DESIGN AND DEVELOPMENT OF PLANAR WIDEBAND PATCH ANTENNA FOR UHF RFID TAG

BY

MOHD SAIFUL RIZA BIN BASHRI

A dissertation submitted in fulfilment of the requirement for
the degree of Master of Science
(Electronics Engineering)

Kulliyyah of Engineering
International Islamic University Malaysia

MARCH 2014

ABSTRACT

Radio Frequency Identification (RFID) technology utilizing Ultra-high Frequency (UHF) band has become significantly popular due to ever growing use in various sectors such as supply chain management, animal and human tracking, automatic access, automatic toll collection and healthcare goods monitoring which can be attributed to long read range, high transmission data rate and large storage capacity. Basic components of UHF RFID system consists of a reader and a tag where tag is made up of a microchip and an antenna. A passive tag operates in the absence of its on board power source or battery. Hence it depends intensely on the antenna to harvest the energy from the transmitting electromagnetic wave emitted by enquiring reader. Typically, tag antenna is designed as modified printed dipole antenna. However, this type of antenna suffers severe performance degradation when mounted on metallic object. As a result, several methods have been proposed to mitigate the problem such as by separating the printed dipole antenna from the metallic surface using foam spacer or the use of grounded type antenna such as Inverted-F antenna (IFA), planar Inverted-F antenna (PIFA) or microstrip patch antenna. Most of the proposed microstrip patch antennas have narrow bandwidth which limits its operation to certain region or country. Moreover, its complex structure that uses of via hole and shorting wall or plate would increase the fabrication cost. Two different types of wideband planar patch antenna for UHF RFID tag have been designed, simulated and fabricated to overcome the limits of the existing patch antenna. Unlike typical microstrip antenna, impedances of the proposed antennas are complex conjugate matched with the reference microchip impedance ($Z_{chip} = 31 - j212\ \Omega$) by using an inductively coupled loop structure. For impedance bandwidth enhancement, a multi planar resonator technique has been used to excite two and three resonance frequencies close to each other to form a wide impedance bandwidth between155 MHz (return loss$\leq$−3 dB) and 117 MHz (return loss$\leq$−6 dB). Simulation and parametric refinement have been done by using FEM based electromagnetic simulator, Ansoft HFSS v13. The overall sizes of the antennas are 87 mm x 45 mm x 1.6 mm and 130 mm × 63 mm × 1.6 mm respectively. The simulated and measured complex impedances of the antennas show a good agreement. The radiation pattern of the prototype antennas have been measured in an anechoic chamber and then compared with the simulated results which also show a good agreement and they are well matched. The maximum gains of the antennas are −7.2 dBi and −5.5 dBi respectively. These results suggest that the UHF RFID tag with proposed antennas can be useful for large metallic object such as metal containers where it can be shipped all over the world.

ملخص البحث

أصبحت تكنولوجياتحديد الهوية باستخدام موجات الراديو (RFID) بواسطة نطاق تردد فوق العالي (UHF) مشهورة نظراً لتزايد استخدامها في مختلف القطاعات مثل إدارة سلسلة التوريد، و تتبع الحيوانات والبشر، والوصول التلقائي، وجمع ضريبة الطرق السريعة التلقائي، ومراقبة منتجات الرعاية الصحية بإمكانية قراءة بعيد المدى، ومعدَّل إرسال البيانات العالي، وطاقة التخزين الكبيرة. المكونات الأساسية لنظام UHF RFID تتكون من القارئ والرقاقة المتضمنة من شريحة صغيرة وهوائي. تعمل الرقاقة السلبية دون اعتماد على مصدر القدرة على لوحة الدائرة أة البطارية. ومن ثم فإنها تعتمد دائمة على الهوائي لحصاد الطاقة من الموجات الكهرومغناطيسية المنبعثة من القارئ. عادة، تم تصميم هوائي الرقاقة المعدلة هوائي ثنائي القطب المطبوعة. ولكن، يعاني هذا النوع من الهوائي تدهور الأداء الشديد عندما شنت على كائن معدني. لذا، تم اقتراح عدة طرق للتخفيف من المشكلة فعلى سبيل المثال بفصل هوائي ثنائي القطب المطبوعة من السطح المعدني باستخدام فاصل رغوة أو باستخدام الهوائي الأرضي مثل هؤائي-F-المقلوب (IFA)، هوائي -F- المقلوب السطحي (PIFA) أو هوائي الشريحة الصغيرة. معظم هوائيات الشريحة الصغيرة المقترحة تعرض النطاق الترددي الضيق الذي يحد من عملها إلى منطقة أو بلد معين. علاوة على ذلك، فإن بنيتها المعقدة من خلال ثقب وتقصير الدائرة أو اللوحة ستؤدي إلى زيادة تكلفة التصنيع. وقد تم تصميم نوعين مختلفين من رقاقة هوائي UHF RFIDالصغرية السطحية الواسعةومحاكاتها وتصنيعها للتغلب على حدود رقعة الهوائي الحالي.بخلاف شريحة الهوائي الصغيرة العادية، ممانعات من الهوائيات المقترحة هي المكورات معقدة المتطابقة مع ممانعة رقاقة المرجعية ($Z_{chip} = 31 - j212\ \Omega$)باستخدام هيكل حلقة بالحث.لتعزيز ممانعة عرض النطاق الترددي، وقد استخدمت تقنية جهاز رنان مستو المتعددة لإثارة اثنين وثلاثة ترددات الرنين قريبة من بعضها البعض لتشكيل مقاومة النطاق الترددياالواسعة بين 155 ميغاهيرتز (فَقْدُ الإرتداد ≥ -3 ديسيبل) و 117 ميغاهيرتز (فَقْدُ الإرتداد ≥ -6 ديسيبل).وقد تم القيام بالمحاكاة والصقل البارامتريباستخدام محاكاة Ansoft HFSS v13الكهرومغناطيسية على أساس FEM. الأحجام الإجمالية للهوائيات هي87 مم × 45 مم × 1.6 مم و 130 مم × 63 مم × 1.6 مم على التوالي.وتظهر ممانعات المعقدة المقلدةوالمقيسة من الهوائيات اتفاقا جيدا.وقد تم قياس نمط الإشعاع من الهوائيات النموذجية في دائرة عديم الصدى ومن ثم مقارنة نتائج المحاكاة التي تظهر أيضا اتفاقا جيدا وأنها مطابقة تماما. تحققت مكاسب الهوائيات في الحد الأقصى عند -7.2 ديسيبلو-5.5 ديسيبلعلىالتوالي.هذه النتائج تشير إلى أن رقاقة UHF RFID مع هوائيات المقترحة يمكن أن تكون مفيدة لكائن معدني كبير مثل حاويات معدنية حيث يمكن شحنها إلى جميع أنحاء العال

APPROVAL PAGE

I certify that I have supervised and read this study and that in my opinion it conforms to acceptable standards of scholarly presentation and is fully adequate, in scope and quality, as a thesis for the degree of Master of Science Electronics Engineering.

………………………………
Muhammad Ibn Ibrahimy
Supervisor

………………………………
S. M. A. Motakabber
Co-Supervisor

I certify that I have read this study and that in my opinion it conforms to acceptable standards of scholarly presentation and is fully adequate, in scope and quality, as a thesis for the degree of Master of Science Electronics Engineering

………………………………
Md. Rafiqul Islam
Internal Examiner

………………………………
Mandeep Singh
External Examiner

This dissertation was submitted to the Department of Electrical and Computer Engineering and is accepted as a fulfilment of the requirement for the degree of Master of Science Electronics Engineering.

………………………………
Othman O. Khalifa
Head, Department of ECE

This dissertation was submitted to the Kulliyyah of Engineering and is accepted as a fulfilment of the requirement for the degree of Master of Science Electronics Engineering.

………………………………
Md. Noor Salleh
Dean, Kulliyyah of Engineering

DECLARATION

I hereby declare that this thesis is the result of my own investigations, except where otherwise stated. I also declare that it has not been previously or concurrently submitted as a whole for any other degrees at IIUM or other institutions.

Mohd Saiful Riza Bin Bashri

Signature…………………..…… Date……………………………..

INTERNATIONAL ISLAMIC UNIVERSITY MALAYSIA

DECLARATION OF COPYRIGHT AND AFFIRMATION OF FAIR USE OF UNPUBLISHED RESEARCH

DESIGN AND DEVELOPMENT OF PLANAR WIDEBAND PATCH ANTENNA FOR UHF RFID TAG

Affirmed by MOHD SAIFUL RIZA BIN BASHRI

…………………………… ……………………………
        Signature   Date

ACKNOWLEDGEMENTS

My gratitude and thanks to Allah s. w. t who granted me strength and knowledge to finally been able to successfully complete my thesis.

I am especially indebted and would like to express my sincere appreciation and gratitude to Assoc. Prof. Dr. Muhammad Ibn Ibrahimy, my supervisor, for his patience, kindness, support, guidance and suggestions throughout the research and preparation of this thesis.

Sincere gratitude is also extended to Asst. Prof. Dr. S. M. A. Motakabber as my co-supervisor for his kind helps, valuable advices, supports and suggestions in my graduate studies.

I would like to thank Br. Mohd. Shukur Bin Ahmad and Br. Shahlan Bin Dalil for their expertise and assistance during the fabrication and measurement process of the antenna.

I also extend my special thanks to the authority and staff of the Institute of Space Science (ANGKASA), Universiti Kebangsaan Malaysia for helping me to measure the radiation pattern of my developed antennas in their anechoic chamber.

I would like to express my sincere appreciation to my wife, my daughter, my mother, my parent in law and my brothers and sisters for their unfailing support, patience, du'a and encouragement during the period of my research.

Finally, the financial support from the Ministry of Higher Education Malaysia sponsorship is gratefully acknowledged.

TABLE OF CONTENTS

LIST OF TABLES

LIST OF FIGURES

LIST OF SYMBOLS

λ	Wavelength
R	Distance from the antenna
H	Largest dimension of the antenna
D	Directivity of the antenna
U	Radiation intensity in a given direction
U_0	Average radiation intensity
P_{rad}	Total radiated power
e_0	Total antenna efficiency
P_{in}	Total accepted power
e_r	Reflection coefficiency
e_c	Conductor efficiency
e_d	Dielectric efficiency
Γ	Voltage reflection coefficient
Z_{in}	Input impedance of the antenna
Z_0	Characteristic impedance of the transmission line connected to antenna
e_{cd}	Radiation efficiency
G	Gain of an antenna
ε_r	Relative permittivity of the substrate
c	Speed of light
h	Thickness of the antenna substrate
f_0	Operating frequency of the antenna
Y	Admittance of a circuit
G	Conductance of a circuit
B	Susceptance of a circuit
$\bar{E}$	Electric field
$\bar{H}$	Magnetic field
J_0	Bessel function of the first kind of order zero
ε_0	Permeability of free space
μ_0	Permittivity of free space
L	Length of the patch antenna
W	Width of the patch antenna
W_e	Effective width of the patch antenna
Z_{chip}	Input impedance of the microchip
Z_{loop}	Impedance of the feed loop
Z_{rb}	Impedance of the radiating body of the antenna
M	Mutual inductance
L_L	Length of the rectangular loop

W_L	Width of the rectangular loop
s	Width of the loop strip
$\hat{n}$	Unit vector normal to the surface of the perfect electric conductor

LIST OF ABBREVIATIONS

RFID	Radio Frequency Identification
RF	Radio Frequency
RLTS	Real Time Location Service
LF	Low Frequency
HF	High Frequency
UHF	Ultra-High Frequency
IC	Integrated Circuit
PEC	Perfect Electric Conductor
PIFA	Planar Inverted-F Antenna
HFSS	High Frequency Simulator Software
VNA	Vector Network Analyser
RL	Return Loss
VSWR	Voltage Signal Wave Ratio
AR	Axial Ratio
MoM	Moment of Methods
FEM	Finite Element Method
FDTD	Finite Difference Time Domain
EM	Electromagnetic
FIT	Finite Integration Technique
SDM	Special Domain Method
LOS	Line of Sight
AIDC	Automatic Identification and Data Collection
OCR	Optical Character Recognition
DC	Direct Current
FCC	Federal Communication Commission
ETSI	European Telecommunication Standard Institute
EIRP	Effective Isotropic Radiated Power
ISO	International Standard Organisation
IEC	International Electronical Commission
EPC	Electronic Product Code
ASK	Amplitide Shift Keying
DSB	Double Side Band
MMS	Miller Modulated Subcarrier
PIE	Pulse Interval Encoding
SSB	Single Side Band
PR-ASK	Phase Reversal Amplitude Shift Keying
FM0	Bi-phase space
PET	Polyethylene Terephthalate

IFA	Inverted-F Antenna
PVC	Polyvinyl Chloride
RCS	Radar Cross Scattering
PTFE	Polytetrafluoroethylene
ERP	Effective Radiated Power
PCB	Printed Circuit Board
ASICS	Application Specific Integrated Circuit
NPR	Negative Photo Resist
UV	Ultra Violet
KOH	Potassium Hydroxide
$FeCl_3$	Iron (III) Chloride
DI	De-ionised Water
SMA	Subminiature version A
SOL	Short-Open-Load

CHAPTER ONE

INTRODUCTION

1.1   OVERVIEW

Radio Frequency Identification (RFID) is an automated identification technology that utilizes radio frequency (RF) wave to automatically identify an object and its location. Although the technology have been in existence for more than half a century, it was not until the last two decades, the technology finally started to gain widespread attention in various sectors such as supply chain, logistics, automatic access, toll collection, real time location service (RTLS) and many more (Dobkin, 2008). These rapid adoptions of RFID can be mainly attributed to the increased capabilities of integrated circuits and the accompanying significant cost reduction thus making it feasible especially for large scale implementation. The basic configuration of RFID system consists of a tag (transponder) or multiple of tags and reader (interrogator) (Finkenzeller, 2003). In a nutshell, tag is a small wireless device attached to an object such as manufactured products, vehicles, animals or even human beings for the purpose of monitoring and tracking its movement while reader is used to read the information carried by the tag. Normally, the information stored in the tag's microchip is its unique identification number along with other useful information such as production date and place of origin. In common, RFID can be classified into several categories based on its operating frequency bands which are low frequency (LF), high frequency (HF), ultra-high frequency (UHF) and microwave system. The interaction between tag and reader for LF and HF systems are realized by inductive coupling between tag's and reader's coil since it operates in the near field where the wavelength

is much larger than the coil. On the other hand, UHF and microwave systems are operating in the far field where electromagnetic wave travels between the antennas at both tag and reader. The overall performance of RFID specifically for UHF system is mostly determined by the capabilities of the antennas for both tag and reader. As such, antenna design plays a pivotal role in realizing a reliable and robust RFID system.

1.2   PROBLEM STATEMENT AND ITS SIGNIFICANCE

It has been reported that commonly used label-typed printed antenna for UHF RFID applications have been observed to suffer from performance degradation when attached to a metal object. Some of the effects were distorted radiation pattern and shift in antenna impedance thus resulting in impedance mismatch between the microchip and the antenna (Ukkonen et al., 2005; Prothro et al., 2006; Ghannay et al., 2009). This prevented reader from reading the tag correctly which would jeopardize the overall monitoring operation. This unwanted scenario is caused by the cancellation of electromagnetic waves of the incoming signal by the reflected waves from the antenna which can be explained through image theory of the electrical current at the boundary of perfect electric conductor (PEC).

Many attempts have been proposed in the literature to solve the problem since many applications requires tag to be mounted on the metallic objects such as metallic box and container at the warehouse and vehicle recognition. One of the approaches is by using microstrip patch antenna due to its working mechanism that operates on a ground plane. As such, when the antenna is mounted on the metallic objects, the surface of that object will act as if it was an extension of the patch antenna ground plane thus no major effects was observed on its performance (Delzo, 2010).

2

One of the challenges in designing patch antenna for UHF RFID tag is to realize the complex impedance matching between the antenna and the microchip. Unlike typical microstrip antenna where the antenna needs to be matched with the 50 Ω coaxial probe or transmission line, the input impedance of the tag antenna must present the required inductance value to cancel out the capacitive reactance of the microchip. This complex impedance matching is very important to harvest maximum energy to power up the microchip since passive tag does not have on-board power source.

Another limitation of patch antenna is it has narrow bandwidth (Garg et al., 2001; Kumar and Ray, 2003). Since the operating frequency for UHF RFID system of each country differs from one another, normally, tag employing microstrip patch antenna is only capable of working within a specific country or region (GS1, 2012). For tag to operate in universal scale, the tag antenna must have a minimum half-power impedance bandwidth (return loss ≤ -3 dB) of 11.16% to cover the entire frequency range of UHF RFID (860 MHz−960 MHz). A wideband tag antenna will avoid the need to individually tuning the antenna to a specific operating frequency. Instead, tag antenna can be directly mass produced regardless of the country it is intended to operate as well as to provide antenna fabrication tolerance. In addition, it also permits continuous tracking of tagged items as they are being transferred from one country to another.

Normally, the proposed patch antennas for RFID application were complex due to cross and multi-layered structure (via hole, double substrate, shorting wall/plate). These antennas were difficult to fabricate and is also required additional process such as soldering and drilling which could lead to increased cost.

As such, a new planar wideband microstrip antenna design capable of mounting on metallic objects is required. With wideband characteristic, the tag antenna will be able to operate worldwide. Furthermore, a complete planar structure without having cross or multi-layered construction is crucial for ease of fabrication and to reduce overall manufacturing cost of tag. This cost reduction will permit implementation of RFID for metallic application in a larger scale.

1.3   RESEARCH OBJECTIVES

The main objective of this research is to design a planar wideband patch antenna for UHF RFID tag which can work when attached to a metallic object. Although several works were done on this problem, many were narrowband and thick in size which subsequently limit its applications. Moreover, most of the proposed wideband design exhibit complex structure due to incorporated cross and multi-layered construction (via hole, double layered substrate) which is challenging to fabricate due to involvement of various additional processes (drilling and soldering) hence lead to higher cost. In order to design a new microstrip patch antenna such as to solve the problem mentioned above, this research work aims at achieving the following objectives:

(1) To design a planar wideband patch antenna of UHF RFID tag for tagging the metallic object.

(2) To realize complex impedance matching between the tag antenna and the referenced microchip.

(3) To increase the bandwidth of the antenna to cover the operating frequency of UHF RFID band (860 MHz-960 MHz) by using multiple resonating patches.

(4) To fabricate the proposed tag antenna on a single copper cladding board by using photolithographic and etching techniques.

(5) To measure and compare the performance of prototype antenna with similar existing antennas.

1.4   RESEARCH METHODOLOGY

In this research, the methods taken in designing the proposed tag antenna are listed below and summarized in Figure 1.1. The methods are chosen to solve the problem statements and to achieve the objectives mentioned above.

(1) *Develop analytical model of planar wideband microstrip patch antenna.* The initial shape of the antenna is derived from the rectangular shape patch. Then, the impedance matching is realized using inductively coupled loop structure. The bandwidth of the antenna is increased using several co-planar resonator patches.

(2) *Simulate the antenna design using commercial electromagnetic simulation software.* After the analytical model is successfully developed, the model is then simulated using Ansoft High Frequency Simulator Software (HFSS). Further parameter refinement is performed using the simulator to achieve optimal design.

(3) *Fabricate the proposed antenna*. The fabrication of the antenna design is conducted using photolithography and etching technique after satisfactory simulation results are obtained.

(4) *Measure the performance of the prototype antenna*. The prototype antenna is measured using vector network analyzer (VNA) and the result is recorded.

(5) *Compare and analyze the results of both simulation and measurements*. The simulation and measurement results are compared and analyzed for validation. Then, the performance of proposed tag antenna is compared with similar existing tag antenna.

(6) *Final report*. The final report of the research is finalized.

Development of analytical model of the antenna

Simulation of the antenna design

Fabrication of the prototype

Measurement of the prototype

Analysis and performance comparison of the design

Final report
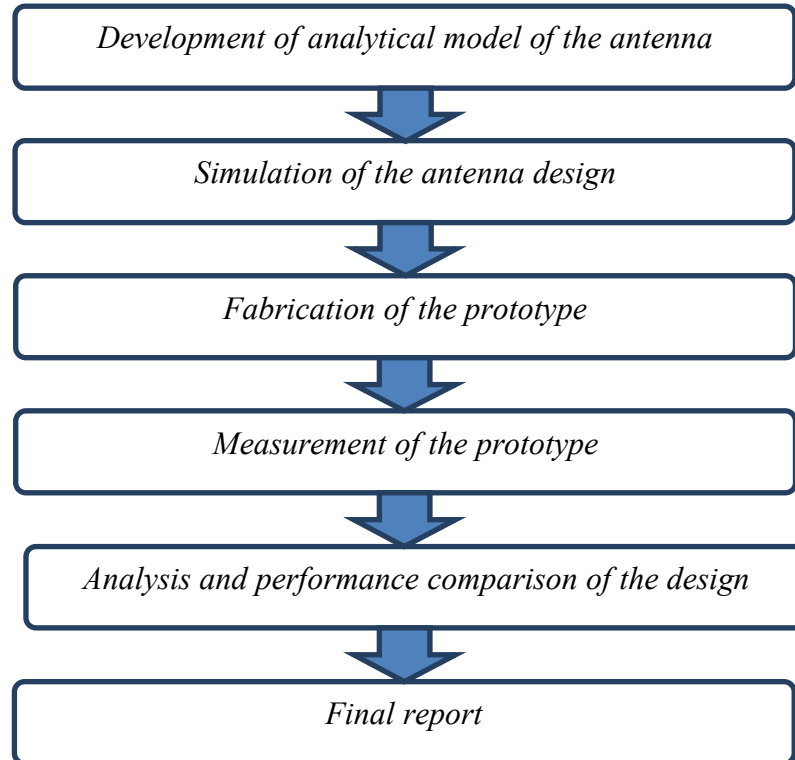
Figure 1.1: Summary of the research methodology

1.5   RESEARCH SCOPE

The research focuses on the design, simulation and fabrication of the antenna for UHF RFID tag. The antennas were designed to be used in UHF RFID operating frequency band of 860 MHz to 960 MHz. The proposed antennas were conjugated matched to referenced microchip which is Alien Higgs-3 with input impedance of $31 - 212j\Omega$. The substrate used was epoxy glass FR-4. The antenna design is simulated using FEM based electromagnetic simulator, Ansoft High Frequency Simulator Software (HFSS) v13. The fabrication of the antennas is carried out using photolithographic and etching technique. The performance of the antenna is measured in term of its impedance bandwidth and radiation pattern and compared with other similar antenna design.

1.6   ORGANIZATION OF DISSERTATION

The thesis consists of six chapters. The first chapter begins with a brief explanation of RFID technology. Then, research problem and its significance are highlighted based on recent literature. The objectives of the research as well as research methodology are also explained in this chapter. Chapter 2 defines the fundamental parameter describing the performance of an antenna where some of them will be later used for performance comparison between the proposed antenna design and the existing ones. A comparative study of existing antenna for UHF RFID tag are presented in detail and further summarized in tabulated form for easy comparison. An overview of general process of designing tag antenna and its requirements are presented in Chapter 3. This is followed by actual antenna requirement according to the research statement. The theory and design of a new antenna is later presented and supplemented with the simulation results for validation. Further parametric refinement was carried out to

produce an optimal antenna design. Chapter 4 demonstrates the fabrication process of the proposed antenna design and the measurement setup used to measure the antenna performance parameter. In Chapter 5, the simulated and measured results were compared to validate the design. In addition, the antenna is also compared with several similar existing antennas. Finally, conclusion and future works are given in Chapter 6.

CHAPTER TWO

LITERATURE REVIEW

2.1   INTRODUCTION

This chapter begins with the description of a typical rectangular patch antenna based on the transmission line model. Afterwards, the RFID system is explained thoroughly. Later, several tag antenna designs from recent literatures are analyzed and discussed in details. The advantages and limitation of each design are highlighted. Comparisons of each tag antenna design are done in terms of impedance matching techniques, miniaturization techniques, broad-banding techniques, radiation characteristic and fabrication level of difficulties. In addition, effects on tag antenna's performance when mounted on metallic surface are also studied and analyzed.

2.2   TRANSMISSION LINE MODEL

Since rectangular patch forms a basic structure of the proposed antenna in this thesis, its working mechanism, fundamental characteristics and the transmission line model for the antenna are discussed. In transmission line model, rectangular patch is represented as two radiating slots (aperture) connected by a parallel plate transmission line (Kumar and Ray, 2003). The width and height of the slots are denoted as W and h as illustrated in Figure 2.1.
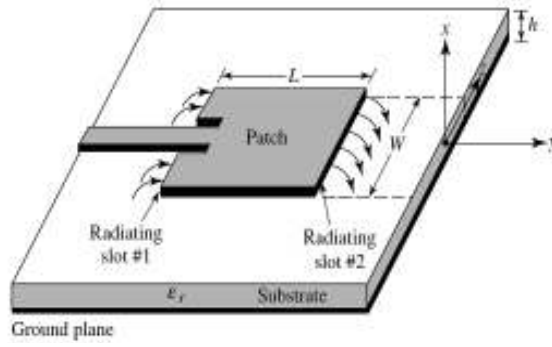
Figure 2.1: Two radiating slots separated by transmission line of length, L

Due to fringing field effect, the resonant length of the patch is longer than that of the physical length. The effective electrical length can be calculated by using the expression below.

$$L_{eff} = L + \Delta L \tag{2-1}$$

where ΔL is given by equation (2-2).

$$\frac{\Delta L}{h} = 0.412 \frac{(\varepsilon_r + 0.3)\left(\frac{W}{h} + 0.264\right)}{(\varepsilon_r - 0.258)\left(\frac{W}{h} + 0.8\right)} \tag{2-2}$$

ε_r is the relative permittivity of the substrate. By using the calculated value of the effective length of the patch, the dominant resonant frequency of TM_{010} can be determined by

$$f_0 = \frac{c}{2L_{eff}\sqrt{\varepsilon_r}} \tag{2-3}$$

For efficient radiator, the W of the patch is given by

$$W = \frac{c}{2f_0}\left(\frac{2}{\varepsilon_r + 1}\right)^{1/2} \tag{2-4}$$

10

In general, the resonant frequency at any TM_{mn} modes can be excited by using the following expression (Balanis, 2005)

$$f_0 = \frac{c}{2\sqrt{\varepsilon_r}}\left[\left(\frac{n}{L}\right)^2 + \left(\frac{m}{W}\right)^2\right]^{\frac{1}{2}} \tag{2-5}$$

where m and n are the modes along the W and L respectively.

The resonant input resistance of the patch can be determined by first finding the equivalent admittances of the two finite width radiating slots, $Y_1 = G_1 + jB_1$ and $Y_2 = G_2 + jB_2$ respectively by using equations (2-6) and (2-7) below (Kumar and Ray, 2003)

$$G_1 = \frac{W}{120\lambda_0}\left[1 - \frac{1}{24}(k_0 h)^2\right]\frac{h}{\lambda_0} < \frac{1}{10} \tag{2-6}$$

$$B_1 = \frac{W}{120\lambda_0}[1 - 0.636\ln(k_0 h)]\frac{h}{\lambda_0} < \frac{1}{10} \tag{2-7}$$

Since slot #2 is identical to slot #1, $Y_2 = Y_1$, $G_2 = G_1$ and $B_2 = B_1$. As a result of the fringing field effect, the length of the patch is electrically longer than the physical length thus making the actual separation between the two slots less than λ/2. By using equation (2-1), the length of the patch can be properly chosen (0.48λ <L<0.49λ) so that the transformed admittance of slot #2 becomes

$$\tilde{Y}_2 = \tilde{G}_2 + j\tilde{B}_2 = G_1 - jB_1 \tag{2-8}$$

$$\tilde{G}_2 = G_1 \tag{2-9}$$

$$\tilde{B}_2 = -B_1 \tag{2-10}$$

Hence, the total resonant input admittance is real as shown in equation (2-11) below

$$Y_{in} = Y_1 + \tilde{Y}_2 = 2G_1 \tag{2-11}$$

The total input resistance at the edge of the patch is then given by

$$Z_{in} = \frac{1}{Y_{in}} = R_{in} = \frac{1}{2G_1} \tag{2-12}$$

However, equation (2-12) above does not take into account mutual effects between the two radiating slots (Balanis, 2005). For better accuracy, the equation (2-12) can be modified to form equation (2-13)

$$R_{in} = \frac{1}{2(G_1 \pm G_{12})} \tag{2-13}$$

where the plus (+) sign is used for modes with odd (asymmetric) resonant voltage distribution beneath the patch and along the length while minus (−) sign is for modes with even (symmetric) voltage distribution. The mutual conductance, G_{12} is expressed as

$$G_{12} = \frac{1}{|V_0|^2} \, \text{Re} \iint_S \mathbf{E}_1 \times \mathbf{H}_2^* \cdot d\mathbf{s} \tag{2-14}$$

where $\mathbf{E}_1$ represents the electric field radiated by slot #1, $\mathbf{H}_2$ is the magnetic field radiated by slot #2 and V_0 is the voltage across the slot. By integrating the fields over a sphere of large radius, equation (2-14) can be expressed as

$$G_{12} = \frac{1}{120\pi^2} \int_0^\pi \left[\frac{\sin\left(\frac{k_0 W}{2} \cos\theta\right)}{\cos\theta} \right]^2 J_0(k_0 L \sin\theta) \sin^3\theta \, d\theta \tag{2-15}$$

where J_0 is the Bessel function of the first kind of order zero and k_0 is the wave number. Furthermore, the resonant input resistance of the rectangular patch antenna can be changed by using an inset feed for impedance matching. The input resistance at a distance y_0 from the edge, as shown in Figure 2.2 is given by equation (2-16) (Derneryd, 1978)
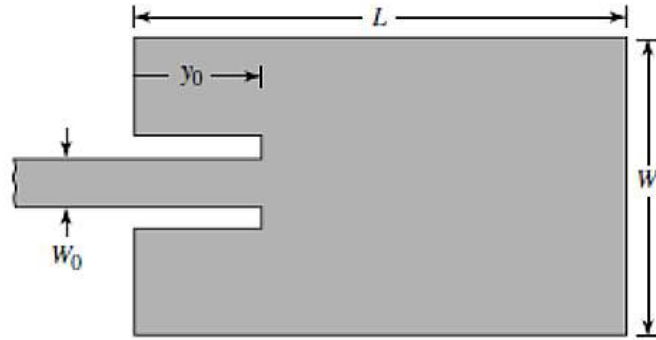
Figure 2.2: Inset feed matching technique for patch antenna (Balanis, 2005)

$$R_{in}(y = y_0) = \frac{1}{2(G_1 \pm G_{12})} \left[\cos^2 \left(\frac{\pi}{L} y_0 \right) \right.$$
$$+ \frac{G_1^2 + B_1^2}{Y_c^2} \sin^2 \left(\frac{\pi}{L} y_0 \right)$$
$$\left. - \frac{B_1}{Y_c} \sin \left(\frac{2\pi}{L} y_0 \right) \right]$$

(2-16)

where $Y_c = 1/Z_c$ and Z_c is the characteristic impedance of the inset feed line with width, w_0 given by equation (2-17a) and equation (2-17b) (Balanis, 1989).

$$Z_c = \begin{cases} \dfrac{60}{\sqrt{\varepsilon_{reff}}} \ln\left[\dfrac{8h}{W_0} + \dfrac{W_0}{4h}\right], & \dfrac{W_0}{h} \leq 1 \qquad \text{(2-17a)} \\[3mm] \dfrac{120\lambda}{\sqrt{\varepsilon_{reff}}\left[\frac{W_0}{h} + 1.393 + 0.667\ln\left(\frac{W_0}{h} + 1.444\right)\right]}, & \dfrac{W_0}{h} > 1 \qquad \text{(2-17b)} \end{cases}$$

For most typical microstrip, $G_1/Y_c \ll 1$ and $B_1/Y_c \ll 1$ thus equation (2-16) reduces to equation (2.18)

$$R_{in}(y = y_0) = \frac{1}{2(G_1 \pm G_{12})} \cos^2\left(\frac{\pi}{L} y_0\right) \qquad \text{(2.18)}$$

The normalized input resistance is illustrated in Figure 2.3. It is observed that the maximum input resistance is found the edge of the patch where the corresponding voltage is maximum while the minimum value (zero) happens at the center of the patch when the voltage is zero and current is maximum.
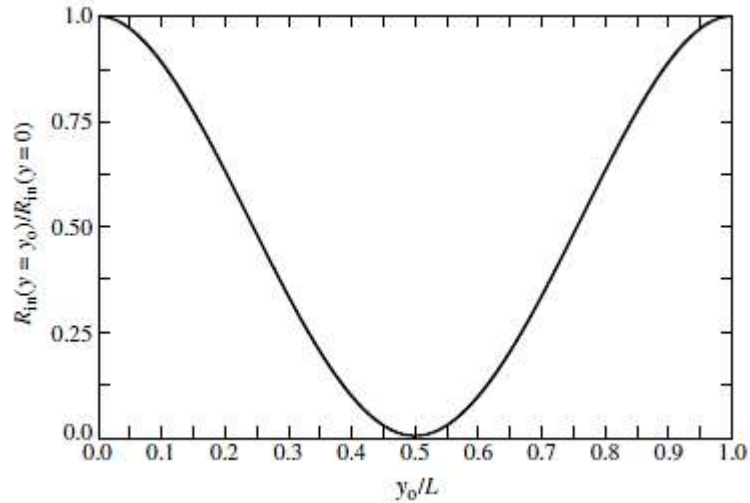
Figure 2.3: Normalized input resistance against y_0 (Balanis, 2005)

2.3 RFID TECHNOLOGY

RFID technology are being implemented rapidly in various sectors for items tracking and monitoring due to its advantages like independent of Line Of Sight (LOS), long

read range, high data speed and large storage capacity. In this subchapter, the basic implementation of RFID, its classification, working mechanism, standard and regulations that govern the technology is presented.

2.3.1 Basic RFID Implementation

The basic component of RFID system consists of a reader (or interrogator) and tag (or transponder). Tag is attached to an object to be identified while reader is used to read the tag just like the operation of a conventional barcode scanner. In most applications, the reader is connected to a host computer or a network to facilitate the interaction between the system and the user so as to perform specific task. However, not all readers are required to be connected to a computer host to work. This type of reader is equipped with its own user interface thus can operate independently although with limited capability. Figure 2.4 shows the diagram of a typical RFID system (Dobkin, 2008). Unlike other types of automatic identification and data collection (AIDC) like optical barcode and optical character recognition (OCR), RFID has numerous advantages such as it does not need for physical contact or line of sight (LOS), large information storage capacity, high data rate and able to simultaneously read or write multiple tags within its proximity (Finkenzeller, 2003).

Reader antenna

downlink (R→T)

Tag antenna

PC

Reader

uplink (T→R)

Tag

Microchip
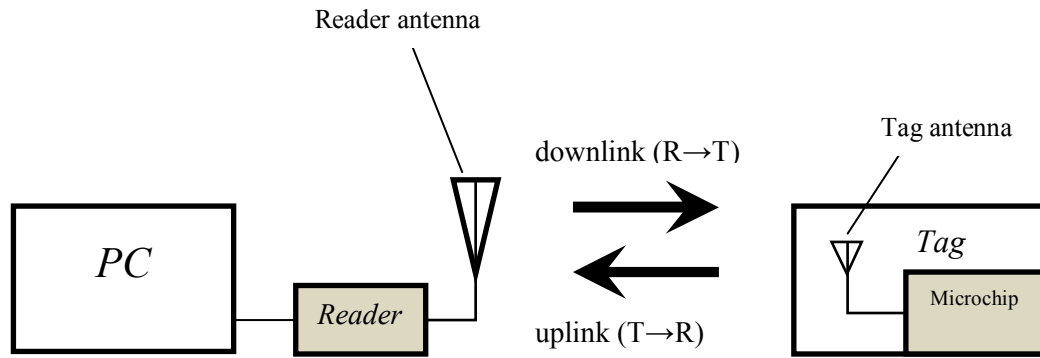
Figure 2.4: Overview of RFID system

Reader is a device to read and sometimes write data to the tag. Generally, it can be classified as stationary and handheld reader depending on its application (Weinstein, 2005). The main components of a reader are transmitter, receiver, reader antenna and processing unit. Transmitter functions to transmit radio frequency (RF) power and the clock signal via reader antenna. Reader antenna is used to radiate and receive RF wave. Receiver receives the signal from the reader antenna and subsequently sends it to the processing unit. The function of the processing unit is to implement the reader protocol which will allow the communication between reader and tag. It also performs encoding, decoding as well as error checking. Figure 2.5 shows photographs of the two types of the RFID reader mentioned above.

Figure 2.5: Stationary (left) and handheld (right) RFID reader

To identify and track an object, a small device relative to the object size is attached to the object. This wireless device is known as tag (or transponder). Tag is able to store and transmit data to a reader using radio waves. Normally, it is made up of an antenna and microchip as depicted in Figure 2.6. In passive system, tag antenna draws the energy from the reader transmitted RF signal to energize the microchip in addition to sending and receiving data to and from the reader (Rao et al., 2005). Microchip, as the processing unit for the tag, performs several tasks such as converting the RF power from the reader signal to DC power, extracting the clock signal, modulating the received reader signal for tag's response and also implementing the communication protocol between the tag and the reader.

2.3.2 Classification of RFID System

Basically, tag can be categorized into three distinct types depending on how it gets the power to turn on its microchip. There are passive, semi-active (also known as battery-assisted) and active tag. Passive tag as the name suggests does not have an on board power source (i.e. a battery) and needs to draw power from external source which in

this case the transmitted RF signal from the reader (Finkenzeller, 2003). Due to its simple construction and cheaper cost, it finds many applications in RFID compared to other types of tag. In order to conserve the energy, passive tag will only be switched on when there is a reader in its vicinity in which the reader will start to communicate first (Dobkin, 2008). As for the realization of tag to reader communication for passive tag, a special modulation technique called back-scattering modulation is used. By changing its RF front end input impedance between two states (matched and mismatched) according to the digital bit '1' and '0' of the information stored, the tag is able to modulate the reflected signal to the reader. Then, based on the two distinct amount of power received (high power received corresponds to mismatched state, low power received corresponds to matched state) the reader is able to demodulate the signal properly. On the other hand, semi-active tag and active tag both have on-board power source in order to provide energy to the tag for its operation. Both types of tag are particularly useful for applications requiring very long read range, or complex circuitry like having a sensor. However, unlike active tag, semi-active tag still uses backscattering modulation to interact with the reader.
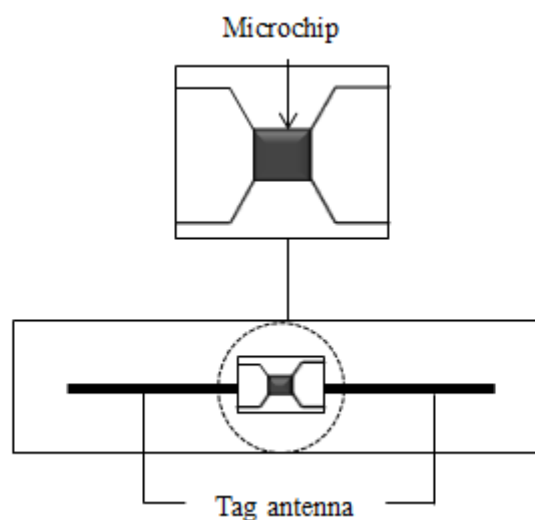
Figure 2.6: Diagram of RFID passive tag for UHF band

The RFID systems are also distinguished by the frequency band they are operating on. The most commonly encountered frequency bands are low frequency (125/134 kHz), high frequency (13.56 MHz), ultra-high frequency (860 MHz-960 MHz) and microwave (2.4 GHz and 5.8 GHz) (Rao et al., 2005; Dobkin, 2008).

2.3.3 Near Field and Far Field Communication

The communication between tag and reader can be classified into three main categories which are capacitive coupling, inductive coupling, and electromagnetic coupling (Dobkin, 2008). Both the capacitive and inductive couplings occur within the near field region while electromagnetic interaction happens at the far field. The near field RFID systems are operating at low frequency regions since the tag antenna is placed at a distance smaller than its wavelength. Low frequency (LF) and high frequency (HF) systems both operate at near field by quasi-static magnetic flux coupling between the reader's and tag's coils hence resulting in low read range (Marrocco, 2008). On the other hand, UHF and microwave systems operate at higher frequency where travelling electromagnetic waves is sent from the transmitting antenna to the receiving antenna. As a result, UHF systems are capable of communicating over longer distance.

2.3.4 Regulation and Standards for UHF RFID System

A brief explanation on regulations and standards for UHF RFID system is given in this subchapter. RFID technology utilizes the electromagnetic spectrum to realize its communication. As such, to ensure it is able to work in parallel with other RF applications, a standard to determine the allocation of operating frequency band and

allowable transmitted power is required. The regulations of UHF RFID systems vary among country or region and they are set by the regulatory body of that specific country (Guha and Antar, 2011). In United State, Federal Communication Commission (FCC) acts to govern the RFID in the country while European Telecommunication Standard Institute (ETSI) serves the European continents in regulating the standards for the technology. Some of the regulations for the operating frequency and the maximum allowable transmitted power define as Effective Isotropic Radiated Power (EIRP) is summarized in Table 2.1.

Table 2.1
Operating frequency of UHF RFID system for several countries (GS1, 2012)

Country/ region	Operating frequency, f (MHz)	EIRP (W)
North America	902-928	4
Europe	865-868	3.3
Japan	952-956	4
Australia	920-926	4
Malaysia	919-923	4

Another important regulation is the air interface standards and protocols where it permits inter-operability between readers and tags manufactured by different companies. The air interface protocol governs the communication between tag and reader. Two standard bodies; International Standard Organization (ISO) and International Electrotechnical Commission (IEC) defined the standards for RFID system. To achieve worldwide adoption and standardization, a family coding scheme

known as electronic product code (EPC) was created and its usage is being promoted by an organization body known as EPCglobal.

Table 2.2
Air interface standards and protocol parameter for UHF RFID (Delzo, 2010)

Parameters	Standard/ protocol		
	ISO/IEC 18000-6A	ISO/IEC 18000-6B	ISO/IEC 18000-6C EPC Class 1 Gen 2
Forward link modulation	ASK	ASK	DSB-ASK SSB-ASK PR-ASK
Forward link encoding	PIE	Manchester	PIE
Return link modulation	ASK	ASK	ASK PSK
Return link encoding	FM0	FM0	FM0 MMS
Collision arbitration	ALOHA	Binary tree	Random slotted
Forward link bitrate	33kbps(mean)	10kbps to 40kbps(depends on regulation)	26.7kbps-128kbps
Return link bitrate	40kbps-160kbps	160kbps	FM0:40kbps-640kbps MMS:5kbps-320kbps

ASK: Amplitude Shift Keying   SSB: Single Side Band
DSB: Double Side Band   PR-ASK: Phase reversal ASK
MMS: Miller Modulated Subcarrier   FM0: Bi-phase space
PIE: Pulse Interval Encoding

From 2006, EPC Class 1 Gen 2 is the commonly used protocol in UHF RFID system since it provides robust performance in dense reader environment and enhanced security compared to previous standards (Delzo, 2010). Table 2.2 lists the air interface parameters for three standards for comparison.

2.3.5 Tag Antenna Read Range

The read range of the tag antenna can be calculated theoretically by using Friis free space equation as expressed below (Rao et al., 2005)

$$d_{max}(\theta,\varphi) = \frac{c}{4\pi f_c} \sqrt{\frac{EIRP_R}{P_{th}} G_{tag}(\theta,\varphi)\tau} \tag{2-19}$$

where EIRP$_R$ is the equivalent isotropic radiated power, G_{tag} is the tag antenna gain, P_{th} is the threshold power of the tag microchip and τ is the power transmission coefficient with value ranging from 0 to 1. τ is given by

$$\tau = 1 - |RL|^2 \tag{2-20}$$

From equation (2-19), it shows half power impedance bandwidth (RL$\geq$ 3 dB) is accounted for at least half of the power is delivered to the microchip, τ=0.5. For more stringent requirement, 6 dB return loss and 10 dB return loss can be used for antenna performance evaluation which corresponds to only 25% and 11% of incident power being reflected back due to the impedance mismatch between tag antenna and the microchip. As with other presented patch antennas for RFID tag, 3 dB return loss should be enough for RFID requirement since in many cases the read range of the tag is only a few meters.

2.4   EFFECTS OF METALLIC SURFACE ON TAG PERFORMANCE

To understand the effect of metal objects toward the performance of tag antenna, a relationship between impinging electromagnetic wave on the perfect electric conductor (PEC) is investigated. Based on equation (2.21), it is shown that the

tangential components of the electric field, $\vec{E}$ on the surface of the PEC is zero at any point of the surface (Park and Eom, 2011).

$$\hat{n} \times \vec{E} = 0 \tag{2.21}$$

where $\hat{n}$, is the unit vector normal to the surface of the PEC. As such, when travelling electromagnetic wave emitted by an antenna impinges upon the surface of PEC material, opposite current is induced on the surface plane of the PEC to cancel out the tangential component of electric field of the incoming wave. In the case of label-typed printed tag antenna, when the tag is attached on the metal objects, the object surface plane can be assumed to act as a perfect conductor. By using an image theory, the metallic surface can be replaced with an antenna whose currents are opposite of the original antenna as illustrated in Figure 2.7 (Balanis, 2005).
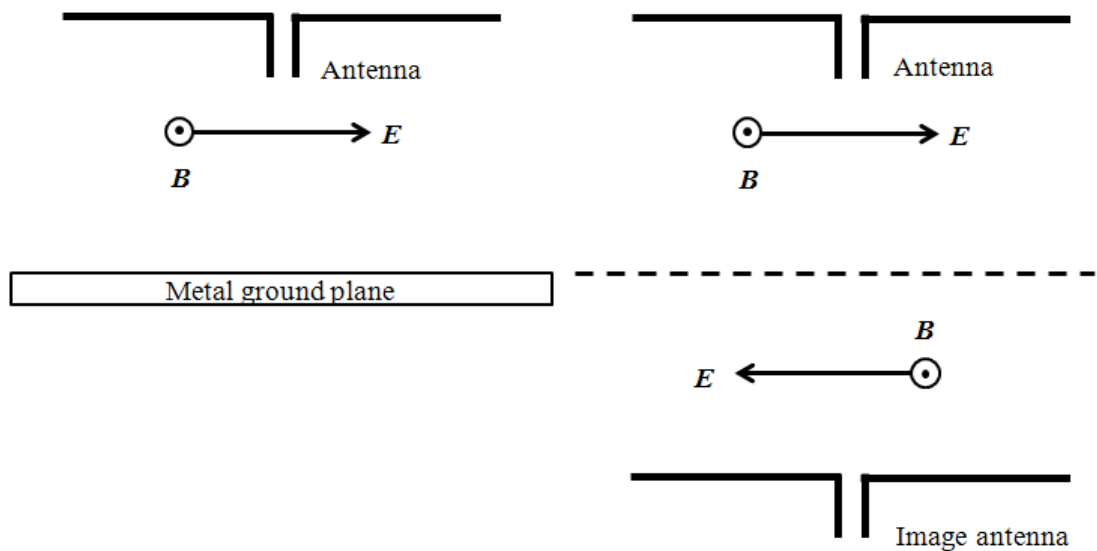
Figure 2.7: Illustrative example of image theory when antenna is near the metal plane.

This image theory method assumes that the metal ground plane is a perfect conductor with infinite dimension. Although the above assumption is not accurately reflecting the scenario of tag antenna placed on the metallic objects, however it is still a good approximation considering the separation between tag and the metal surface is very close as with the case with the label-typed tag antenna (Prothro, 2007).

As a result of this phenomenon, power emitted by the reader could not be harvested by the tag. As a result, the tag does not receive sufficient power to energize its microchip hence preventing it from responding to the reader command. This scenario can have detrimental effects to the overall operation of RFID system where items cannot be tracked and monitored properly.

2.5 RELATED WORK

There have been extensive and numerous works on tag antenna design to cater for various requirements of the RFID system. An overview of the design process of passive UHF tag antenna has been presented by Rao et al., (2005) and Marrocco (2008). As presented by Ukkonen et al., (2005), Prothro, (2007) and Delzo (2010), the commonly used label typed printed dipole antenna suffers performance degradation when used for tagging metallic objects. The observed effects are shift in operating frequency, degraded impedance matching and distortion of radiation pattern.

2.5.1 Label-type Printed Dipole Antenna

Some of the works on printed dipole antenna can be found in (Choi et al., 2006; Yang and Feng, 2008; Choi et al., 2009; Monti et al., 2010). The structure of typical printed dipole antenna is a half-wavelength thin copper strip printed on a polyethylene

terephthalate (PET) substrate. As a mean of miniaturizing the dipole antenna, the dipole arm are bend to give a much shorter projected length as presented by Choi et al., (2006), Yang and Feng(2008), Choi et al., (2009), Pongpaibool (2009) and Monti et al., (2010). The increase of the electrical length due to the resulting meandered dipole reduces the resonant frequency of the antenna. As such, the dipole arm can be squeezed so that the final dimension of the antenna is smaller than that of typical dipole without meandering. The structure of the meandered dipole is displayed in Figure 2.8.
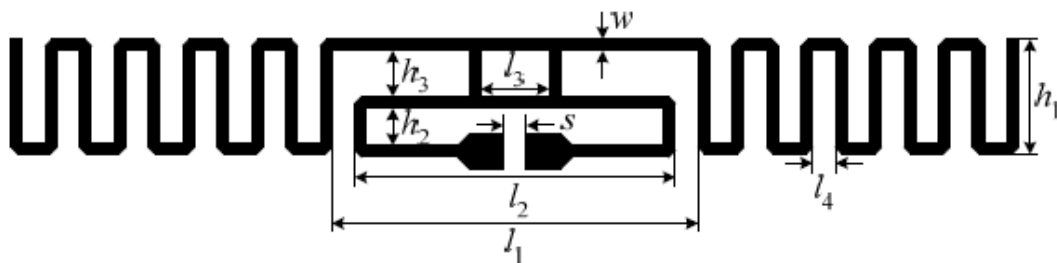
Figure 2.8: Meandered dipole tag antenna for UHF RFID (Pongpaibool, 2009)

2.5.2 Printed Dipole Antenna with Foam Spacer

Although label-type printed dipole antenna proposed above offers low cost construction and can be easily attached to objects surface due to its flexible structure, it has several limitations when used for metal application. To present a solution to this problem, a foam spacer was used to provide enough separation between dipole tag antenna and the metal surface which would provide constructive interference between the incoming and the reflected electromagnetic waves (Delzo, 2010). Cho et al., (2008) presented a novel antenna made up of spiral inner dipole and bend dipole printed on PET substrate. The antenna is then attached on top of a 3 mm thick form to separate the antenna from the metal surface as shown in Figure 2.9. For the impedance

matching part, double T-matching network is adopted. The reported half-power

impedance matching (return loss ≤ -3 dB) and read range for free space were both

7.6% and 2.8 m while on metallic surface were 0.8% and 1.8 m respectively.

However, the antenna bandwidth is reduced significantly by 6.8% when attached on

metallic surface.
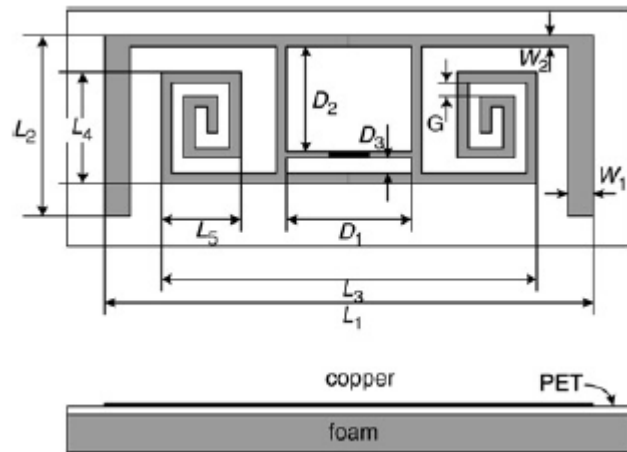
Figure 2.9: Printed spiral dipole antenna attached to foam spacer (Cho et al., 2008)

Another approach that has gotten serious consideration to provide better

solution to mitigate the metal problem is the use of grounded antenna. The reason

behind the idea is that the metallic surface on which the tag is embedded would act as

an extension of the antenna ground plane hence becoming part of the antenna

structure. Due to this, it is anticipated that only slight variation on antenna

characteristic has been observed.

2.5.3 Inverted-F Antenna (IFA)

To present a solution to the problem faced by the printed dipole antenna for RFID

metal application, inverted-F antenna was proposed byUkkonen et al., (2004) as

shown in Figure 2.10. The length of the antenna is 67 mm while the height is 10 mm.

The antenna was experimentally tested on several different substrate materials namely Teflon, two substrate layer and no substrate. The experimental results shows read range between 0.5 m and 1 m when the antenna was mounted on metal. The limitations posed by the design are its narrow bandwidth of 17 MHz (return loss≤ -10 dB) and it is difficult to fabricate due vertical feeding method used for connecting the antenna and the microchip.

Figure 2.10: A fabricated IFA antenna (Ukkonen et al., 2004)

2.5.4 Planar Inverted-F Antenna (PIFA)

Another type of antenna proposed for metal surface improvement is planar inverted-F antenna (PIFA). The name of the antenna came from F-shaped structure seen when view from the antenna side due to shorting plate used to connect the patch to the ground plane. Hirvonen et al., (2004) proposed a small and low-cost PIFA. The antenna configuration can be seen in Figure 2.11. The antenna impedance is directly matched to the microchip input impedance to achieve good power transfer. To evaluate its performance, several platforms consists of free space, metal, wood, PVC and water canister were used to attach the antenna. The results show only slight

performance variation in terms of bandwidth and read range thus verifying that the antenna is suitable for various applications including metal. The reported read range varies from 2 m to 5.1 m depending on the material the antenna is attached to. This is mainly due to the variation of the antenna gain where metal acts as a reflector thus increasing the directivity in the main lobe while free space and water canister absorbs some of the wave thus reducing the efficiency of the antenna. However, the drawbacks of the design are narrow bandwidth around 15 MHz (return loss≤ -3 dB). In addition, the adoption of shorting plate and the vertical feeding method increase the complexity of the antenna structure which makes it difficult to fabricate.
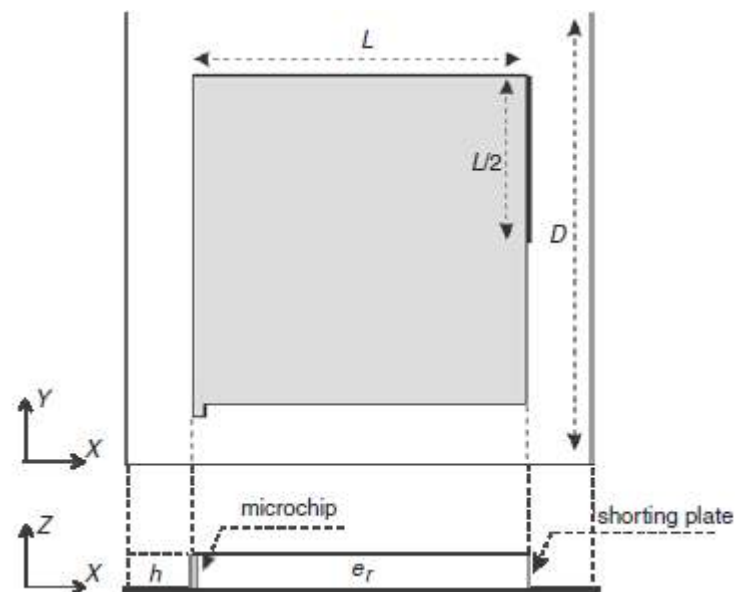
Figure 2.11: Antenna configuration of PIFA (Hirvonen et al., 2004)

Kwon and Lee (2005) proposed a compact slotted PIFA antenna whose dimension is 50 mm x 30 mm x 4mm for metallic applications. The antenna structure is shown in Figure 2.12. The microchip can be easily attached on the center of the U-slotted. To realize a low cost antenna, foam substrate with $\varepsilon_r \sim 1$ was used. The

maximum measured read range is 4 m and the 3dB bandwidth (based on RCS performance specification) is 25 MHz. Although small form factor is achieved, it does not exhibit low profile structure due to thick substrate. Furthermore, the bandwidth is still below the required minimum value for worldwide application and the fabrication is challenging due the folded radiating body.
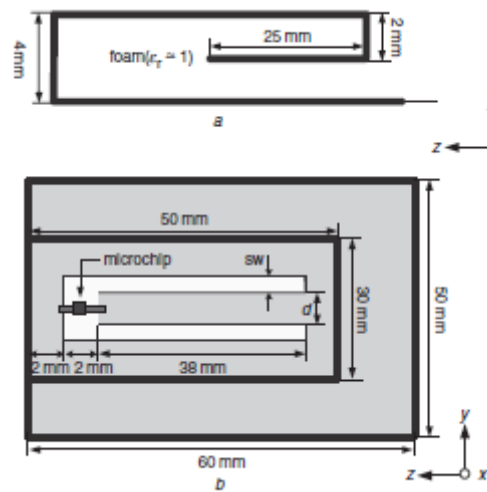
Figure 2.12: Slotted PIFA tag (Kwon and Lee, 2005)

Another PIFA utilizing U-slot on the radiating body for size reduction was reported by Choi et al., (2006). The total dimension of the final design is 40 mm x 40 mm x 2.36 mm. To feed the microstrip, coplanar waveguide is placed at the center of the feeding layer as shown in Figure 2.13 for easy integration with the microchip. Furthermore, several shorting pins are employed at the edge of the patch to connect it to the ground plane for size miniaturization. Two layers are used between the patch and the metallic surface consists of dielectric substrate with ε_r=2.5 and a thickness of 2.36 mm and foam with ε_r=1.07 of thickness 1mm hence making the total separation distance between tagged metal surface and the antenna about 3.36 mm. The reported

measured maximum read range is 4.5 m which is obtained only when the antenna is mounted on metal due to the absence of actual ground plane in the antenna design. The disadvantages of the proposed antenna are low bandwidth and consist of cross and multi-layered configuration where it is difficult and costly to fabricate.

(a)

(b)
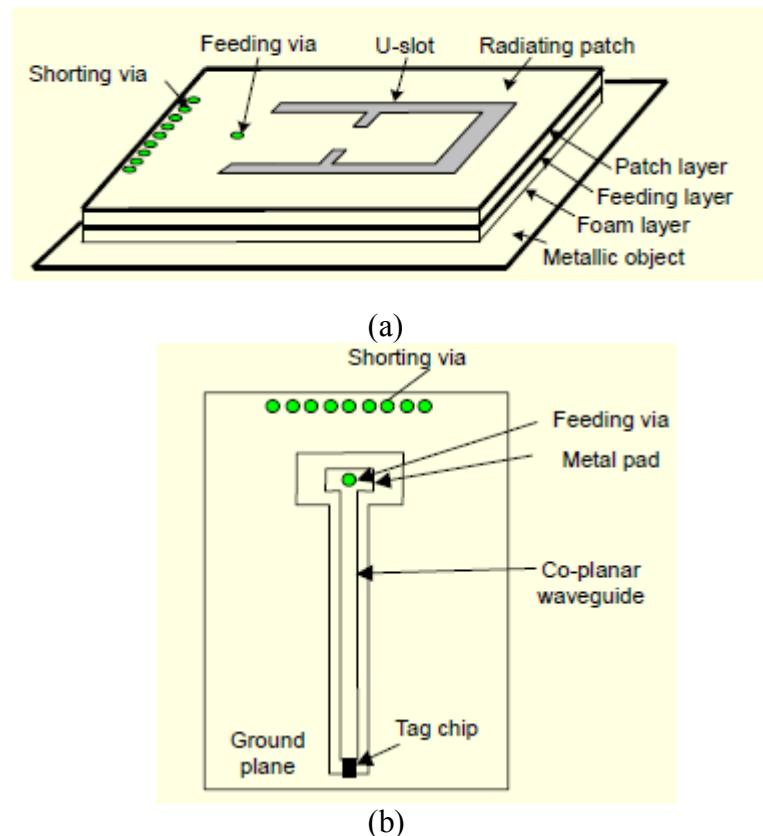
Figure 2.13: (a) Overall view and (b) feeding layer view of U-slot tag antenna

2.5.5 Microstrip Patch Antenna

Microstrip antenna is one of the most research antenna types due to its versatility and numerous advantages. Since the working principle of microstrip antenna requires a conductor to act as its ground plane, the problem presented by the metallic objects on

label-type printed dipole antenna will have little effects on the performance of patch antenna since the metal surface would act merely as an extension to its ground plane. However, microstrip antenna inherits several limitations such as low gain, inefficient and limited bandwidth.

Numerous works on microstrip antenna for RFID application have been proposed utilizing various feeding methods for impedance matching and patch shapes for specific radiation pattern. Son et al., (2006) presented a low cost wideband planar antenna by employing proximity-coupled feed structure orthogonal to that of the length of the radiating patch thus eliminating the need for additional matching network as illustrated in Figure 2.14. The radiating patch, the shorting plate and ground plane are constructed by bending a thin copper sheet into U-shaped. A polystyrene foam with ε_r =1.1 and tangential loss, $tan\,\delta$ =0.001 is used for the substrate. For the feeding part, a microstrip feedline is printed on a small piece of PTFE dielectric substrate which is then connected to the ground plane. The microchip is connected to one end of the microstrip feed line while the other end is terminated with a meander-shaped printed inductor. The input impedance of the antenna, $Z_A = R_A + jX_A$, depends on the self-reactance of the feed line. By properly adjusting the distance between the feed line and the shorting plate and the width of the meander-shaped inductor, good matching between the antenna and the microchip impedance is obtained. The overall dimension of the antenna at the operating frequency of 915 MHz is 74.5 mm x 24.5 mm with 3 mm in height. The achieved impedance bandwidth of 3 dB return loss is 57 MHz which is sufficient to cover the 26 MHz bandwidth requirement in North America region. The drawbacks of the antenna lie on its complex feeding method and the use of multi-layer substrate which could increase the

31

total construction cost of the antenna. In addition, the required 100 MHz half-power impedance bandwidth for universal application is not met by the proposed antenna.
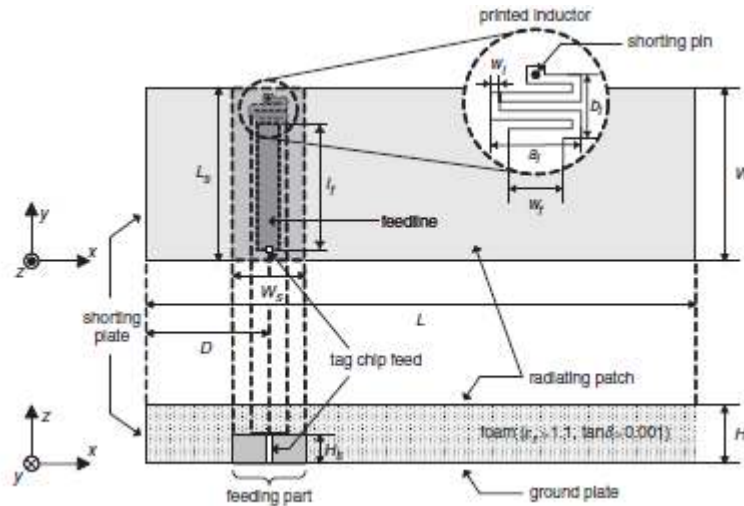
Figure 2.14: Patch antenna with proximity-coupled feed structure (Son et al., 2006)

A fork-shaped RFID antenna for mounting on metallic object was proposed byKim et al., (2007). The structure of the antenna is a folded dipole type with two parasitism patches which allows easy control of impedance matching with various microchip complex impedance values. The metal patch is printed on the FR-4 substrate with ε_r=4.6 with thickness of 3.2 mm. The geometry of the antenna is given in Figure 2.15. The resistance of the antenna was mainly controlled by changing the length of the parasitic patch or the distance between the feeding line and the parasitic patch while the reactance value was varied by changing the width of the radiating patch or the distance between the radiating patch and the ground patch. Parametric refinement was done to get good impedance matching between the antenna and the microstrip. The final dimension of the antenna is 120 mm x 30 mm x 3.2 mm. The measured read range when mounted on 200 x 200 mm and 400 x 400 mm metal plate

are 4.0 m and 3.8 m respectively. However, the antenna was intended to be operating within the 902 -928 MHz UHF RFID band and the thickness of the antenna at 3.2 mm can be further reduced to make it more conformable to the attached metallic objects.
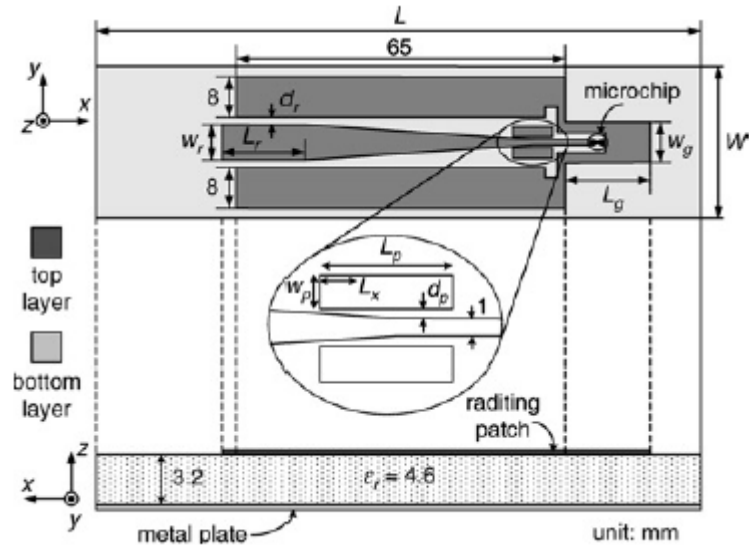
Figure 2.15: Fork-shaped patch antenna (Kim et al., 2007)

An attempt to increase the impedance bandwidth of the microstrip antenna was presented by Mo et al., (2008). By cutting a pair of U-slot at the non-radiating edge of the rectangular patch, a new adjacent resonant mode close to the fundamental mode of the radiating patch is excited to form a wide impedance bandwidth. The antenna was matched to the microchip through a thin microstrip line deep inset at the radiating edge where it is divided into inset feed line and short stub line. A via hole was used to connect the short stub line to the ground plane as shown in Figure 2.16. The impedance matching was done by adjusting the inset feed line and the distance between the microchip and the via hole. In order to match the new resonant mode excited by the U-slot to the microchip, the slot arm length, the distance between the slot and the patch edge as well as the slot width was tuned to achieve good impedance

matching. The measured half-power impedance bandwidth (return loss ≤ -3 dB) of the proposed antenna is 133 MHz (14.5%) which is able to cater the entire frequency range of UHF RFID band. The reported read range for the European band and North America band is between 2.8 m and 4.5 m. However, the use of via hole contributes to cross-layered structure hence require additional process such as drilling and soldering. Moreover, the operation of the antenna for the upper frequency range in UHF band (952-954 MHz) which is used by Japan and some of the South East Asian countries was not performed to verify it universal feature.
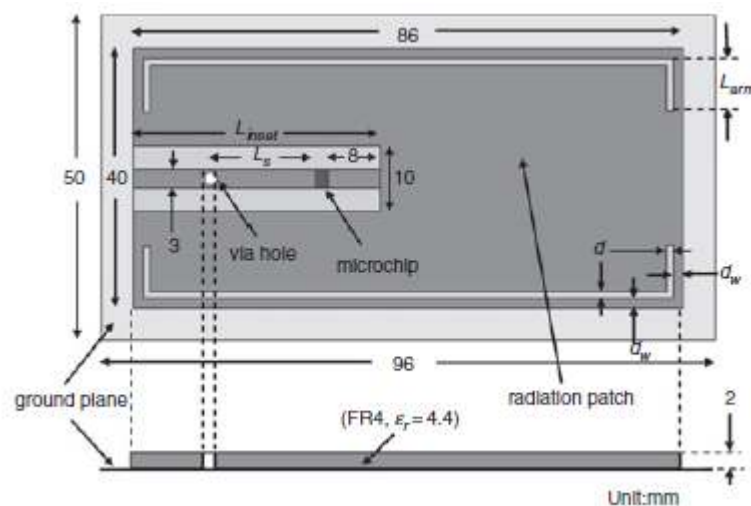
Figure 2.16: Rectangular patch antenna with U-slot (Mo et al., 2008)

Rao et al., (2008) presented a wideband tag antenna for mounting on metallic object as shown in Figure 2.17. The antenna structure consists of offset coplanar tapered feeding to feed the microchip and outer rectangular ring to form a virtual ground. Two resonant frequencies were excited to form a wideband performance. The lower frequency was produced by the outer rectangular ring while the upper frequency came from the inner radiator length. To present an inductive reactance to the

microchip, the patch trace that connects the outer and inner patch element was tapered. The design was fabricated with two form factors, which are 155 mm x 32 mm x 10 mm (large) and 79 mm x 31 mm x 10 mm (small). The read range measurement was carried out to evaluate the performance of the antenna where minimum read range of 7.62 m and 3.048 m throughout the UHF band were obtained for both types of tag when mounted on metallic surface. However, the size of the tag antenna is very thick.

(a)

(b)
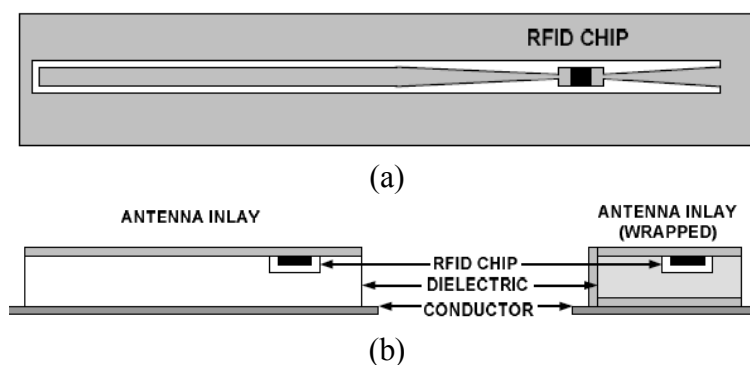
Figure 2.17: (a) Top view and (b) side view of wideband tag antenna (Rao et al., 2008)

A novel antenna with broadband characteristic incorporating T-matching network and double symmetrical radiating patches shorted to the ground plane shown in Figure 2.18 was presented by Xu et al., (2008). The FR-4 layer with ε_r=4.7 and a thickness of 1.6 mm is used as the antenna substrate. A foam layer was inserted between the FR-4 layer and the ground plane to fix its position. The conjugate matching was attained by adjusting the dimension and the width of the loop of the matching network. The measured half-power bandwidth is 118 MHz (12.9%) covering the whole frequency range of UHF band. Maximum read ranges of over 6.2 m and 2.9 m for free-space and on metal were reported. On the other hand, several disadvantages

of the design are thick structure at 4 mm in height due to use of two different types of substrates and the adoption of shorting plate which is challenging to implement.
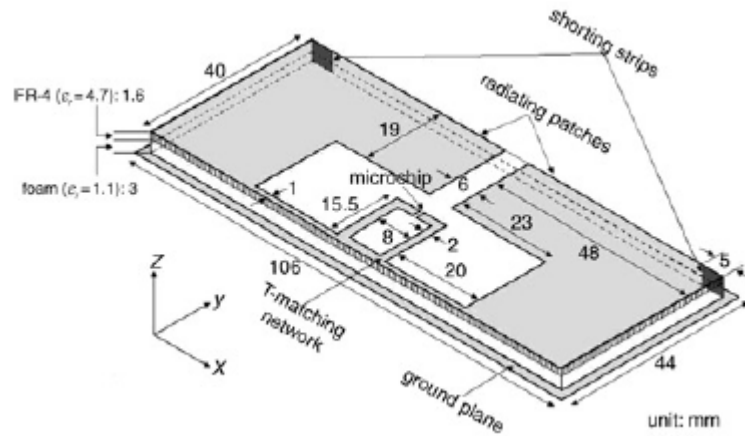
Figure 2.18: Patch antenna with double symmetrical radiating patches (Xu et al., 2008)

Chen (2009) presented a miniature RFID tag antenna consists of two rectangular patches electrically connected to the ground plane through vias. A non-contacting inter-conductive layer was placed between the patches and the ground plane to increase the capacitive reactance of the antenna which shifted the self-resonant frequency of the antenna to low frequency band. This enables high imaginary part of the antenna input impedance to be achieved with small size tag antenna. The configuration of the proposed antenna is described in Figure 2.19. The self-resonant frequency of the antenna was mainly affected by the length of the inter-conductive layer and the distance between two via hole. The optimal size of the antenna is 32 mm x 18 mm x 3.2 mm. The experimental results showed maximum read range of 1.5 m when placed on metal surface. The simulated and measured half-power bandwidth is reported to be 6.02 % (890-945 MHz) and 6.05 % (898-954 MHz) respectively. A

trade-off was made between the antenna size and the antenna impedance bandwidth. In addition, double layer substrate and the vias structure also increase the manufacturing process hence fabrication cost.
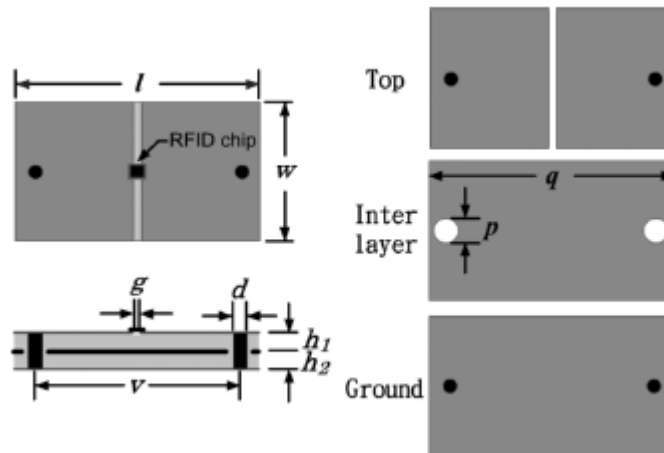
Figure 2.19: Miniature RFID tag antenna (Chen, 2009)

A compact tag antenna with broadband characteristic was proposed by Huang et al., (2009). Owing to the inset feed techniques and two thin asymmetrical slots deep inset into the center of the non-radiating edge, two resonant frequencies with similar radiation characteristic were excited to form wide impedance bandwidth. The impedance matching was performed using microstrip line inset feed at the radiating edge thus provide easy control of the antenna resistance impedance value to match that of the microchip. The other end of the feed line was shorted to the ground to present inductive reactance which would cancel the capacitive reactance of the microchip. Figure 2.20 shows the antenna configuration and the current path density for both of the resonant modes. The final dimension of the design is 65 mm x 65 mm x 2 mm. The measured half-power bandwidth is 115 MHz (855 MHz-970 MHz) with

37

read range of over 2 m. The limitations of the design are high cross polarization based on the current path density and the implementation of via hole.

(a)

(b)
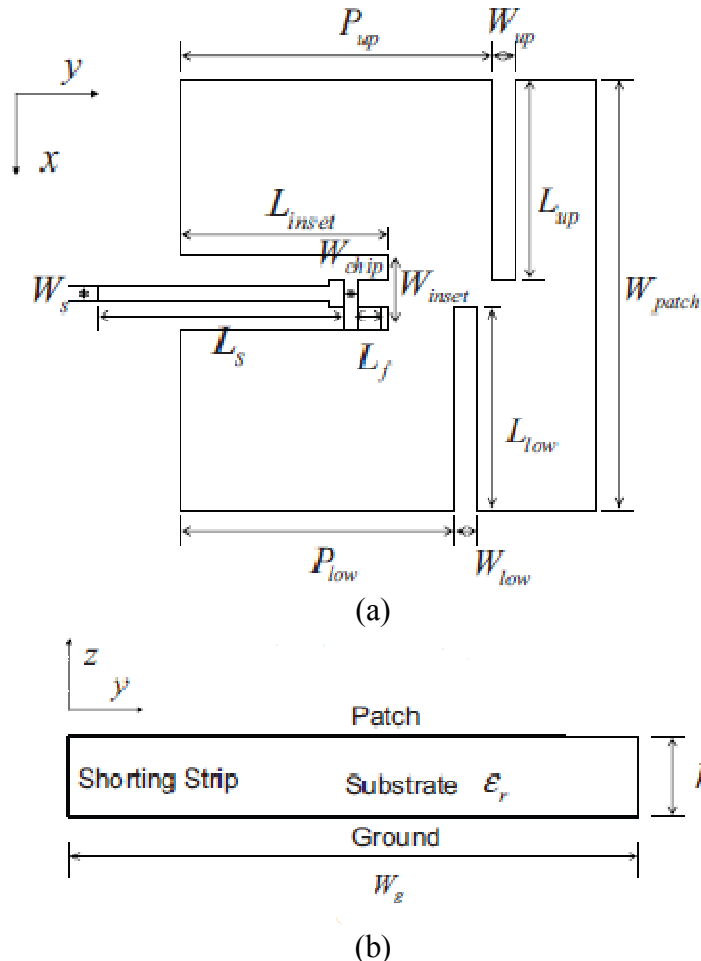
Figure 2.20: Structure of slotted patch antenna (a) top view (b) side view
(Huang et al., 2009)

Figure 2.21 shows the tag antenna proposed by Lu and Zheng (2011) which exhibits broadband feature for use on metal objects. It can be seen that two branch structures resembles half-wavelength dipole that excites two resonant modes close to each other. Two shorting pins were used to connect with the grounded metal plate to reduce the capacitive effect between the branch and the metal plate thus increasing the resonant frequency to higher frequency region. The total dimension of the antenna is

70 mm x 30 mm x 2.9 mm where two layers of FR-4 substrate and air were used. The half-power bandwidth is reported to be 112 MHz (12.5 %) with maximum read range of 5.2 m when operated on metal. The use of the antenna is limited by its complex structure with shorting pins and two layers substrate configuration which lead to increase manufacturing complexity and cost. Moreover, at about 3 mm, the antenna can be considered as thick and might not suitable to some of RFID applications.
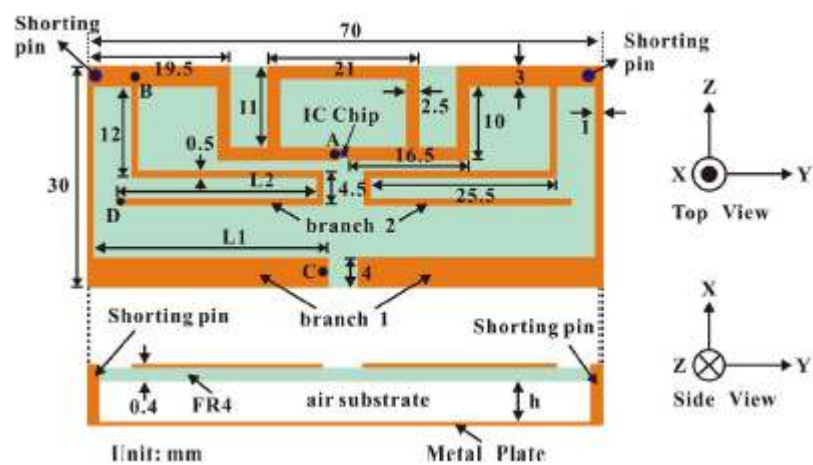
Figure 2.21: Metal tag antenna with dual branch strips (Lu and Zheng, 2011)

Son and Jeong (2011) presented wideband patch antenna using proximity coupled feed method. The feed line lies in parallel between the radiating patch and ground plane which is filled with foam of ε_r=1.1 and tan δ=0.001. The feedline was printed on small dielectric substrate and bonded on the ground plane. The microchip is connected to one end of the feed line and grounded by shorting via while the other opposite end of the feed line is connected to the ground also by shorting via. The input impedance of the antenna was controlled by varying the microstrip feed line length and the distance between tag chip feed and the radiating edge to present complex conjugate matching with that of microchip complex impedance as illustrated

in Figure 2.22. Both 53 MHz and 49 MHz simulated and measured half-power impedance bandwidth (return loss ≤ -3 dB)were reported with measured read range of 8.9 m when mounted on 200 x 200 m metal plate. However, the bandwidth of the antenna is not sufficient to cover the entire UHF band for worldwide operation and the feeding method employed is very difficult to fabricate.
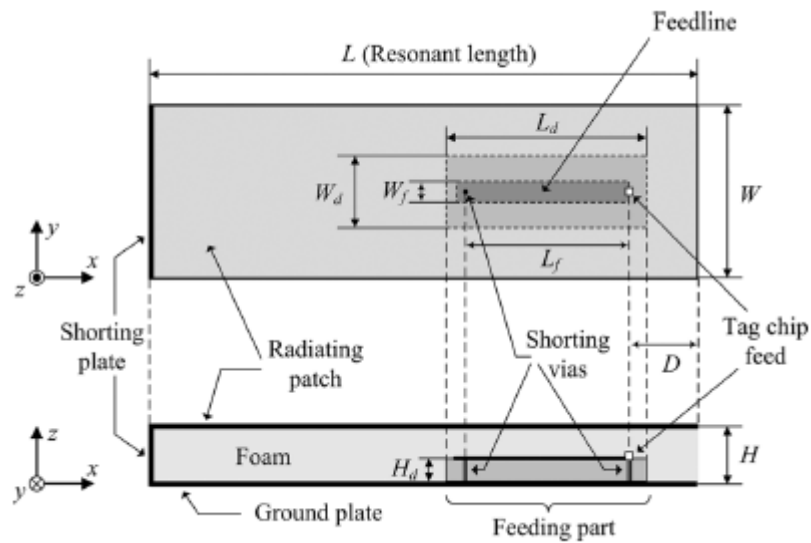
Figure 2.22: Microstrip patch antenna with proximity-coupled feed structure
(Son and Jeong, 2011)

A planar inverted-E patch antenna was presented by Lu and Hung (2010) incorporating three slit at the radiating edge of the patch to excite new resonant mode near the fundamental mode of the antenna to realize wide impedance bandwidth (return loss$\geq$3 dB) of 123 MHz (13.7%). The antenna geometry is given in Figure 2.23 with total dimension of 70 mm x 22 mm x 1.6 mm. The substrate used in the design is inexpensive FR-4 with ε_r=4.7 and tan δ=0.0245. The measured maximum read range of the antenna when mounted on three different metal plates with dimension of 75 x 22 mm, 150 x 150 mm and 300 x 300 mm are 1.5 m, 2.2 m and 2.5 m. Although the

antenna is thinner compared to most of the metal tag antenna presented, the structure still inherits the cross-layered configuration.
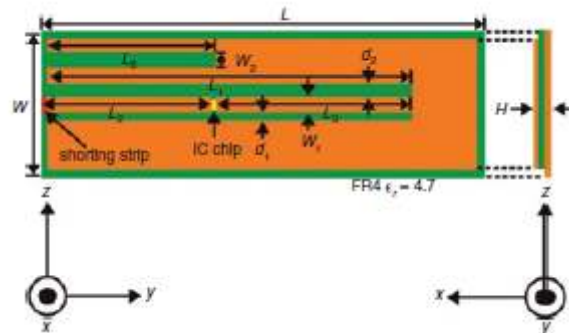
Figure 2.23: Inverted-E patch antenna (Lu and Hung, 2010)

A complete planar patch antenna was studied and proposed by several researchers (M. Eunni, 2007; Sahin and Deavours, 2009; Mo and Qin, 2010; Tashi et al., 2011). The antenna were realized without cross and multi-layered configuration which lead to ease of fabrication and reduced cost. The geometry of the antennas proposed by M. Eunni (2007) and Tashi et al., (2011) are illustrated in Figure 2.24 and 2.25 respectively. For impedance matching, nested slot and T-matching network were used. The simulated half power bandwidth of 5.1 MHz and 46 MHz were reported for both designs. However, both of the designs were narrowband.

Figure 2.24: Microstrip patch antenna with T-matching network
(M. Eunni, 2007)
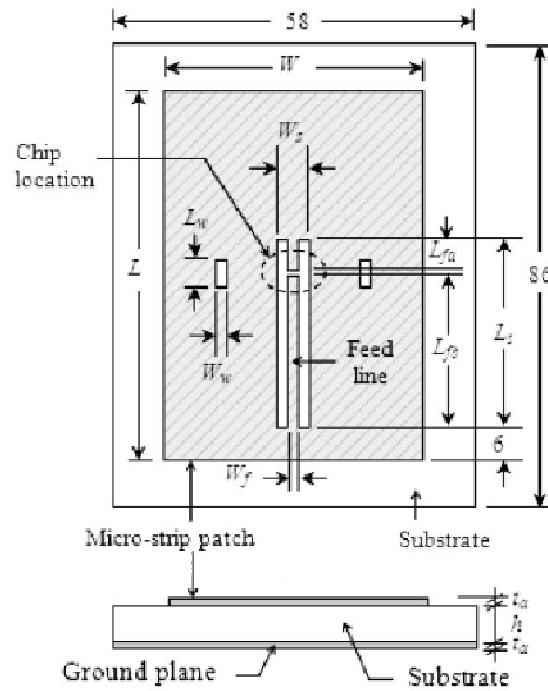
Figure 2.25: Rectangular patch antenna with nested slot (Tashi et al., 2011)

An embedded-feed type microstrip patch antenna was proposed to realize the conjugate impedance matching to the microchip (Cho et al., 2010) as shown in Figure 2.26. The overall size of the antenna is 82.6 x 49.8 x 1.6 mm^3. This planar microstrip patch antenna has an impedance bandwidth (return loss ≤ -3 dB) of 65 MHz covering from 885 MHz and 950 MHz which is enough to operate within the North America region. However, the required impedance bandwidth for universal use was not achieved. Mo and Qin (2010) had proposed a new method to feed patch antenna

without the need to have any connection between the patch and the ground plane by using an open stub feed line as illustrated in Figure 2.27. The advantage of the feeding method other than easy to fabricate is that the input impedance of the patch antenna can be match to almost any reactance value of the microchip it is connected and its simple antenna configuration. However, the limitation of the proposed patch antenna is its narrow bandwidth.
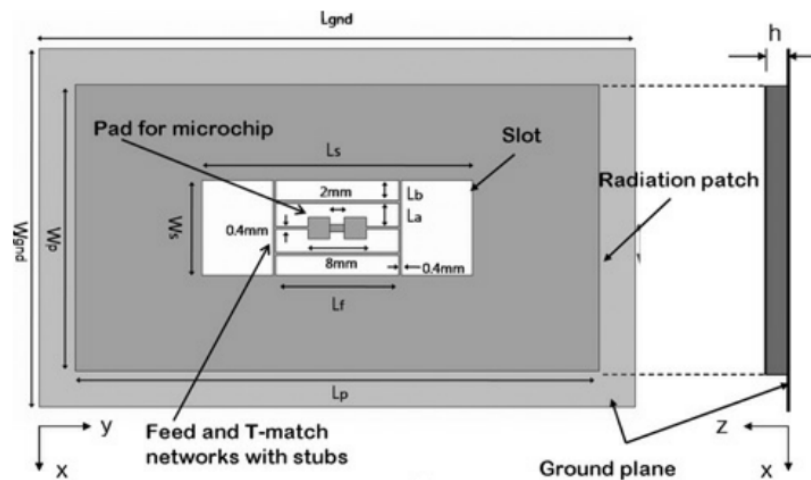
Figure 2.26: Planar embedded feed type microstrip patch antenna
(Cho et al., 2010)
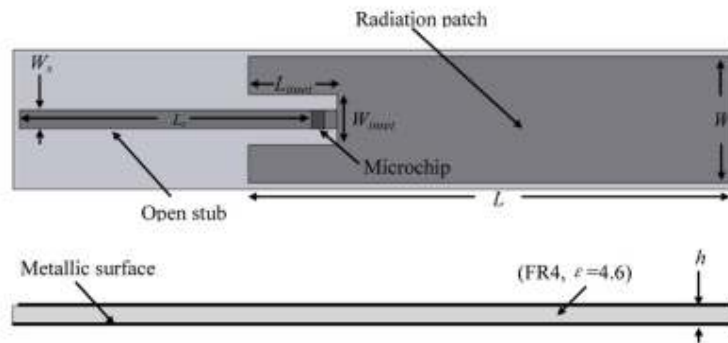
Figure 2.27: Patch antenna with open stub feed for metallic objects
(Mo and Qin, 2010)

The printed dipole antennas presented in Section 2.5.1 were not able to work when it was placed on the metallic surface due to the cancellation of the incoming electromagnetic wave by the field produced by the image current. Although numerous

efforts have been put to realize tag antenna that are able to function properly when mounted on metallic surface, most of them are either narrowband or have complicated structure.

These factors prohibit it from being used worldwide and make it difficult to fabricate. It is very important to reduce the fabrication complexity to reduce cost since tag is always intended to be mass produced. In this research, a new antenna design capable of mounting on metallic surface with wideband characteristic is proposed. A minimum half-power impedance bandwidth (return loss≤ -3 dB) of 100 MHz is aimed for worldwide operability. To greatly simplify the fabrication process and to reduce fabrication cost, a complete planar structure without cross or multi-layered configuration is aimed. The proposed tag antenna will also be compact in size as possible and low-profile making it conformable to the objects to be tagged. The list of antenna design for UHF RFID tag is summarized in Table 2.3.

Table 2.3
Summary of literature review on antenna design for UHF RFID tag

Previous works	Type of antenna	Advantages	Limitations
(Choi et al., 2009)	Label type printed modified folded dipole antenna	• Low cost • Flexible and conformable on curvy surface	• Suffers performance degradation when tagging metal objects
(Monti et al., 2010)	Label type printed dipole antenna	• Low cost • Flexible and conformable on curve surface • Broadband	• Suffers performance degradation when tagging metal objects
(Pongpaibool, 2009)	Label type printed meandered dipole antenna	• Low cost • Flexible and conformable on curve surface • Broadband	• Suffers performance degradation when tagging metal objects
(Cho et al., 2008)	Label type antenna backed by foam spacer	• Able to work on free space and metal object	• Narrow bandwidth

(Ukkonen et al., 2004)	Inverted-F antenna	• Can be used for tagging metal made object	• Complex antenna structure • Narrow impedance bandwidth
(Kwon and Lee, 2005)	Planar inverted-F antenna	• Designed for tagging metal object	• Have narrow bandwidth • Complex antenna configuration
(Choi et al., 2006)	Planar inverted-F antenna	• Designed for tagging metal objects • Compact in size	• Complex antenna structure which could increase the tag cost • Narrow bandwidth
(Son et al., 2006)	Folded patch antenna	• Designed for tagging metal objects	• The impedance bandwidth is below 100 MHz for universal operation • Have cross-layered structure thus hard to fabricate
(Kim et al., 2007)	Folded dipole tag antenna with parasitism patches	• Able to work on metal object	• Small impedance bandwidth
(Mo et al., 2008)	Patch antenna with pair of U-slot	• Designed for tagging metallic goods • Have half-power impedance bandwidth of 133 MHz	• Required via hole • Performance of the proposed antenna for upper region of UHF RFID band was not justified
(Rao et al., 2008)	Patch antenna	• Offers high read range	• Very bulky and thick structure at 10 mm
(Xu et al., 2008)	Tag antenna with double symmetrical patches	• Have half-power impedance bandwidth of 118 MHz	• Thick structure at 4.6 mm • Required two layered substrate
(Huang et al., 2009)	Patch antenna with two asymmetrical slots	• Compact in size • Offers half-power impedance bandwidth of 115 MHz	• Required via hole structure • High cross polarization is expected
(Lu and Zheng, 2011)	Planar tag antenna with dual-branch strips with shorting pins	• Offers half-power impedance bandwidth of 112 MHz	• Thick structure at 3 mm
(Lu and Zheng, 2011)	Planar inverted-E tag antenna	• Able to provide half-power bandwidth of 123 MHz	• Required via hole for impedance matching
(Mo and Qin, 2012)	Tunable compact planar inverted-F antenna	• Small size compared to microstrip patch antenna design	• Low impedance bandwidth

(Eunni et al., 2007)	Planar microstrip patch antenna	• Complete planar structure without cross and multi layered structure for ease of fabrication	• Narrow bandwidth
(Mo and Qin, 2010)	Planar patch antenna with open stub feed line	• Simple antenna design	• Narrow bandwidth
(Cho et al., 2010)	Microstrip patch antenna with embedded-feed	• Planar antenna design	• Narrow bandwidth for universal use
(Tashi et al., 2011)	Microstrip patch antenna	• Eliminate the need for electrical connection between the patch and the ground plane	• Designed for use in North America region only

2.6 SUMMARY

This chapter aims to provide a brief introduction to antenna technology and its performance parameters. An explanation with regards to RFID technology is also presented. The problem faced by commonly used label typed printed dipole antenna is studied. In addition, several types of antenna used for UHF RFID tag are discussed thoroughly where its advantages and limitations are highlighted. In the next chapter, design and simulation of the proposed tag antenna is discussed in detail.

CHAPTER THREE

PROPOSED TAG ANTENNA - DESIGN AND SIMULATION

3.1   INTRODUCTION

The chapter starts with a brief explanation of general design requirements of UHF RFID tag antenna followed by the design process involved. Then, detailed and specific design requirement of the proposed antenna according to the problem statements are described. The antenna design begins with initial determination of antenna parameter by using closed form expression derived from transmission line model. For impedance matching, an inductively coupled loop feed method is adopted. Several techniques to enhance the bandwidth of microstrip antenna are explored. A miniaturization technique is also performed to realize a more compact structure. The final design is simulated using electromagnetic field solver, Ansoft HFSS v13 based on the calculated theoretical parameter and further parametric refinement is carried out to produce the optimal antenna design.

3.2   GENERAL DESIGN REQUIREMENT OF RFID TAG

One important criteria in designing RFID tag is the size and form. Tag must be built in such a way that it can be attached or embedded to the objects to be tagged. The examples of the objects are cardboard boxes, airline baggage strips or identification cards. On the other hand, some applications require tag to be fit inside a printed label. This is intended for easy attachment of the tag to the tracked items. Since antenna

occupied most of the tag volume, the miniaturization of tag mainly depends on the success of reducing the size of the antenna. However, the reduction of antenna size is often accompanied with a trade-off between several antenna parameters. In most cases, the optimization of one parameter will lead to degradation of another. For example, if the antenna size is reduced, the effective aperture for transmitting and receiving EM signal is also reduced hence lead to lower gain and decrease in bandwidth compared to its initial form. As such, it is important to study the actual requirement demanded from RFID application in order to arrive at the optimal design.

Read range plays a very critical aspect in RFID since most of the applications require long read range. The operating frequency of the systems mainly determines the achievable maximum read range. However, there are few cases that require short read range for more secured communication especially those with sensitive data. The read range is also determined by other factors such as the allowable power radiated by RFID reader, material of tagged objects, its surrounding and tag orientation. The maximum power radiated by reader is controlled by the local regulatory body. The two most commonly allocated power radiated by reader in passive UHF system are 4 W effective isotropic radiated power (EIRP) and 2 W effective radiated power (ERP) which is equivalent to 3.3 EIRP (GS1, 2012). The performance of tag is affected when it is attached on different objects or when the tagged objects are placed in the vicinity of other objects. To solve this problem, most of the tag is tuned for optimal performance for mounting on particular objects. Also, to avoid the effects of the surrounding objects, the tag is designed to be less sensitive to its environment. Orientation of tag can also affect the read range of the system. Normally, a specific directivity pattern is required such as omni-directional or broadside radiation by RFID applications.

For RFID application, the overall cost of the tag must be made minimal. It is only possible when, the antenna structures, the type of material used and the IC must be low in cost. Typically, the conductor of the antenna is printed by using copper, aluminum and silver ink while the dielectrics are chosen from flexible polyester and rigid PCB substrates such as FR-4. This is one of the reasons for label type dipole antenna is widely used in RFID. To implement patch antenna for metallic application, the chosen substrate as well as the fabrication involved play a big role in dictating the overall cost. Reliability of the tag is also imperative to ensure the tag is able to sustain environmental effects such as temperature, stress, humidity. The overall tag design requirements are summarized below.

i) *Frequency band*: The frequency band of which the antenna operates depends on the regulations of the country the antenna is intended to work and type of application.

ii) *Cost*: RFID tag should be made as cheap as possible to ensure large scale implementation can be achieved. This is realized by simplifying the antenna constructions so as to reduce the number of process involved. Moreover, materials used must be chosen carefully by taking into consideration the main requirement of the application.

iii) *Gain*: The antenna should have acceptable gain to provide the minimum required read range.

iv) *Compatibility to the tagged objects*: It is observed that the performance of tag antenna is affected when it is attached to different objects. In order to mitigate this problem, antenna is usually designed for optimum performance when mounted on particular object.

v) *Size*: The size of the tag must be small enough relative to the tagged objects where the objects can take various sizes.

vi) *Orientation*: Based on the requirements, tag can be designed to have linear polarization or circular polarization.

3.3   OVERVIEW OF DESIGN PROCESS OF TAG ANTENNA

In designing the tag antenna particularly for passive UHF system, several design steps need to be followed. Figure 3.1 shows the flow of the tag antenna design process. First and foremost, a specific RFID application is determined. Then based on the application, system requirements are set. These requirements are analyzed to facilitate the design process of the tag antenna. Then, the parameters of the antenna are defined. Due to numerous IC for RFID tag are available in the market, a suitable one for the application must be chosen. In the next step, the material for the antenna construction is selected according to the design specification.

Each tag IC has its own complex impedance value which needs to be conjugate matched with the input impedance of tag antenna. The impedance of the tag IC can be measured experimentally by using vector network analyzer or the value stated in the tag IC datasheet can be used as reference.
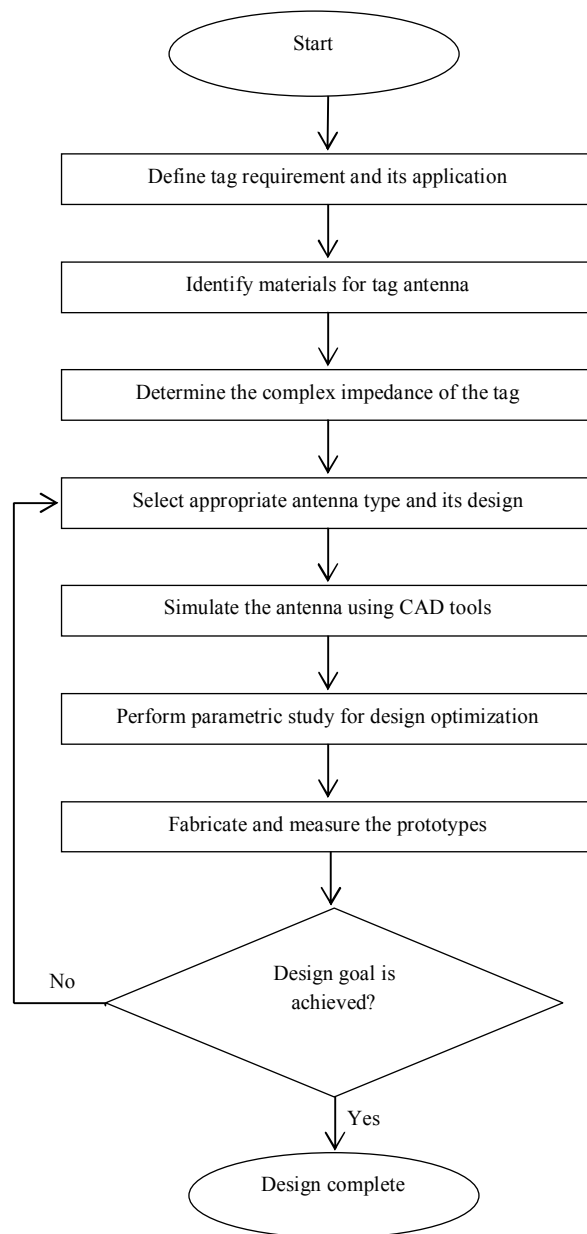
Figure 3.1: Design process of RFID tag antenna

In preliminary design stage, the approximate values of antenna parameters are calculated based on closed form expression derived from transmission line model. Afterward, parametric refinement and optimization is carried out until the optimal antenna design is met in the simulation. Since most of the antenna designs are too complicated for analytical solution, advanced electromagnetic modeling and

simulation tools are often used. For planar designs, MoM solution is able to give accurate result while for three dimensional structure; FEM and FDTD are of better choice. Once satisfactory simulation results are obtained, the antenna prototype is fabricated and their performance is evaluated. If the performance of the prototype antenna is in good agreement with the simulation, the antenna is ready to be used. In case of major disagreement between both results, further modification and optimization are required.

3.4 DESIGN REQUIREMENT OF THE PROPOSED TAG ANTENNA

Based on the problem statements, the design requirements of the proposed antenna are developed. In this research, the application of the RFID is specified for realizing the tag antenna that can work when mounting on metallic surface. These applications are normally encountered in supply chain sectors where shipment containers or boxes used to store good are made of metal. Since typical label-typed printed dipole antenna is severely affected when attached on the metal objects, a new antenna design is needed.

The UHF band systems operate within the frequency of 860 MHz to 960 MHz worldwide. Each country is operating at different UHF frequencies set forth by its local regulatory organization. So, the tracking and monitoring of the movement of tagged items as they are being transported from one country to another might pose a problem since most of the tag antennas are built to work only within a specific country or region it is intended to (Obsiye, 2009; Guha and Antar, 2011). Moreover, the operating frequency of a tag antenna might be slightly shifted due to fabrication inaccuracy. To mitigate these problems, a wideband patch antenna is chosen and the

antenna able to operate within the whole UHF frequency band is required. Hence, the proposed antenna is designed with wideband characteristic which enable it to function on universal scale. In addition, it is also able to provide fabrication tolerance. To greatly simplify the fabrication process so as to reduce cost, a complete planar structure with inexpensive substrate is chosen. Furthermore, the size and form factor of the tag must be compact to make it conformable with the tagged metallic objects. The design requirements of the tag antenna are summarized in Table 3.1.

Table 3.1
Summary of the design requirements of the proposed antenna

Design parameters	Requirement
Application	Mounting on metallic objects i.e. metal boxes or containers.
Type of antenna	Microstrip patch antenna.
Operating frequency	860 MHz-960 MHz for worldwide operation.
Bandwidth (measured at 3 dB return loss)	Should have minimum impedance bandwidth of 100 MHz (return loss ≤ -3 dB) (11.16%)
Minimum read range	Should provide least 1 m throughout the entire UHF band.
Form	The antenna should be completely planar in structure for ease of fabrication.
Size and thickness	Footprint must fit into a standard 15.24 mm × 10.16 mm label (Rao et al., 2005). Thickness should be less than 2 mm.
Fabrication difficulty	The proposed antenna should be able to be fabricated with ease for cost reduction.
Cost	FR-4 substrate is used due to its cheap cost.

3.5   DESIGN METHODS OF THE PROPOSED TAG ANTENNA

Based on general design flow and the design requirement of the tag antenna explained earlier, the design process for the proposed wideband RFID tag antenna is presented. To present a solution for metallic application, microstrip patch antenna is chosen since it needs a ground plane to operate and have been experimentally observed to work well when being mounted on metal objects. Moreover, it can also avoid the use of foam spacer which would make the tag bulky and not suitable most of the application. Several limitations of microstrip patch antenna for UHF RFID tag like low impedance bandwidth and costly fabrication process will be addressed in the proposed design.

3.5.1   Rectangular Patch Antenna

The antenna design begins with the selection of the rectangular as the initial shape of the radiating patch. Typical rectangular patch antenna offers versatility in terms of excited modes and it is easy to analyze. Initially, a single rectangular patch antenna with various width and length were designed and simulated to operate at different frequencies within the UHF band.

Based on transmission-line model, the length, L and effective width, W_e with operating frequency, f_0 of the rectangular patch antenna was calculated using equations (2-1), (2-2), (2.3) and (2.4) as depicted in Figure 3.2. The substrate of the antenna was chosen to be FR-4 whose ε_r=4.4 and $tan\,\delta$=0.02. The selection of the substrate is driven by its low cost and is readily available in the lab. Due to its low dielectric constant value, the Q-value of the antenna is reduced hence able to increase the bandwidth. The height, h of the dielectric as shown in Figure 3.2 was set to 1.6 mm to provide low-profile structure to the overall dimension of the antenna. It is

important to keep the thickness of the patch antenna as thin as possible to ensure conformability of the tag with the tagged items. However, very thin substrate will significantly reduce the gain of the patch antenna and should be chosen properly. Table 3.2 shows the calculated L and W_e of the rectangular patch antenna for several operating frequencies in UHF band.

(a)

(b)
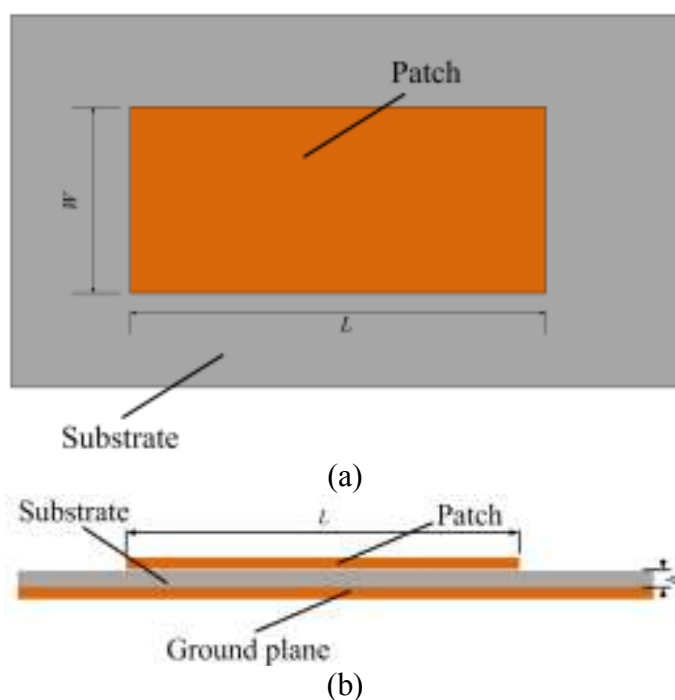
Figure 3.2: Rectangular patch antenna

Next, the antenna has been simulated by using EM solver, Ansoft HFSS which is based on finite element method to validate the calculated parameter. Table 3.3 displays the comparison between the simulated operating frequency and the calculated value of the patch dimensions. The design is again simulated based on the new parameter values and the results is listed Table 3.4.

Table 3.2

Theoretically calculated parameters values of various sizes rectangular patches

Operating frequency, f_0(MHz)	Width, W (mm)	ε_{reff}	ΔL(mm)	Length, L (mm)	L_e (mm)
866	105.412	4.263	0.715	82.396	83.886
915	99.767	4.257	0.745	77.967	79.456
954	95.689	4.251	0.744	74.767	76.256

Table 3.3

Comparison between calculated and simulated operating frequency of rectangular patch antenna

Width (W)	Length (L)	Calculated operating frequency (MHz)	Simulated operating frequency (MHz)
105.412	82.396	866	833.6
99.767	77.967	915	876.4
95.689	74.767	954	909.5

Table 3.4

Simulated operating frequency of rectangular patch antenna with reduced width

Width, W (mm)	Length, L (mm)	Simulated operating frequency (MHz)
10	85.25	867.3
10	81.8	914.6
10	77.85	954.3

3.5.2 Impedance Matching

This section describes one of the important methods in designing the UHF RFID tag antenna. Typically, an antenna is designed to match with the 50 Ω transmission line such as coaxial cable. However, because the tag antenna is intended to be connected to

the microchip, a totally different impedance values are presented by the microchip to the antenna input terminal. Due to inclusion of energy-storage stages in microchip, tag antenna needs to be conjugate matched to the capacitive impedance value of the microchip. Most of the available RFID ASICS (application-specific integrated circuits) exhibit an input reactance ranging from $-j50$ Ω to $-j400\Omega$. As for the resistance, the values are normally smaller lying between 5Ω to 50 Ω. As such, the antenna must present an inductive reactance to achieve conjugate matching with the tag microchip to ensure sufficient power is delivered to the microchip.

To investigate the effects of conjugate impedance matching to the performance of the RFID system, Friis free space equation is used to determine the maximum read range, d_{max} along the (θ, ϕ) as expressed in equation (2-19). It is evident that the read range can only be improved by increasing the tag antenna gain and providing good conjugate impedance matching since other parameters are fixed by local governing body.

Several methods for conjugate impedance matching have been summarized by Marrocco (2008). Some of the methods used are T-match network, microstrip line shorted to ground plane, inductively coupled feed loop, proximity coupling, nested slot and lumped components (Delzo, 2010). To present appropriate impedance value at the antenna input terminal where the antenna is connected to the microchip, a reference microchip value is needed. In this thesis, Alien Higgs-3 made by Alien Technology is used as reference IC (Alien, 2012). The impedance value of the chip at operating frequency of 915 MHz is $31-j211$ Ω. For maximum energy transfer, tag antenna must present conjugate value of $31+j211$ Ω at its input terminal. To achieve wideband characteristic, the main aim is to provide good impedance matching

throughout the entire UHF band. As such, 3 dB return loss of 100 MHz should suffice to guarantee satisfactory read range worldwide.

An inductively coupled feed loop initially proposed by Son and Pyo (2005) is used in the design to provide the needed inductive reactance to cancel out the capacitive reactance of the reference microchip. The loop is made of a small width patch and is coupled to the radiating element as shown in Appendix I along with its equivalent circuit diagram. The radiation of the antenna is mainly due to the radiating body and not from the loop.

The strength of the coupling is controlled by the shape of the loop and the distance between the loop and radiating body. The input impedance at the feed terminals is given by equation (3-1) (Son and Pyo, 2005)

$$Z_{in} = R_{in} + jX_{in} = Z_{loop} + \frac{(2\pi f M)^2}{Z_{rb}} \tag{3-1}$$

where Z_{rb} and Z_{loop} are the impedances of the radiating element and the feed loop respectively. M is the mutual inductance between them. The Z_{loop} and Z_{rb} near the resonant frequency can be derived from equations (3-2) and (3-3) (Son and Pyo, 2005)

$$Z_{loop} = j2\pi f L_{loop} \tag{3-2}$$

$$Z_{rb} = R_{rb} + jR_{rb,0}Q_{rb}\left(\frac{f}{f_0} - \frac{f_0}{f}\right) \tag{3-3}$$

where L_{loop} is the self-inductance of the loop, R_{rb} is the radiation resistance and Q_{rb} is the quality factor near the resonant frequency of the radiating patch. From equations

(3-1), (3-2) and (3-3) the resistance and the reactance values of Z_{in} can be expressed

as

$$R_{in} = \frac{(2\pi f M)^2}{R_{rb,0}} \frac{1}{1+u^2} \tag{3-4}$$

$$X_{in} = 2\pi f L_{loop} - \frac{(2\pi f M)^2}{R_{rb,0}} \frac{u}{1+u^2} \tag{3-5}$$

where u is given in equation (3-6)

$$u = Q_{rb} \left(\frac{f}{f_0} - \frac{f_0}{f} \right) \tag{3-6}$$

where at resonance, $f = f_0$, the input impedance of the antenna at the input terminal

can be calculated by equations (3-7) and (3-8)

$$R_{in,0} = R_{in,0}(f = f_0) = \frac{(2\pi f M)^2}{R_{rb,0}} \tag{3-7}$$

$$X_{in,0} = X_{in,0}(f = f_0) = 2\pi f L_{loop} \tag{3-8}$$

One of the advantages of the above method is that an individual adjustment can be

performed on resistance and reactance components of the antenna as shown in

equations (3-7) and (3-8). To implement the inductively feed loop method in the

design, a rectangular patch is coupled at one side of the loop as shown in Figure 3.3.
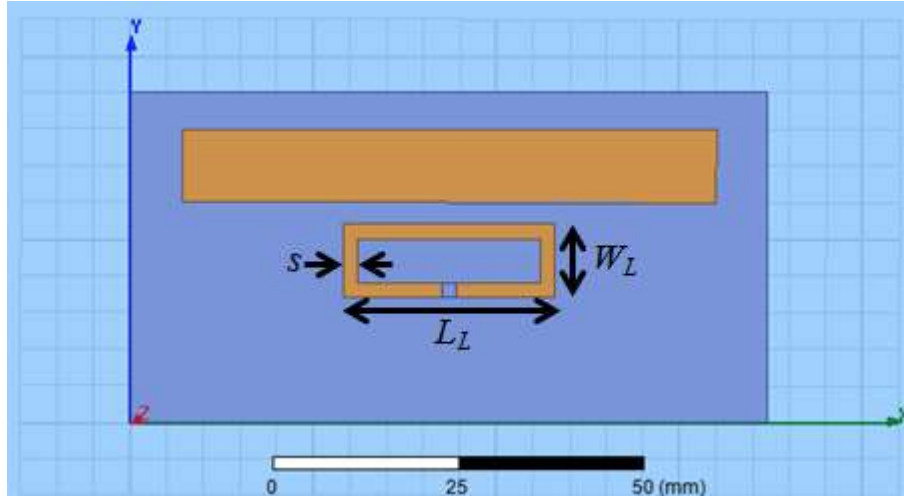
Figure 3.3: Rectangular patch with inductively coupled feed loop

The dimension of the feed loop can be approximated using equation (3-9) expressed below (Yang et al., 2011)

$$L_{loop} = 0.4(L_L + W_L) \ln\left[\frac{2L_L W_L}{s(L_L + W_L)}\right] (\mu H) \qquad (3\text{-}9)$$

where L_L, W_L, and s are the parameters of the loop strip in meter. The approximated dimension of the feed loop to present the required inductance value, $X_{in} = j212\ \Omega$ to conjugate match with the capacitive reactance of the microchip is given in Table 3.5.

Table 3.5
Parameter of the rectangular feed loop

Loop parameter	Value (mm)
L_L	35 mm
W_L	10 mm
s	2 mm

The simulated reactance of the antenna using the calculated dimension in Table 3.5 is shown in Figure 3.4. It is observed that the simulated reactance value is higher than the calculated value. To achieve the reactance around $+j212$ Ω to conjugate match with the referenced IC, parametric refinement has been carried out. To simplify the process, W_L and s value are fixed at 10 mm and 2 mm respectively while L_L are varied as shown in Figure 3.4. Based on the results, it is found that the required reactance value is obtained when the L_L is set to 28.5 mm.
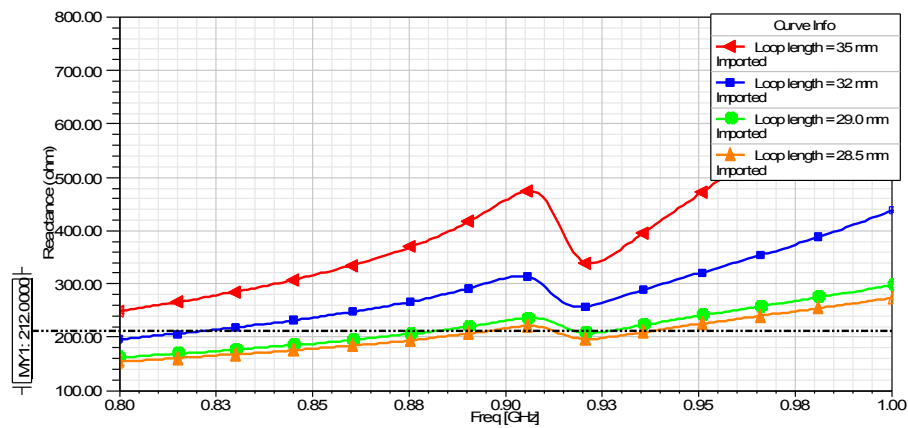
Figure 3.4: Simulated reactance values of different feed loop length, L_L

The antenna input resistance is then matched to the resistance of the microchip by varying the distance between the patches and the feed loop. The effect of the distance between the single patch and the feed loop is shown in Figure 3.5. It is observed that the smaller the distance between them, the higher the input resistance of the antenna whereas the resonant frequency remains unchanged.
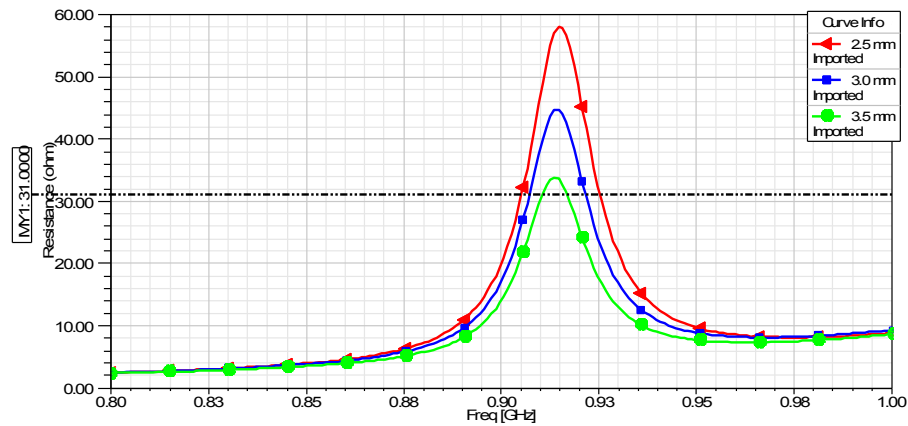
Figure 3.5: Effects of distance between feed loop and the rectangular patch on antenna input resistance

3.5.3 Impedance Bandwidth Enhancement

In order to increase the impedance bandwidth of the antenna, several methods can be utilized as briefly presented by (Kumar and Ray, 2003). Some of the broadbanding techniques involve modified shape patches, planar multi-resonator configurations and multi-layered (stacked) configurations. By modifying the shape of the radiating patch, several resonances close to each other can be simultaneously excited to form wide bandwidth. On the other hand, in planar multi-resonator, several resonators with different resonant frequency are used. The resonators are either gap-coupled or directly coupled to the feeding patch. For multi-layered configurations, several patches on different layers of dielectric are stacked on each other where they are coupled to the feeding line through electromagnetic coupling or by aperture coupling. Although high impedance bandwidth have been reported by employing this technique, its main disadvantages especially for RFID application are thick and complex structure which would lead to substantial production cost.

After evaluating the methods explained above, planar multi-resonator method is chosen due to its low-profile feature where all radiating elements reside at the same plane which suits the design requirement of the antenna. Instead of the initial design

of single rectangular patch antenna shown in Figure 3.3, two rectangular patches are formed by adding another rectangular patch antenna. The second one has slightly different length as illustrated in Figure 3.6 to excite two resonances that are close to each other to form wideband characteristic which will finally cover the entire UHF RFID band.
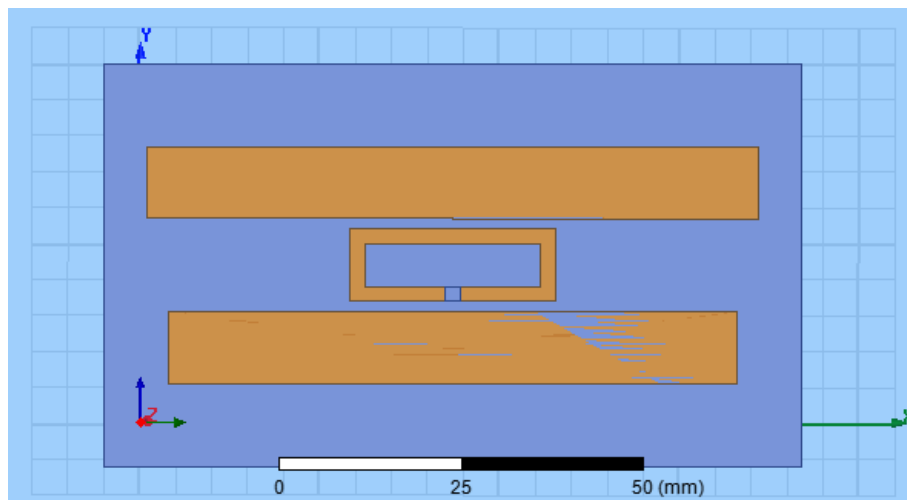
Figure 3.6: Two rectangular patches antenna

The half power impedance bandwidth of the single patch design is about 73.2 MHz as depicted in Figure 3.7 which is lower than the required 100 MHz. However, when two rectangular patches were used to excite two resonance frequencies, the resulted bandwidth is about 155 MHz which is well over the requirement as illustrated in Figure 3.8. It is clearly seen that by incorporating two patches at each side of the feed loop, two resonances were produced by the antenna to form wider bandwidth compared to single patch design.
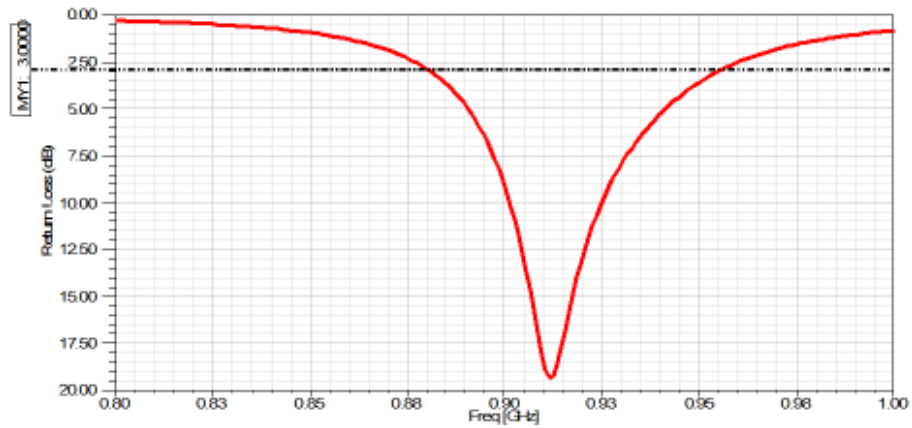
Figure 3.7: Return loss of single radiating patch antenna
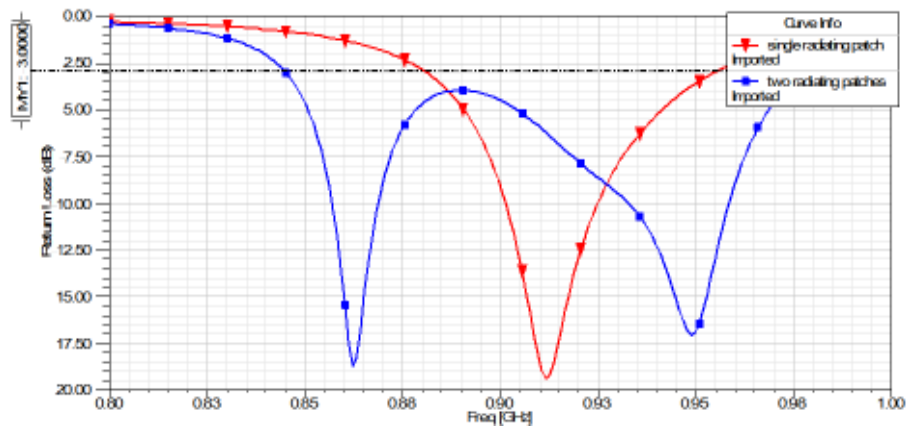
Figure 3.8: Return loss of single radiating patch antenna against two
radiating patches antenna

3.5.4 Antenna Miniaturization

In order to reduce the size of the antenna, several methods have been investigated and evaluated. The miniaturization process always involves trade-off between the bandwidth, efficiency, and size in the antenna design as depicted in Appendix B. As such, antenna design requirement are carefully evaluated to come out

with the best compromise between the related parameters to produce the optimal solution. Some of the miniaturization techniques for microstrip antenna have been summarized by Kumar and Ray (2003). A shorted λ/4 rectangular patch is one of the examples. Another way to reduce the size of the patch is by cutting slots on the radiating patch which will increase the electrical current path on the patch. Longer electrical current permits the antenna to resonate at the lower frequency than that of its original form thus making a miniaturization of the antenna possible. Two rectangular slots are embedded at one side of the patches for miniaturization as shown in Figure 3.10. By cutting the slots, the electrical current path of the patches is increased. The result of miniaturization of the antenna by cutting the rectangular slot at each of the patches shown in Figure 3.10 is illustrated in Figure 3.9.
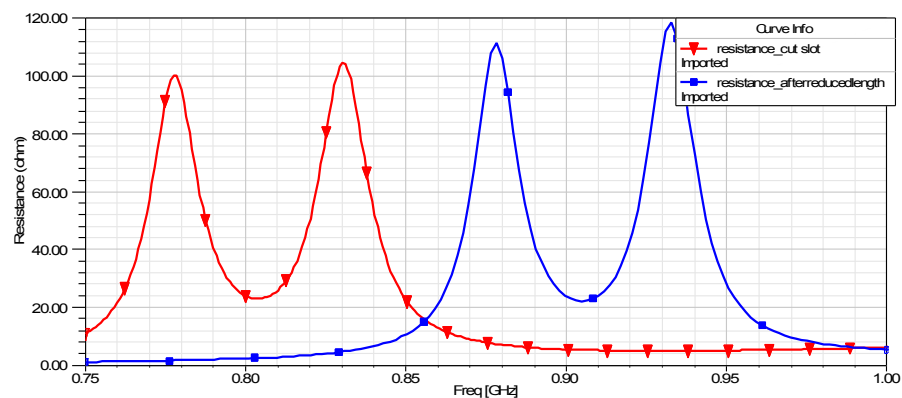
Figure 3.9: Reduced resonant frequencies due to embedded slot and after patch length reduction

Based on the result, the resonant frequencies are shifted to the lower frequencies region due to the increased of electrical current path on the radiating patches. Then, by properly reducing the length of the patches, operating frequencies of the antenna is shifted back towards the UHF frequency band (860 MHz-960 MHz) resulting in

smaller antenna size. In addition, a narrow slot is cut at both of the patches for easy tuning of the resonant frequencies without the need to change the value of the patches' width and length.

The optimal design of the proposed antenna is shown in Figure 3.10 and the final antenna parameter is tabulated in Table 3.6.
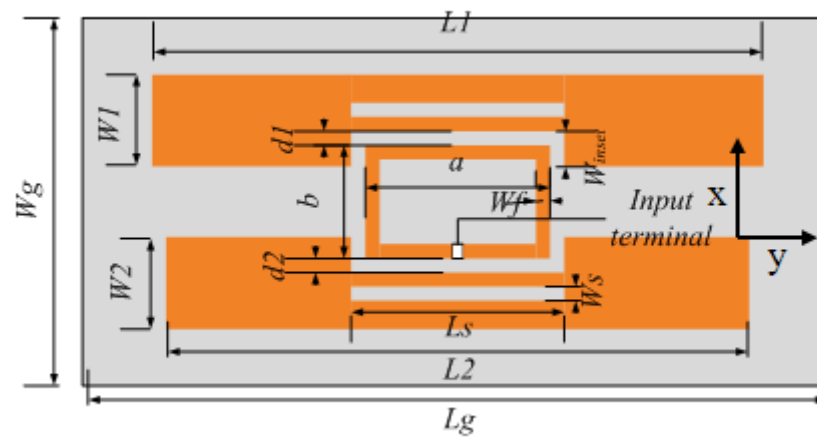
(a)
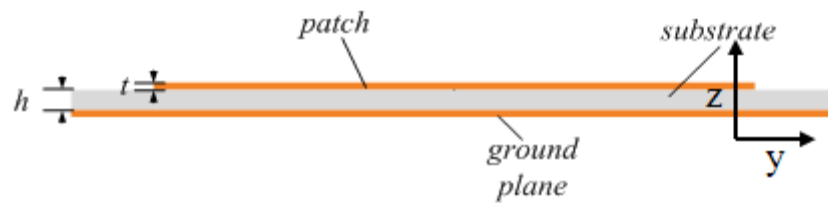
(b)

Figure 3.10: Final antenna design configuration. (a) Top view and (b) side view

Table 3.6

Optimal parameter values of the double resonance antenna

Parameter	Value (mm)
$W1$	10
$L1$	74
$W2$	10
$L2$	69
W_s	1
L_s	30
$d1$	2
$d2$	2
W_{inset}	4
t	0.0358
h	1.6
W_f	2
a	29
b	10
Ground plane and substrate	87 x 45

3.6   TRIPLE RESONANCE MICROSTRIP PATCH ANTENNA DESIGN

The antenna design described previously exhibit half power impedance bandwidth (return loss ≤ -3 dB) of 155 MHz. Theoretically, half of the power accepted by the antenna is lost due to impedance mismatch at the antenna input terminal. To further reduce the power lost, which in turn will increase the read range of the tag, three radiating element fed by modified triangle loop feed network instead of rectangular is proposed. It was anticipated that by having more resonances within 860 MHz to 960 MHz of UHF RFID operating band, the impedance bandwidth can be improved. The improvement is measured by using a more strict impedance bandwidth requirement which is 6 dB return loss. The 6 dB return loss reflects that 75% of accepted power is transferred to the microchip rather than only half of the power in 3 dB return loss measurement.

In order to excite the third radiating patch, the rectangular feed loop structure need to be changed. In this design, a triangle loop is proposed. Although they differ in shape, their function is the same which is to act as a matching structure and to excite the patches. Based on the literature, this is the first time the triangle loop feed shape is used in tag antenna. The dimension of the triangle loop feeding network can be approximated using equation (3-14)

$$
\begin{aligned}
L_{loop} \approx N^2 \frac{\mu_0 \mu_r}{2\pi} \Bigg[&2c \ln\left(\frac{2c}{0.5s}\right) \\
&+ b \ln\left(\frac{2c}{0.5s}\right) \\
&- 2(b+c) \sinh^{-1}\left(\frac{b^2}{\sqrt{4b^2c^2 - b^4}}\right) \\
&- 2c \sinh^{-1}\left(\frac{2c^2 - b^2}{\sqrt{4b^2c^2 - b^4}}\right) - (2c + b) \Bigg]
\end{aligned}
\tag{3-14}
$$

where b, c, and s are the dimension of the triangle loop. N, μ_0, and μ_r are number of turns of the loop, permeability of free space and effective permeability of the substrate respectively.

Due to the triangle shape of the feeding structure, three patches can be magnetically coupled to the feed loop. Figure 3.11 shows the geometry of the antenna. One rectangular patch and two meandered patches derived from rectangular form are chosen as the radiating element. Each of the patches is positioned at each side of the loop where it resonates at three different frequencies. The dimensions of the radiating patches and the feed loop were initially calculated based on equations (2-1), (2-2), (2-3), (2-4) and (3-14).

Table 3.7
Parameter of the triangle feed loop

Loop parameter	Value (mm)
b	34 mm
c	20 mm
s	2 mm

Table 3.7 shows the theoretical calculated dimension of the triangle feed loop. Based on calculation, the feed loop was then simulated. The parameter optimization was then performed to get the required reactance value of $j212$ Ω. To simplify the process, only the parameter c was varied and the result is shown in Figure 3.11. Based on the simulation results, the input reactance is around $j212$ Ω when c is 24 mm.
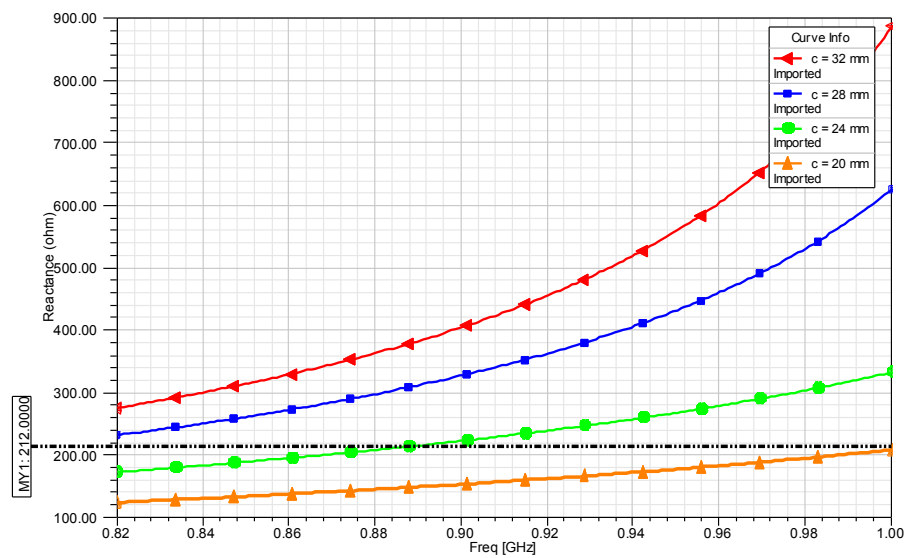
Figure 3.11: Simulated reactance values of triangle loop when varying parameter c.

As for the radiating patches, a thin rectangular patch of width 5 mm was first coupled to the bottom edge of the triangle. Then, the other two patches of width 5 mm and 7 mm were meandered in order to fit them at the other edge of the triangle. Based on the final geometry of the meandered patch, it is expected that only the horizontal segment will contribute to the far-field radiation while the vertical segment will cancel each other due to the opposite current patch. The parametric study and refinement were carried out to reach to the optimal design. The final antenna design illustrated in Figure 3.12 and the optimal parameter value of the antenna is given in Table 3.8.
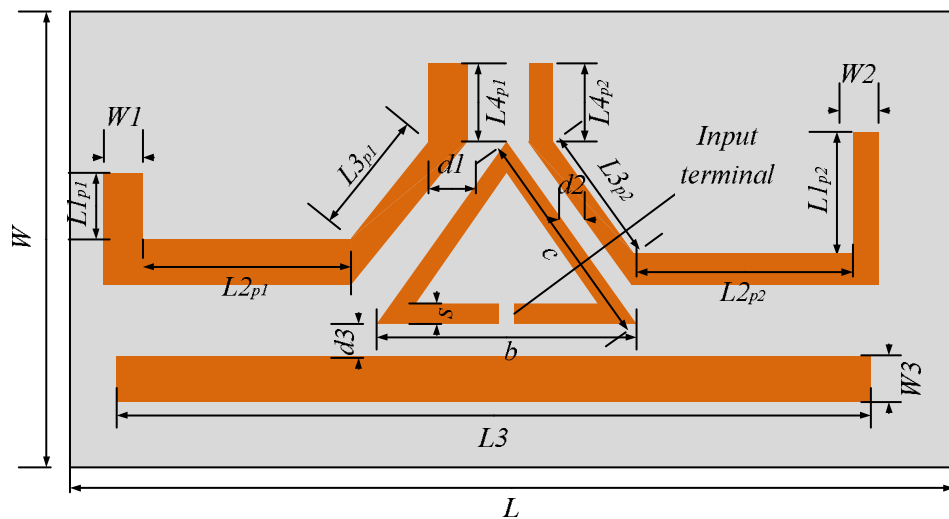
(a)
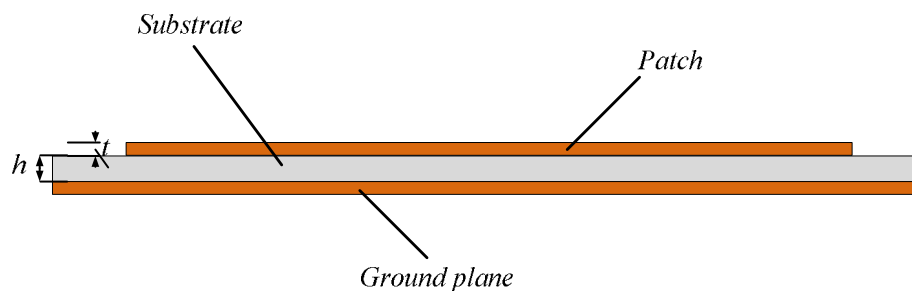
(b)

Figure 3.12: Geometry of the triple resonance antenna. (a) Top view and (b) side view

Table 3.8

Optimized design parameter of the triple resonance antenna

Parameter	Value (mm)
$W1$	7
$L1_{p1}$	10
$L2_{p1}$	37
$L3_{p1}$	10
$L4_{p1}$	12
$W2$	5
$L1_{p2}$	15
$L2_{p2}$	37
$L3_{p2}$	14
$L4_{p2}$	14
$W3$	5
$L3$	86
c	24
b	34
s	2
$d1$	2
$d2$	1
$d3$	2
t	0.0358
h	1.6
Ground plane and substrate	130 x 63

3.7   SUMMARY

This chapter has started with an overview of overall design requirement and the design process involved in designing tag antenna. Then, a detailed tag antenna design requirement for this research was developed according to the research problem. Based on the specification, an antenna model was developed. Impedance matching, bandwidth enhancements and miniaturization techniques were discussed and incorporated to the design so as to achieve the optimal antenna design. At each design stage, simulation results were supplemented to verify the calculated theoretical parameter and the deduction made.

CHAPTER FOUR

ANTENNA FABRICATION AND MEASUREMENT SETUP

4.1   INTRODUCTION

This chapter presents the fabrication and the measurement process of the proposed antenna. There are several techniques for microstrip antenna fabrication. The most commonly used method is using printed circuit board (PCB) technology. This simple and low cost method has been chosen in this research. All the processes involved for the antenna fabrication is explained in this chapter. Then, measurement setup to characterize the performance parameter of the antenna is briefly explained. Since differential signal is fed to the antenna, the impedance measurement setup for the proposed tag antenna is different than that of a typical microstrip antenna. Normally, a microstrip antenna is measured using a 50Ω single ended probe. However, this technique has been proven to be inaccurate for tag antenna measurement with balanced feed structure like the ones proposed in this research. As such, a measurement technique using differential probe technique is used instead.

4.2   FABRICATION PROCESS OF THE ANTENNA

There are various techniques available for microstrip antenna fabrication (Huie, 2002; Pan et al., 2005; Sood et al., 2008). First, a mask is created by drawing the geometrical pattern of the antenna using Eagle software as shown in Figure 4.1. Then, the antenna pattern is printed on a special plastic using laser printer. A double sided copper clad FR-4 substrate is cut based on the actual dimension of the simulated antenna using

CNC milling machine as illustrated in Figure 4.2 and then cleaned to remove the surface impurities by using organic solvents. The substrate is dried to prepare it for negative photo resist (NPR). To precisely transfer the mask pattern onto the substrate, a photolithography technique is used. The substrate is coated at both sides with film using laminating machine at 110 °C. After that, the mask is put on top of the laminated substrate and exposed to ultra violet (UV) light in UV exposure unit for 25 second.
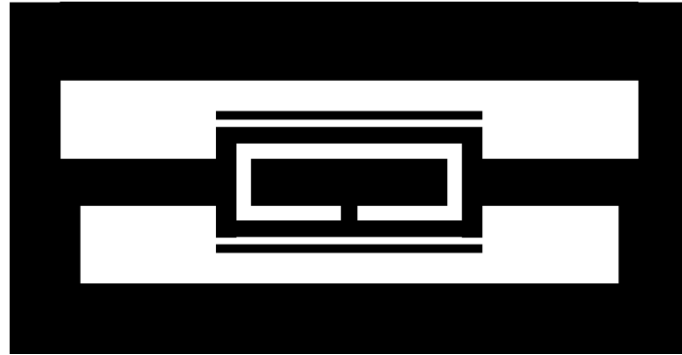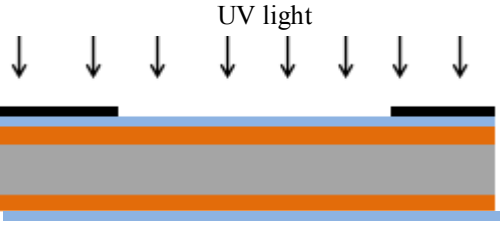
Figure 4.1: Mask of the antenna

The exposed substrate is then developed in 20% K(OH) solution to transfer the mask image onto the surface of the copper. The exposed unwanted copper traces are etched out in solution of FeCl$_3$. Finally, the etched copper pattern is rinsed in DI water and dried. The fabrication steps are graphically illustrated in Figure 4.3. The prototypes of the proposed antenna are shown in Figure 4.4 and Figure 4.5 respectively.

Figure 4.2: Cutting process of the FR-4 substrate using CNC milling machine

Double copper clad FR-4 substrate	
Negative photoresist coated substrate	
Exposing to UV light	
Developing in K(OH)	

Etching in FeCl₃	
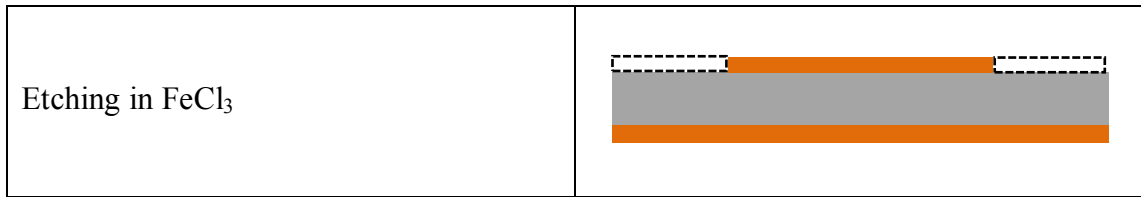
▬ (orange)	Copper
▬ (gray)	Substrate
▬ (blue)	Photoresist
▬ (black)	Mask
⬚ (dashed)	Remove Copper

Figure 4.3: Fabrication steps of proposed antenna

Figure 4.4: Prototype of double resonance patch antenna

Figure 4.5: Prototype of triple resonance patch antenna

4.3   ANTENNA MEASUREMENT

To evaluate the performance of the prototype antenna, the antenna input impedance and its radiation pattern are measured. The measured results have been compared with the simulated results obtained for verification; results are shown in Chapter 5. To perform these two measurements, a proper and suitable test setup is needed. The first measurement conducted is to characterize the input impedance of the tag antenna. It is important to ensure accurate results are obtained since tag performance relies heavily on good impedance matching between the tag antenna and the IC. Secondly, the radiation pattern of the prototype is measured in an anechoic chamber.

4.3.1 Impedance Characterization Methodology

Impedance measurement of RFID tag antenna with high accuracy is very challenging and has been a subject of discussion among RFID practitioners. Previously, small antenna measurements are based on 50 Ω single ended probe system. However, this method cannot be directly applied to RFID tag antenna since tag antennas are being

fed differently from those antennas due to balanced connection to the microchip. As shown in Figure 4.6, a tag antenna is designed to be connected to an RFID strap where it has two identical pads that transmit power into tag antenna (Qing et al., 2009). Due to the symmetrical feed structure, most of tag antennas are considered as balanced antennas.
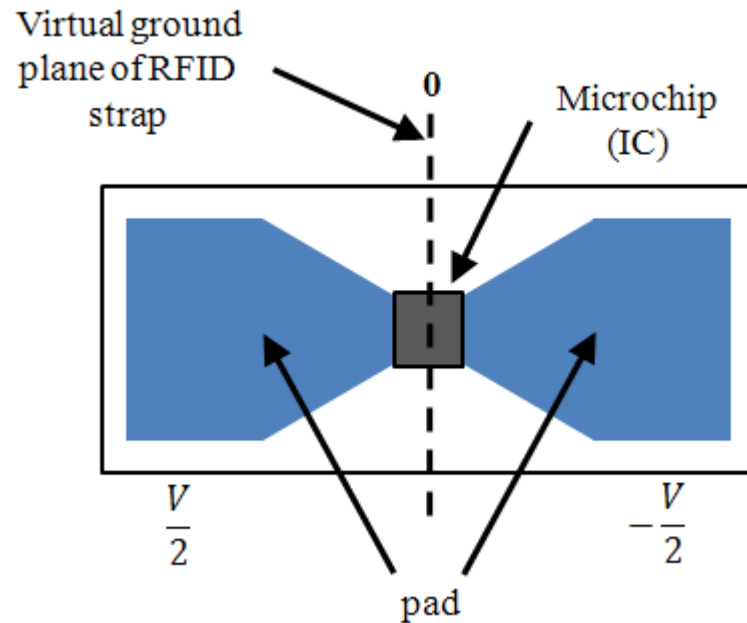
Figure 4.6: Typical diagram of an RFID strap

4.3.1.1 Differential Probe Technique

To present a highly accurate impedance measurement for tag antenna for both balanced and unbalanced tag antenna, a differential probe derived from well-known two-port network model was proposed by Kuo et al., (2008), Qing et al., (2009) and Yao et al., (2011).

To probe the antenna, a text fixture as shown in Figure 4.7 is constructed by using two semi-rigid coaxial cables with diameter of outer conductor of 2.2 mm and length of 10 mm. Both semi rigid cables are soldered together at the outer conductor

which serves as a ground. Two SMA connectors are connected to one end of the cable pair while at the other end is left open with inner conductor extended outward to form the tips. The tips are used to connect to the input terminal of the antenna under test. Then, the test fixture is connected to two test cables from the two ports of the vector network analyzer.

Due to the use of the test fixture, its impact to the impedance measurements needs to be accounted to achieve accurate results. To remove the effects of the test fixture, port extension method is performed as explained below.

Figure 4.7: Test fixture prototype

4.3.1.2 Port Extension Method

In order to remove the effect of the test fixture from the antenna measurement, port extension technique was used by shifting the calibration plane from the end of test cable to the tips of the test fixture as shown in Figure 4.8. The effects of test fixture is eliminated without having to perform the tedious post processing step as required by de-embedding method presented by Palmer and Rooyen (2006). Hence, this method provides a quick and simple way compared to method mentioned above.
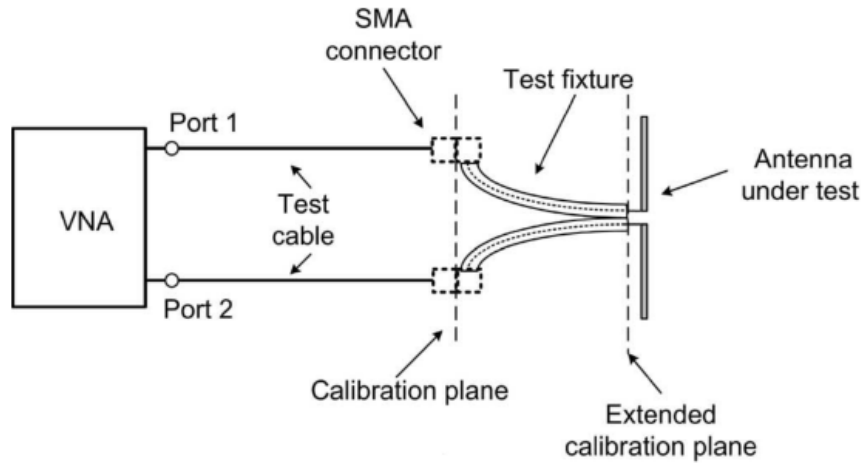
Figure 4.8: Shifting of the calibration plane to the tips of the test fixture

To perform the impedance measurement of the prototyped antenna, a place with minimum environment reflection is chosen. The measurement is then conducted through the following steps.

Step 1: Standard vector network analyzer (VNA) parameters setting and calibration is carried out using Short-Open-Load (SOL) method.

Step 2: The effects of test fixture and cable loss are removed by using port extension method for quick and simple process. First, the test fixture is connected to the test cables. The fixture must be either open or short circuited when performing the port extension procedure. In this case, a short-circuited configuration is performed by soldering the tips of the fixture and the outer conductors of the coaxial cables as illustrated in Figure 4.9. The measured impedance with short-circuited test fixture over 0.8-1.1 GHz before and after port extension is shown in Appendix C.

Step 3:   The input terminal of the proposed antenna is connected to the test

fixture to measure the standard S-parameters illustrated in Figure 4.10

Step 4:   The impedance of the antenna is then calculated by using equation

(4.1) below (Qing et al., 2009)

$$Z_d = \frac{2Z_0(1 - S_{11}S_{22} + S_{12}S_{21} - S_{12} - S_{21})}{(1 - S_{11})(1 - S_{22}) - S_{21}S_{12}}$$ (4-1)

Figure 4.9: Short-circuited configuration of the test fixture
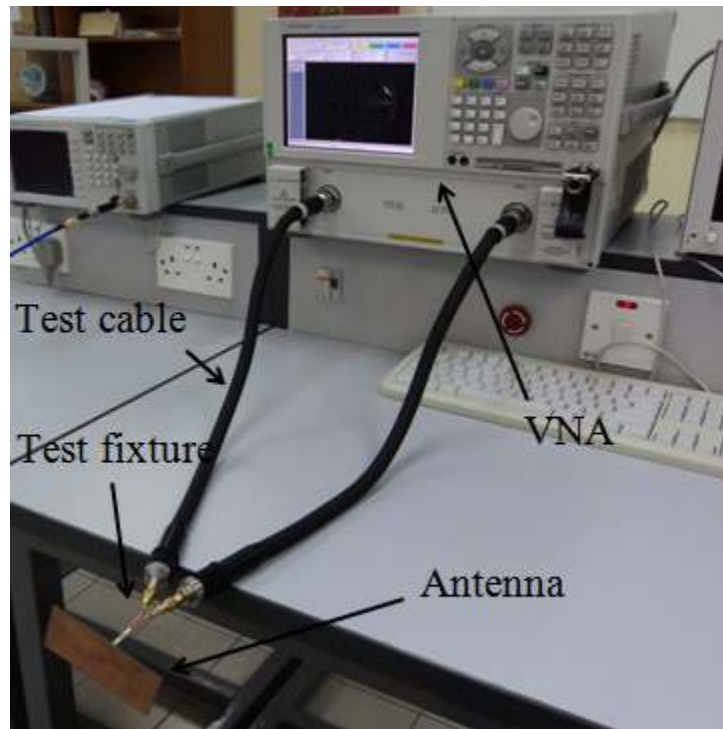
Figure 4.10: Impedance measurement setup using Agilent N5230A vector network

analyzer

4.3.2 Radiation Pattern Measurement

To further analyze and evaluate the performance of an antenna, radiation pattern measurement is carried out. The measurement results obtained from this procedure is used to validate the simulation results achieved in the designing process. The far field radiation pattern measurement was done in an anechoic chamber in Universiti Kebangsaan Malaysia (UKM). Several test equipment were used to perform the measurement as listed below.

i) A transmitter and source antenna with known radiation pattern.

ii) A receiver system to determine the amount of power received by the tag antenna.

iii) A positioning system to rotate the test antenna relative to the source antenna. This will measure the radiation pattern of the test antenna as a function of angle.

The position of the test antenna must be in the far-field so that the electromagnetic field incident on it is a plane wave.

4.4.   SUMMARY

This chapter has presented the fabrication method of the antenna and the measurement setup used to measure the antenna characteristics. The proposed antennas were fabricated using photolithography and etching technique employing negative photo resist. For antenna impedance measurement, differential probe technique was used to provide accurate results. A port extension method was then carried out to remove the test fixture effect on the antenna measurement to improve its accuracy. Moreover, the radiation pattern of the antenna was performed in anechoic chamber.

CHAPTER FIVE

RESULTS AND DISCUSSION

5.1   INTRODUCTION

This chapter presents and compares the simulation and measurement results of the proposed antenna for verification purpose. The antennas are evaluated based on its impedance bandwidth as well as its radiation characteristic particularly its peak gain performance. Analysis on the difference between the simulated and measured results is carried out to find the actual reasons of its discrepancies.   Finally, the proposed antennas are compared with other similar existing antenna for justification of its performance especially in term of impedance bandwidth.

5.2   SIMULATED ELECTRICAL CURRENT PATH OF THE ANTENNA

The simulated electrical current paths of the antennas are shown in Figure 5.1 and Figure 5.2. It can be seen that the first antenna resonates at two different frequencies which are 883 MHz and 953 MHz. The first resonance came from the top patch while the second resonance was attributed to the bottom patch. As for the second antenna, three resonant frequencies are excited at 882 MHz, 908 MHz and 949 MHz. These three resonances were excited by the three radiating patches of the antenna at three different frequencies. The reason for the radiating patches to resonate at different frequency are because of its overall length differs from one another. The patches were designed to have a length of around half of its wavelength of which the radiating element resonates. Based on the direction of the current path on the antenna, it is clear that both of the antenna exhibits horizontal linear polarization.
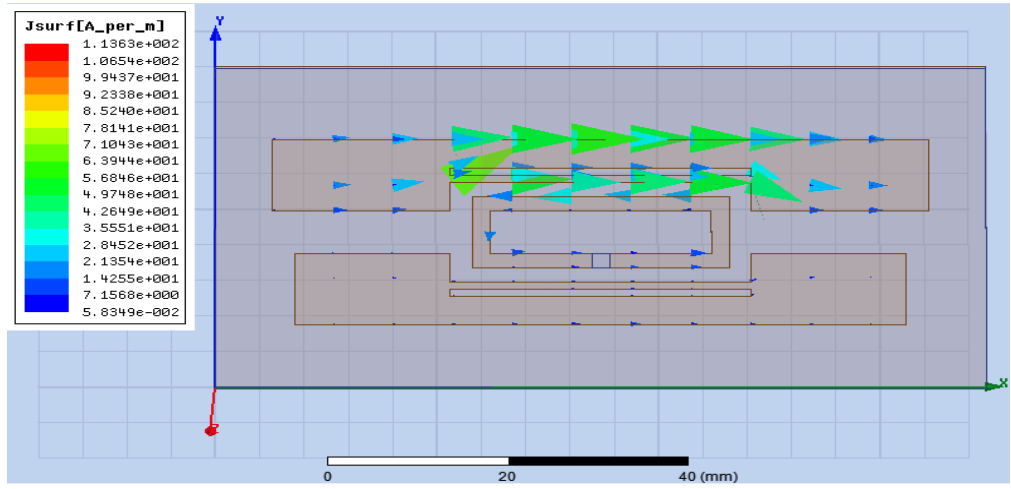
(a)
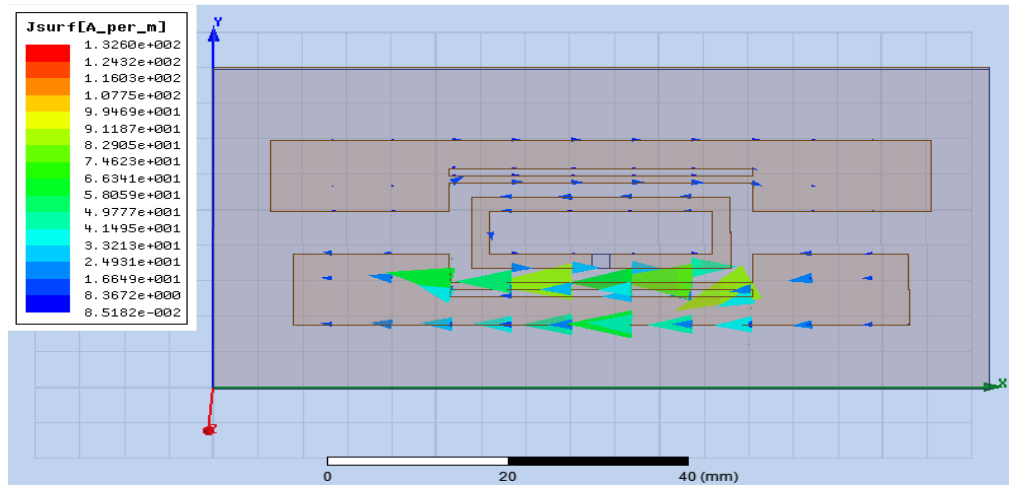
(b)

Figure 5.1: Surface electrical current density of the antenna at two resonant frequencies. (a) At 883 MHz and (b) 953 MHz

(a)

(b)

85
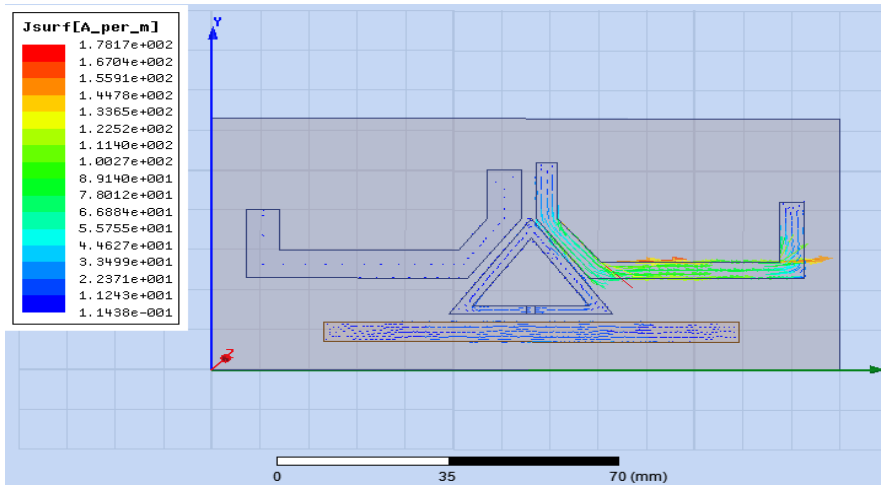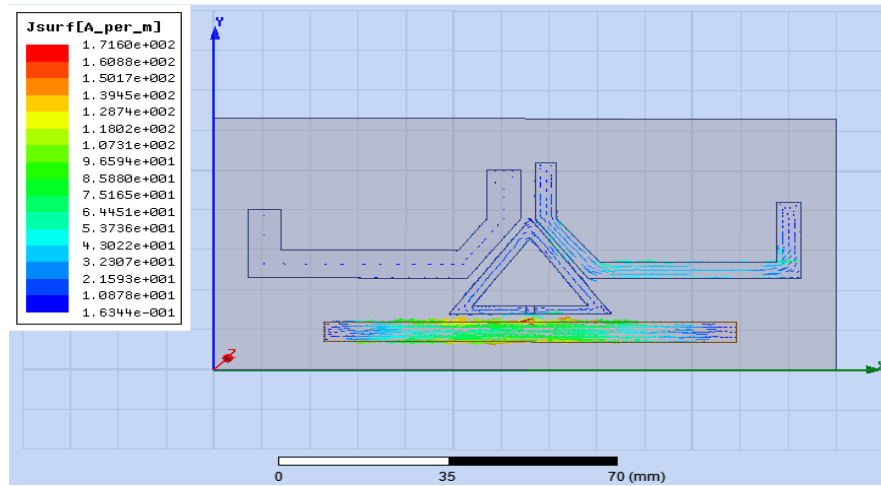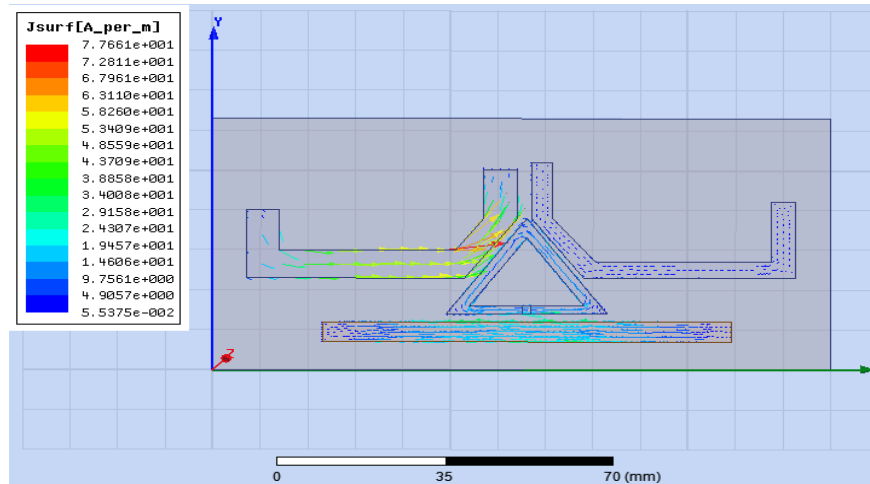
(c)

Figure 5.2: Surface current distribution at three resonant frequencies. (a) 882 MHz, (b) 908 MHz and (c) 949 MHz

5.3   EFFECTS   OF   METALLIC   SURFACE   ON   THE   ANTENNA   PERFORMANCE

The performance of the proposed antenna when mounted on metallic surface has been carried out both in simulation and experiment. In the simulation, the antenna was simulated on a reference metal plane of size 200×200 mm^2 as shown in Figure 5.3. Meanwhile, the prototype antennas were mounted on metal sheet of size 200×200 mm^2 during antenna impedance measurement as depicted in Figure 5.4. The size of the plate was chosen to represent the actual surface and size of the metal box the tag is designed to use.

86
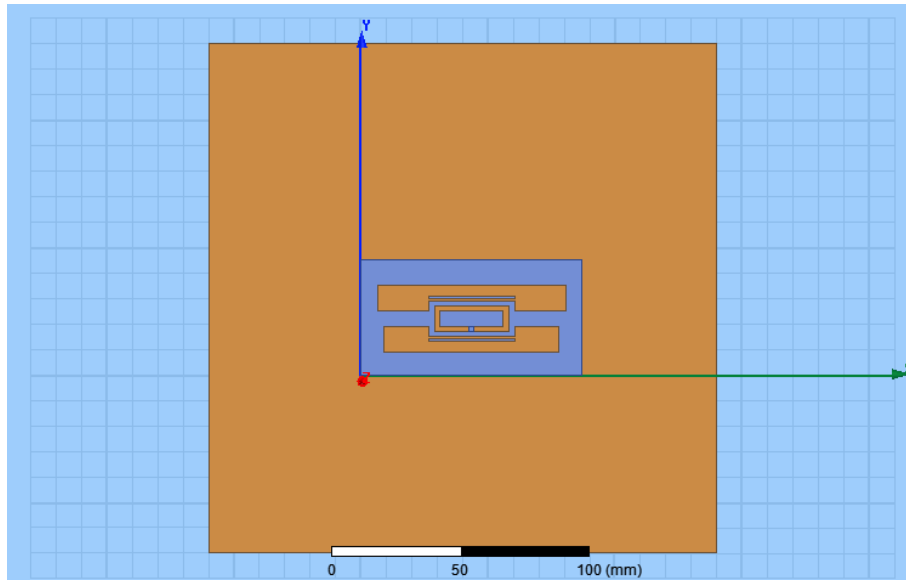
Figure 5.3: Simulation of the antenna when mounted on metal plate

Figure 5.4: Measuring of the antenna input impedance when mounting on metal plate

5.4   IMPEDANCE BANDWIDTH OF THE ANTENNA

As explained in Chapter 4, the impedance of the antenna has been measured using two-port vector network analyzer. The measured S-parameters are used to extract the impedance as shown in equation (4-1).

5.4.1 Double Resonance Microstrip Patch Antenna

The measured S-parameters for the first antenna are shown in Figure 5.5 and its impedance is calculated. The use of the differential probe method to measure the antenna input impedance has produced four S-parameter values which are S_{11}, S_{12}, S_{21} and S_{22}. Unlike single ended probe method that is normally use to probe patch antenna, the impedance of the proposed antenna cannot be directly obtained from the VNA. The impedance of the antenna needs to be extracted from the measured S-parameter by using equation (4.1). In addition, the plot between S_{11} and S_{22} as well as for S_{12} and S_{21} are almost identical because of the symmetrical structure of the antenna.

The effect of the metallic plate on the proposed antenna was recorded in both simulation and experiment. The input impedance for both simulation and measurement are shown in Figure 5.6 for comparison.
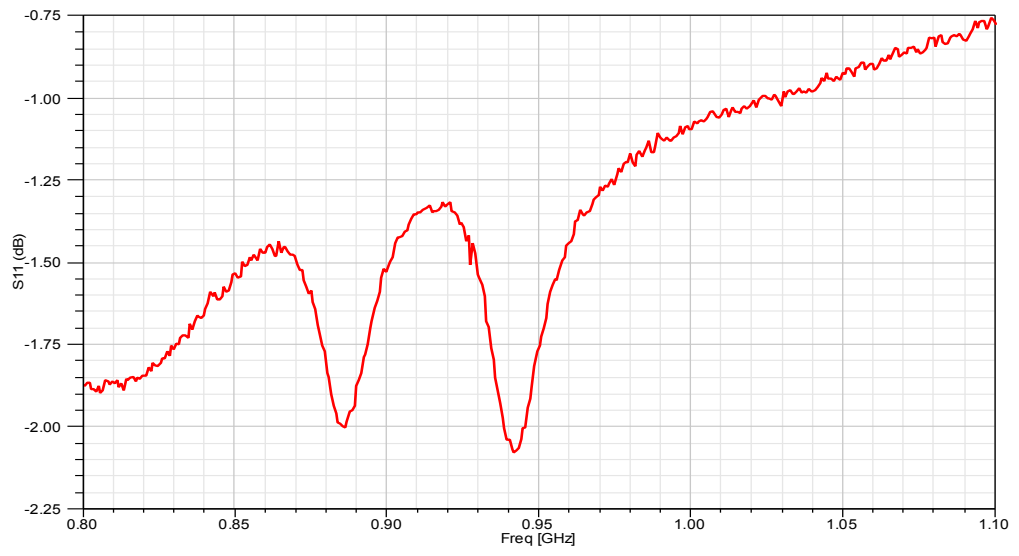
(a)
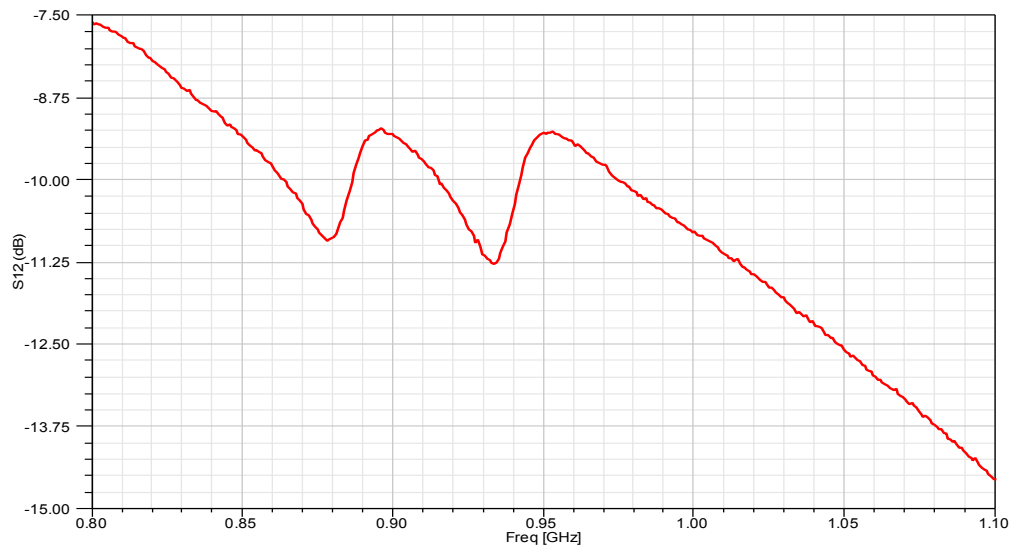
(b)
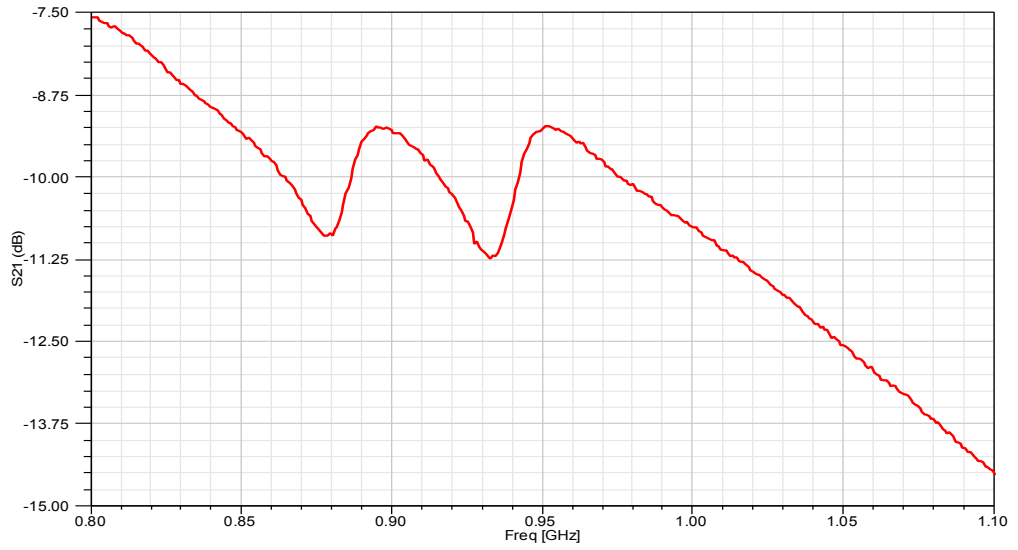
(c)

(d)

Figure 5.5: (a) S_{11}, (b) S_{12}, (c) S_{21} and (d) S_{22} parameters of the double resonance patch antenna.
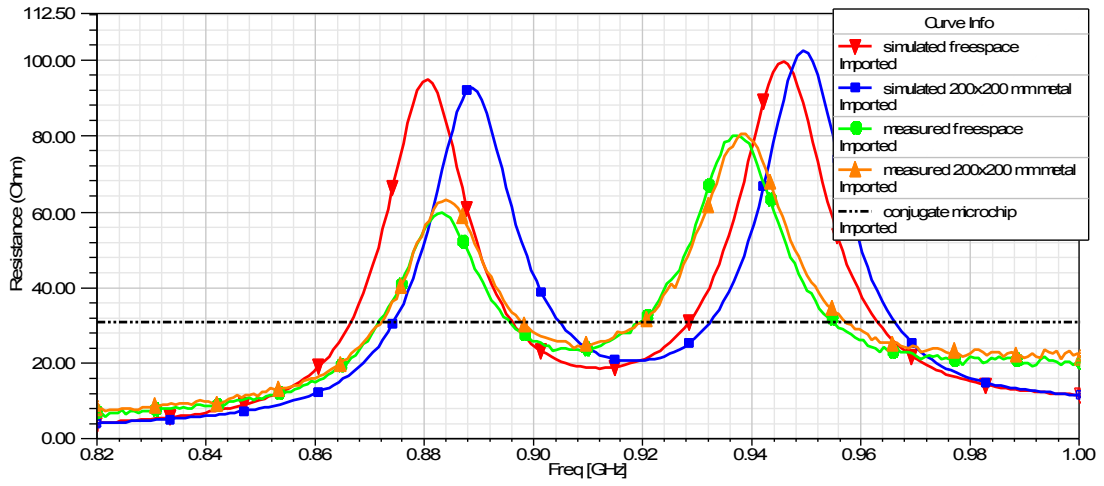
(a)
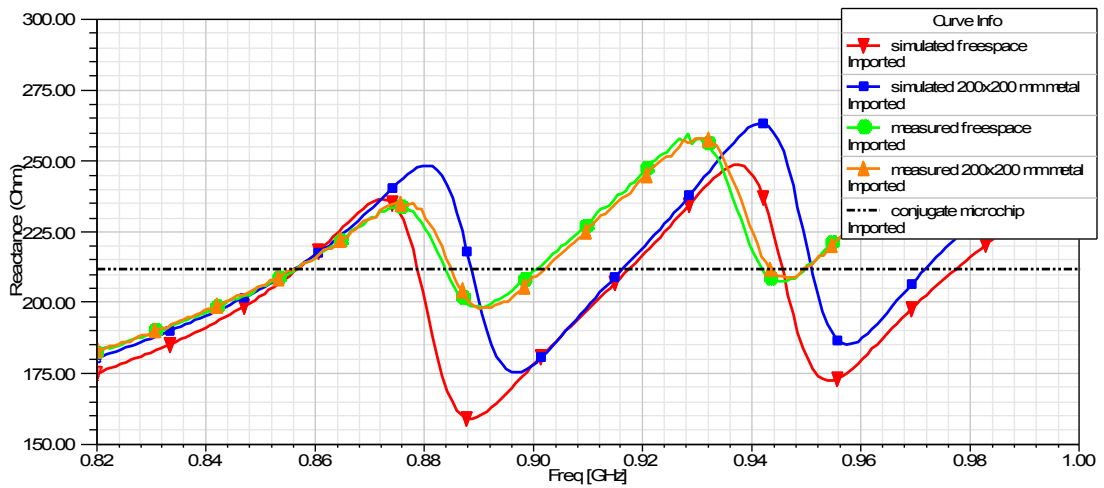
(b)

Figure 5.6: Simulated and measured input (a) resistance and (b) reactance input impedance of the double resonance antenna

Referring to Figure 5.6, it is observed that two resonant occur at two different frequencies in both simulation and measurement. The simulated input resistance and reactance values are higher than that of the measured values for both free space and metal cases. Moreover, the antenna also resonates at a slightly different frequency in the simulation than the prototype. The reasons for these discrepancies might be due to the fabrication inaccuracy as well as the surrounding effects during the antenna

measurement. The antenna was measured in an open space in the lab and not in the anechoic chamber. The interference from the surrounding might have contributed to the inaccuracy in the measurement. In addition, the shift on the resonant frequencies between the free space and when mounted on metal plate is observed in the simulation result whereas in the measurement, the frequency shift is almost negligible. Nevertheless, both results prove that the antenna impedance is only slightly affected when it is mounted on a metallic plate as anticipated.

To investigate the impedance matching performance of the antenna, the simulated and measured half-power impedance bandwidth (return loss ≤ -3 dB) is carried out. The 3 dB return loss impedance bandwidth of the antenna is shown in Figure 5.7. The simulated and measured value of 159 MHz and 155 MHz were obtained which is more than 100 MHz needed to cover the entire operating frequency of the UHF RFID band from 860 MHz to 960 MHz. The wideband feature of the antenna will also be able to compensate for the antenna fabrication inaccuracy during the manufacturing process.

Figure 5.7: Simulated and measured return loss of the double resonance antenna on free space and when mounted on metallic plate

92

5.4.2 Triple Resonance Microstrip Patch Antenna

In order to improve the bandwidth of tag antenna design, a triple resonance microstrip patch antenna was proposed. By utilizing three radiating element coupled fed by triangle loop structure for impedance matching, an improved impedance bandwidth is achieved. In the previous design, the bandwidth was evaluated based on half-power impedance bandwidth (return loss ≤ -3 dB) which attributes to the frequency range of which at most half of the power is reflected back at the input terminal of the antenna due to impedance mismatch between antenna and the microchip.

In this antenna design, three resonances were excited instead of two to improve the impedance bandwidth. To evaluate its bandwidth, (return loss ≤ -6 dB) is used as a benchmark which indicate only 25% of power is reflected at the antenna input terminal at the maximum as compared to 3 dB return loss (half of the power is reflected). The measured S-parameters obtained from the VNA are depicted in Figure 5.8. The input impedance of the antenna for both simulation and measurement are shown in Figure 5.9 for comparison. Based on the results, it is observed that measured resistance is lower than the simulated results while the reactance values are almost identical. Moreover, there is a slight shift of resonant frequencies between the simulation and measurement results. Both of these finding is attributed due to fabrication inaccuracies as well as the surroundings effects during the antenna measurement. Next, the impedance bandwidth of the antenna was calculated to measure its impedance matching performance based on 6 dB return loss. The simulated and measured value of (return loss ≤ -6 dB) 113 MHz and 117 MHz are obtained which is well above 100 MHz as shown in Figure 5.10. The return loss has four distinct minimum values which are -40 dB, -33 dB, -14 dB and -12 dB corresponds to operating frequency of 875 MHz, 887 MHz, 930 MHz and 970 MHz.

These minimum values were obtained since the impedance of the antenna was closely conjugate matched with the impedance of the referenced microchip which is around $31+j212$ Ω at these frequencies.
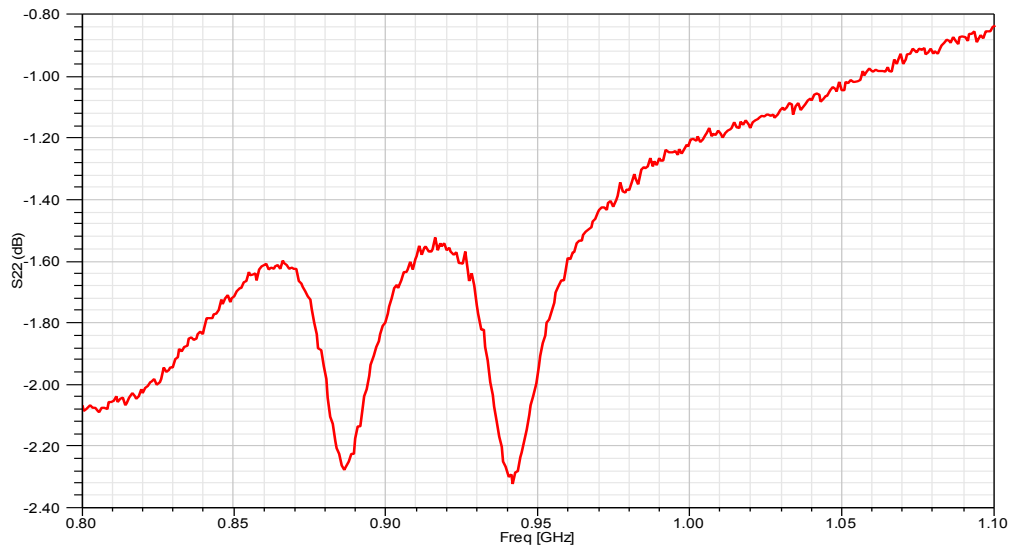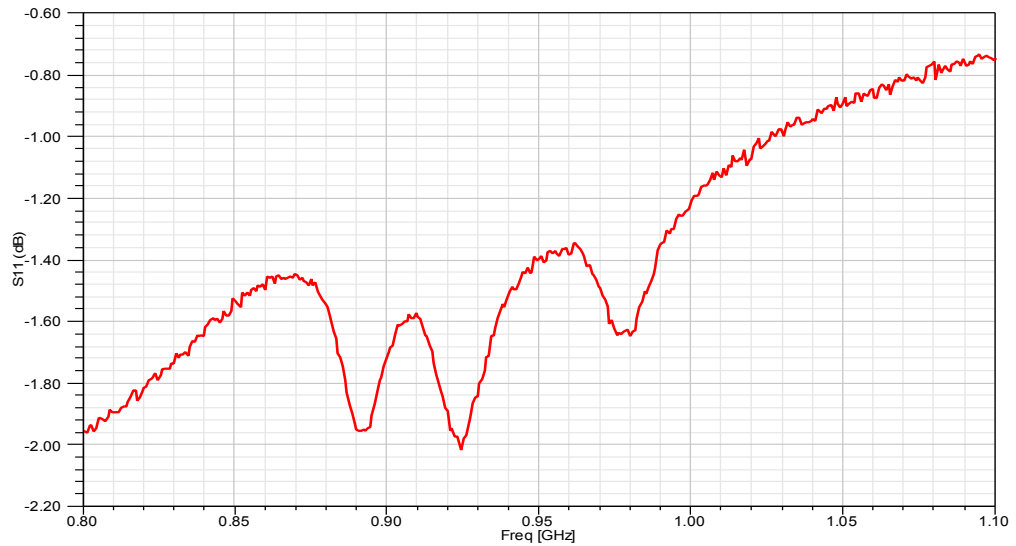

(a)
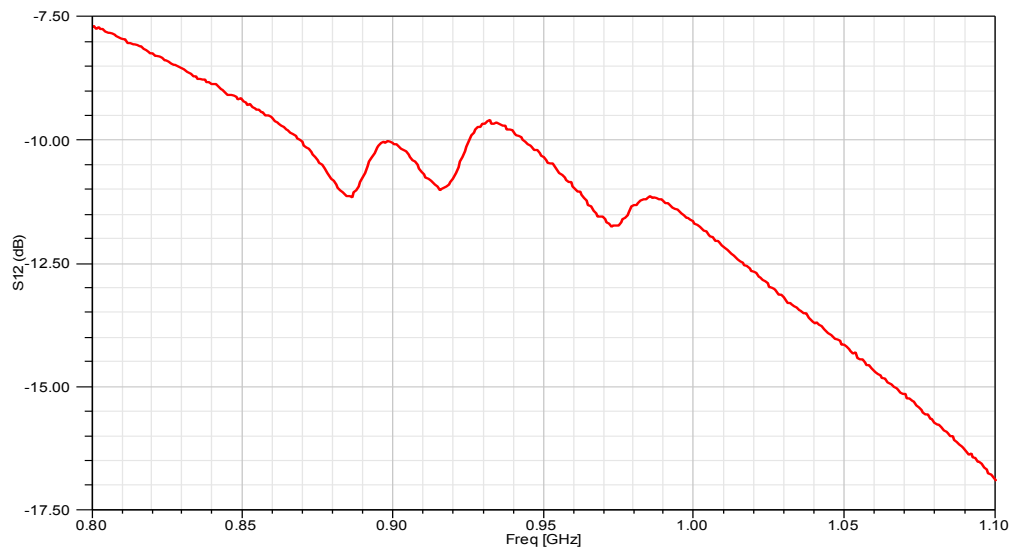
(b)
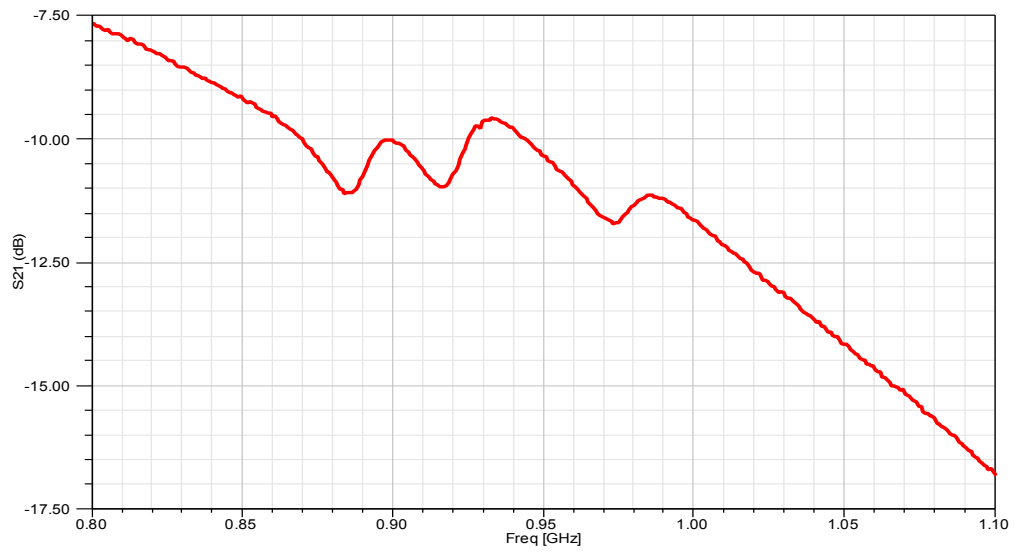
(c)
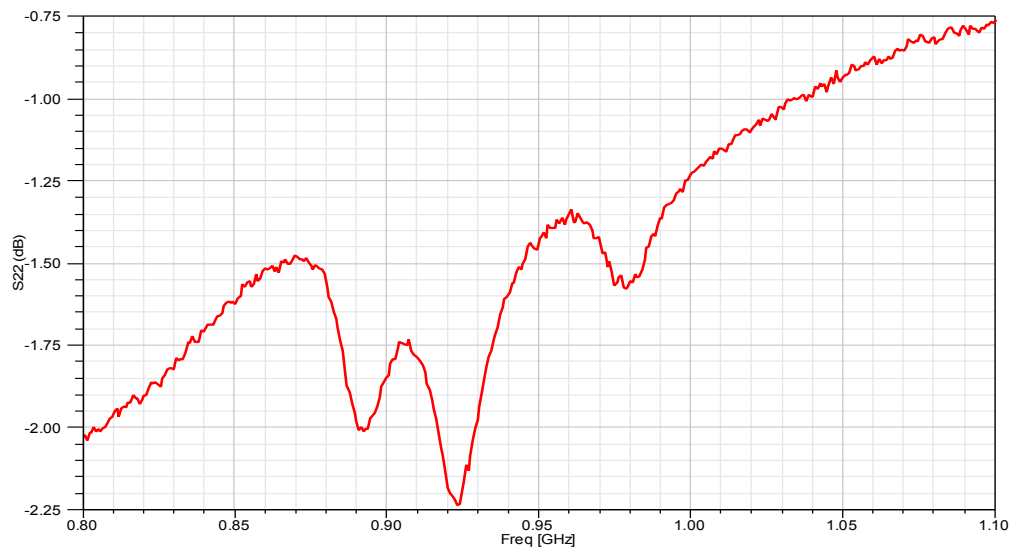
(d)

Figure 5.8: S$_{11}$, (b) S$_{12}$, (c) S$_{21}$ and (d) S$_{22}$ parameters of the triple resonance patch antenna.
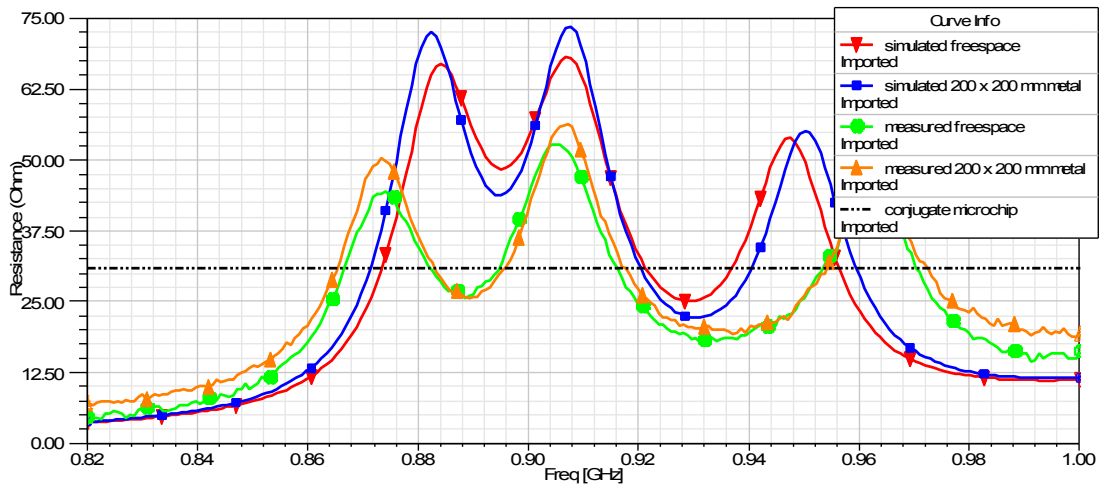
(a)
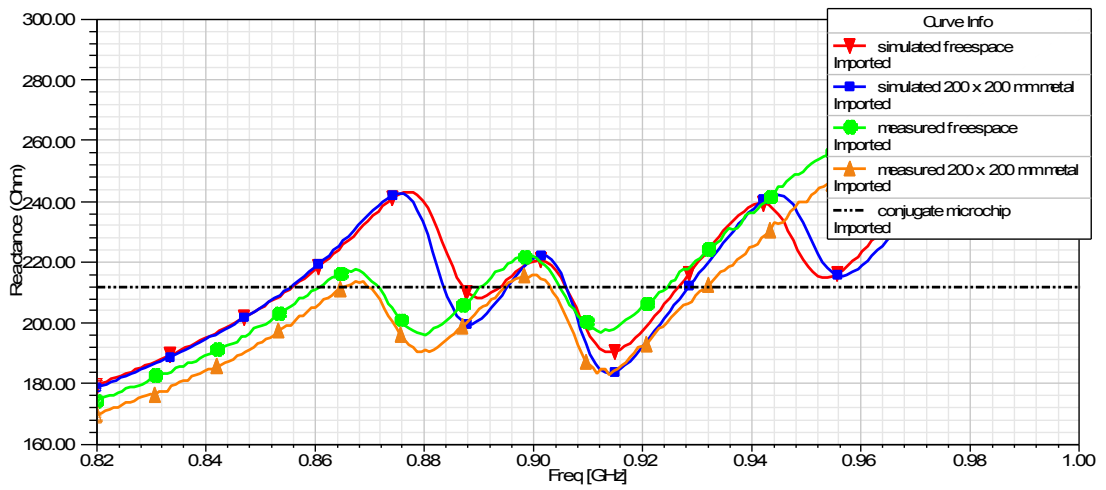
(b)

Figure 5.9: Simulated and measured input (a) resistance and (b) reactance input
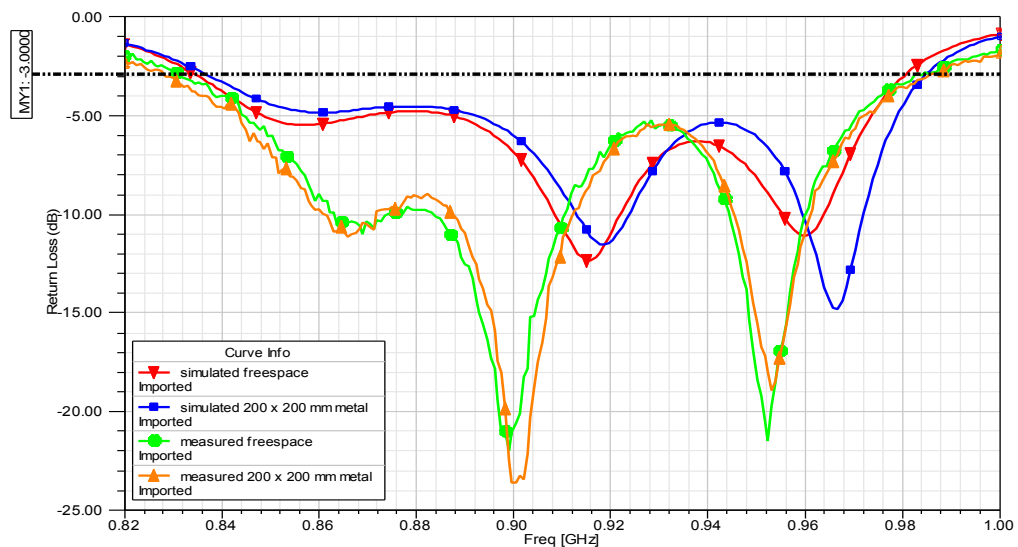impedance of the triple resonance antenna
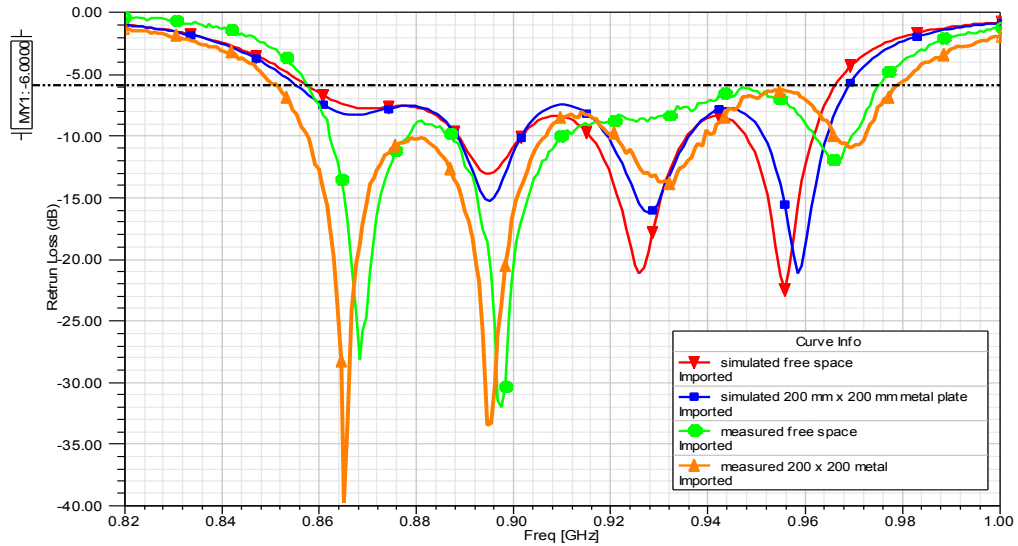
Figure 5.10: Simulated and measured return loss of the second antenna on free space and when mounted on metallic plate

5.5 RADIATION CHARACTERISTIC OF THE ANTENNA

The radiation pattern of the proposed antennas for both simulation and measurement were conducted to further analyze the performance of the antenna. The antenna was simulated on a free space as well as mounted on metallic plate of size 200×200 mm^2 to investigate the effects of conductive plane on the antenna. In addition, the radiation pattern of the proposed antenna on free space was measured in an anechoic chamber.

5.5.1 Radiation Pattern of Double Resonance Microstrip Patch Antenna

In this section, the radiation pattern of the antenna was simulated at the center of operating frequencies of UHF RFID which is 915 MHz. In the simulation part, there were two results obtained which are in free space and when mounted on reference metal plate of size 200×200 mm^2 to observe the effects of large metallic surface to the radiation pattern of the antenna. Meanwhile in the measurement part, only the free space scenario was carried out since by having large metal plate attached to the

97

antenna, the connector and the rotating system might not be able to hold the whole structure. Nevertheless, the comparison of the radiation pattern on free space between the simulation and measurement result should suffice to validate the performance of the antenna.

Figure 5.11 and Figure 5.12 shows the simulated radiation pattern of the antenna at operating frequency of 915 MHz for both free space and when attached on reference metal plate of size 200 mm × 200 mm^2. Broadside radiation pattern were observed for both cases. However, back lobe radiation was significantly reduced when the antenna was simulated on the metallic plane due to reflection of the radiating wave in the direction normal to the patch antenna.
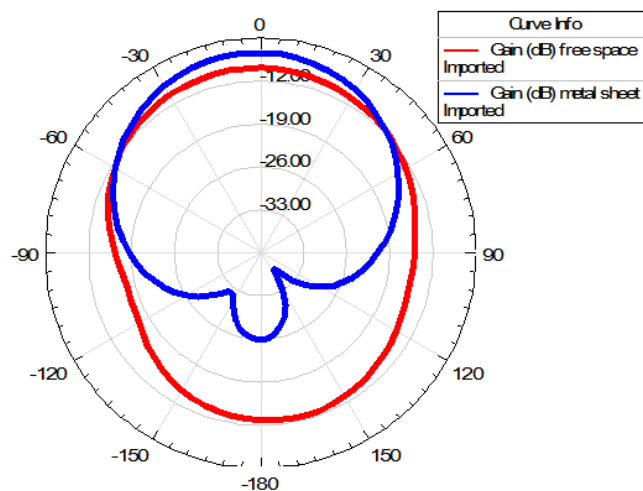
Figure 5.11: Simulated E-field radiation pattern of the proposed double resonance patch antenna at 915 MHz
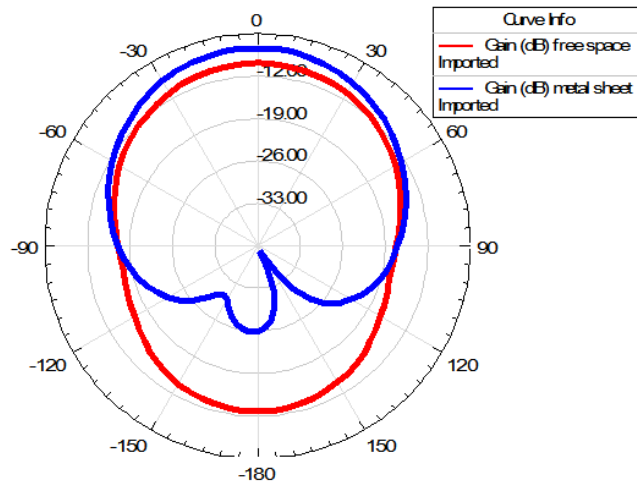
Figure 5.12: Simulated H-field radiation pattern of the proposed double resonance patch antenna at 915 MHz

Meanwhile, for comparison between simulations and measurements results, the simulated and measured radiation pattern of the antenna on free space for both E-plane and H-plane is depicted in Figure 5.13 and Figure 5.14. It is observed that both of the results indicate a quite similar broadside radiation pattern normal to the antenna plane. The backside radiation lobe is quite significant compared to the main lobe. This is due to the small ground plane of the antenna as proven in the previous simulation result.
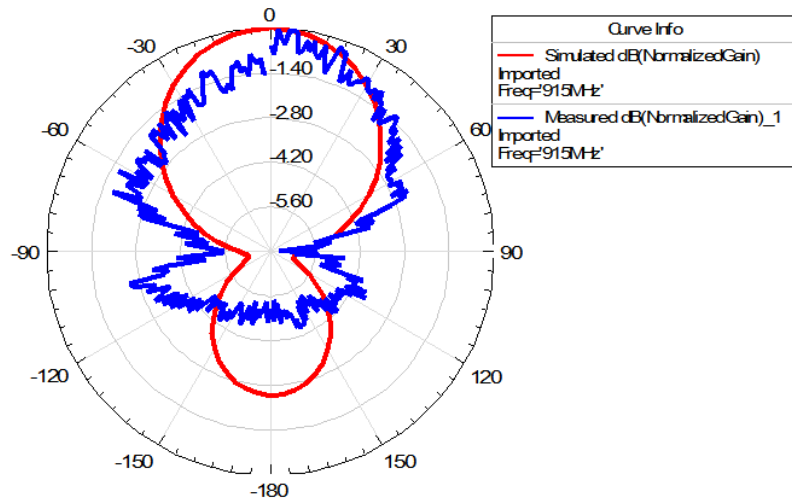
Figure 5.13: Simulated (red) and measured (blue) E-field radiation pattern of the double resonance patch antenna at 915 MHz on free space
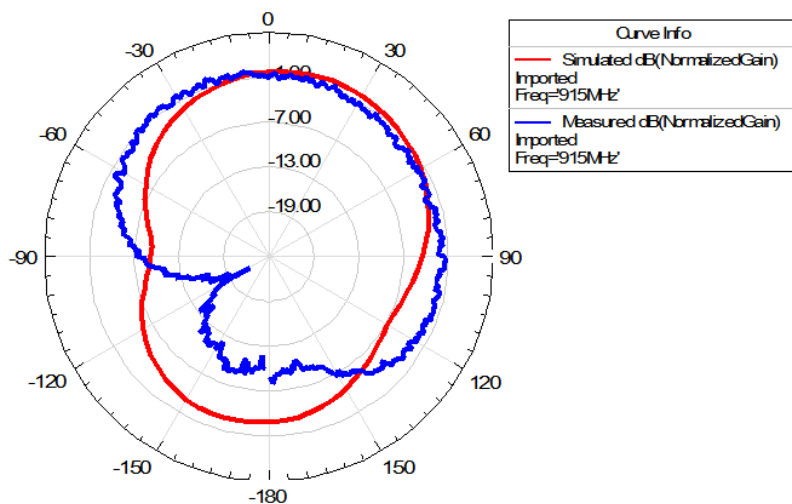
Figure 5.14: Simulated (red) and measured (blue) H-field radiation pattern of the double resonance patch antenna at 915 MHz on free space

5.5.2 Radiation Pattern of Triple Resonances Microstrip Patch Antenna

In this section, the simulation of the radiation pattern for the second antenna was carried out. At first, the simulation was carried out for two cases which are on free space and when mounted on metal plate of size 200×200 mm^2. Then, as with the

previous antenna, the measurement of the radiation pattern in free space at operating frequency of 915 MHz was performed and compared with the simulation results for validation.
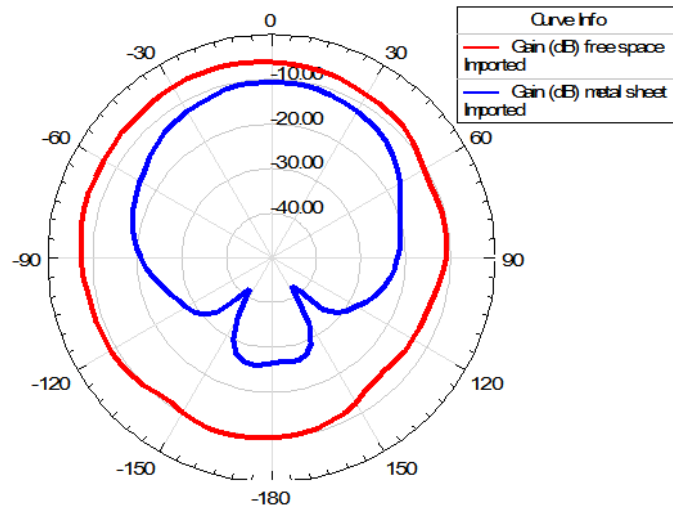
Figure 5.15: Simulated E-field radiation pattern of the proposed double resonance patch antenna at 915 MHz

It is observed in Figure 5.15 and Figure 5.16, the second antenna also exhibit broadside radiation pattern normal to the antenna plane. Furthermore, the back lobe radiation was higher when simulated in free space compared to when the antenna was mounted on referenced metal plate.
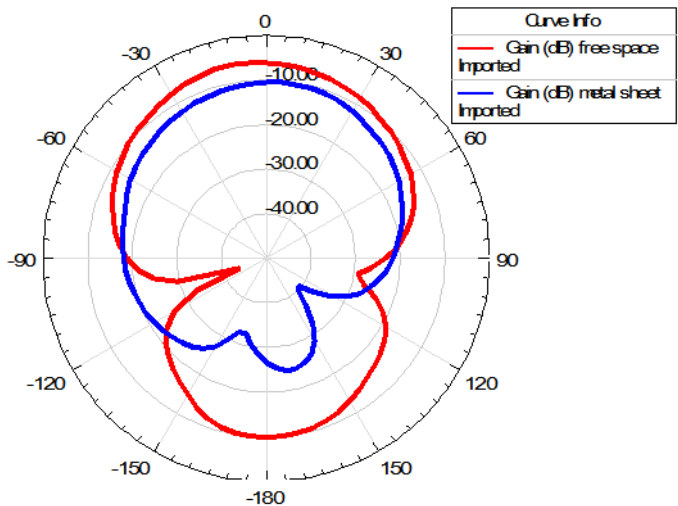
Figure 5.16: Simulated H-field radiation pattern of the proposed triple resonance patch antenna at 915 MHz
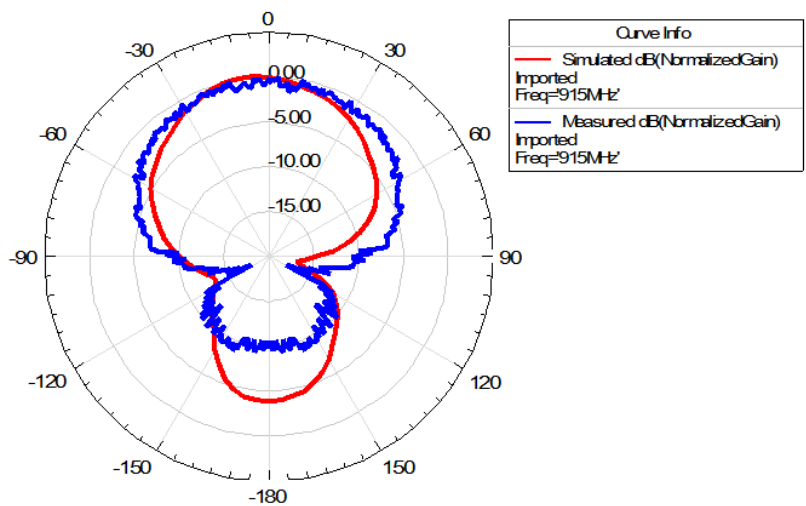
Figure 5.17: Simulated (red) and measured (blue) normalized E-field radiation pattern of the triple resonance patch antenna at 915 MHz

Figure 5.17 and Figure 5.18 show the normalized radiation pattern of the triple resonance antenna for the simulation and the measurement. It can be seen that both simulated and measured radiation pattern is fairly similar. The antenna shows a broadside radiation pattern that is normal to the antenna plane. However, back lobe radiation of the antenna is high due to small ground plane. Nevertheless, it will not be

an issue since the antenna is designed to be attached to metal made object whose surface will be big enough to act as an extension of the antenna ground plane thus reducing the back lobe radiation from the antenna as indicated in Figure 5.7 and Figure 5.11 when the antenna was simulated on top of referenced metal plate of size 200 x 200 mm^2.
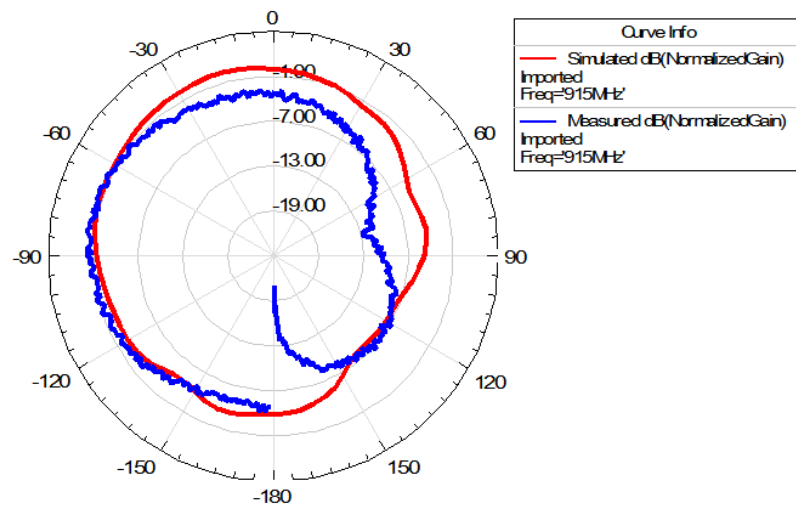
Figure 5.18: Simulated (red) and measured (blue) normalized H-field radiation pattern of the triple resonance patch antenna at 915 MHz

5.6   THEORITICAL CALCULATION OF TAG ANTENNA READ RANGE

The simulated peaks gain of the proposed antenna at the bore sight direction ($\theta = 0, \varphi = 0$) is shown in Figure 5.19. Based on the results, it is seen that the peak gain of antenna is increased as the size of metallic plate it is attached is increased. This gives a clear indication that the performance of the proposed antenna will actually improve when it is mounted on metal objects. It is to be noted that the antenna yield negative gain which indicate the gain is low. However, in the field of UHF RFID tag antenna, such a gain is common as reported by previous works done by Eunni et al. (2007), Lu

and Hung (2010), Ming et al. (2010) and Cho et al. (2010). Other parameters like *EIRP* and P_{th} are set by the countries regulatory body and chip manufacturer.
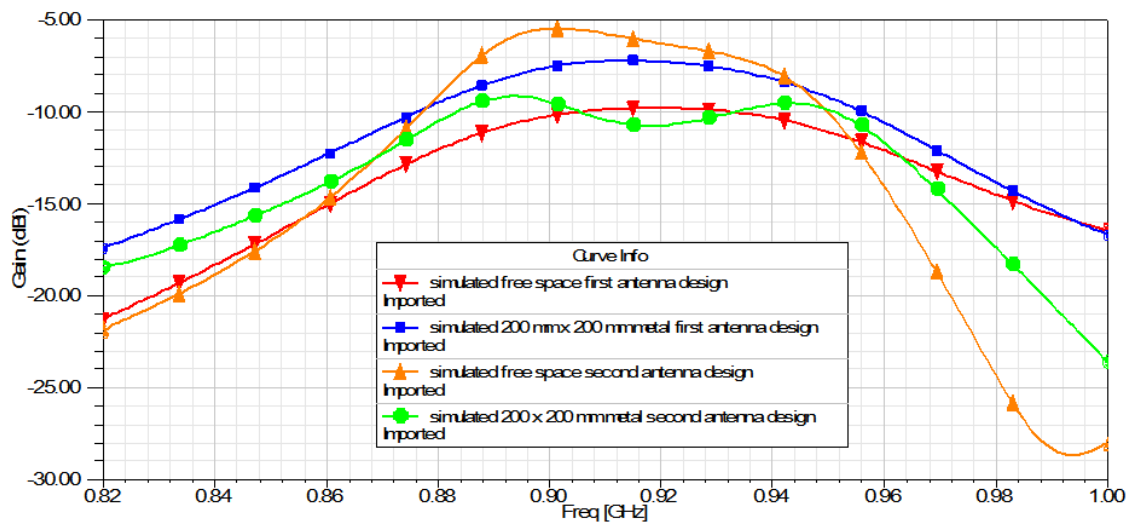
Figure 5.19: Simulated peak gain of the antenna

By assuming the antenna polarization is the same with the reader antenna (no polarization loss), the maximum read range of the proposed antenna at the main operating frequencies across the UHF RFID frequency band can be theoretically calculated using equation (2-19) by incorporating the measured impedance bandwidth and the simulated peak gain above. The calculation results for both antenna designs are presented in Table 5.1. A minimum read range of 2.36 m and 2.68 m are obtained for both antennas. The calculated minimum read range for both antennas are both above the required 1 meter which is the standard distance for the passive UHF RFID system. It is also observed that the read range is actually improved when it was mounted on large metallic plate due to increased peak gain.

104

Table 5.1

Theoretically calculated read range of the proposed antenna

Country/ Region	Center freq., f_c (MHz)	EIRP (W)	Calculated read range (m)			
			Antenna#1		Antenna#2	
			Free space	200 x 200 mm^2 metal sheet	Free space	200 x 200 mm^2 metal sheet
Europe	886	3.3	2.36	3.15	2.68	3.33
North America	915	4	4.08	5.51	6.18	3.61
Japan	954	4	2.91	3.5	2.99	2.80

Note:

Antenna #1: Double resonance patch antenna

Antenna #2: Triple resonance patch antenna

5.7 PERFORMANCE COMPARISON WITH OTHER EXISTING PATCH ANTENNA FOR RFID

In this sub-section, a comparison of the proposed antenna with other similar existing metal mountable tag antenna is presented. For ease of comparison, a comparison table is developed as shown in Table 5.2. Major emphasize will be given towards the impedance bandwidth performance of the antenna since it serves as the main objective of this research. The antenna gains for some of the work were not reported in their paper. As such, the antennas were reconstructed if possible using the electromagnetic simulator, Ansoft HFSS to calculate its gain. It is seen that the proposed antenna has better performance in term of impedance bandwidth than other metal mountable antennas in the literature. As for the gain, the proposed antenna produce a comparable gain with other antennas although was not the highest.

Table 5.2

Comparison of the performance of the proposed antenna with other similar existing
antenna for UHF RFID tag

Author	Antenna type	Size (mm^3)	Substrate	Cross/multi-layer structure	3 dB Return loss bandwidth (MHz)	Peak Antenna gain (dBi)
(Eunni et al., 2007)	Planar patch antenna	105 x 44 x 1.6	Low loss substrate	Planar	-	−1.13
(Tashi et al., 2011)	Planar patch antenna	86 x 58 x 1.6	FR-4 substrate	Planar	46 MHz	3.28
(Mo and Qin, 2010)	Open feed stub patch antenna	77 x 22 x 3	FR-4 substrate	Planar	40 MHz	2
(Chen and Tsao, 2010)	Low Profile meandered patch antenna	100 x 50 x 0.8	FR-4 substrate	Incorporate shorting pin	40 MHz	−6.8
(Mo et al., 2008)	Patch antenna with a pair of U-slots	96 x 50 x 1.6	FR-4 substrate	Incorporate via hole	133 MHz	−3
(Mo and Qin, 2012)	Tunable compact PIFA with open stub feed	40 x 22 x 3	FR-4 substrate	Incorporate shorting wall	37 MHz	2.3
(Ming et al., 2010)	Low Profile Broadband patch antenna	70 x 85 x 1.6	FR-4 substrate	Incorporate shorting plate	153 MHz	−6
(Lu and Hung, 2010)	Planar inverted-E antenna	75 x 22 x 1.6	FR-4 substrate	Incorporate shorting via	123 MHz	−7
(Cho et al., 2010)	Embedded feed patch antenna	83 x 50 x 1.6	FR-4 substrate	Planar	65 MHz	−6
Antenna #1	Planar patch antenna	87 x 45 x 1.6	FR-4 substrate	Planar	155 MHz	−7.2
Antenna #2	Planar patch antenna	130 x 63 x1.6	FR-4 substrate	Planar	160 MHz	−5.5

Note:
Antenna #1: Double resonance patch antenna
Antenna #2: Triple resonance patch antenna

5.8   SUMMARY

This chapter has presented the simulation and measurement results along with the
discussion with regards to the proposed antenna. In addition, the read range of the
proposed antenna was theoretically calculated to investigate its practicality for use in
RFID metallic applications based on Friis free space equation. Lastly, performance

comparison between the proposed antennas with other similar antenna in term of

impedance bandwidth, gain and size were carried out to validate its performance.

CHAPTER SIX

CONCLUSION AND RECOMMENDATION

6.1 CONCLUSION

In this thesis, the design, simulation and fabrication of wideband microstrip patch antenna was presented. The proposed antenna is intended for UHF RFID tag where it can be mounted on metallic objects for monitoring purposes. Moreover, it is also aimed for worldwide usage.

The implementation flow of the proposed antenna was discussed in Chapter 3. The design requirement of the tag antenna was first developed and studied. Then, based on the requirements, the antenna design was carried out using existing closed form expression for the calculation of the antenna parameters. The design was simulated using full wave electromagnetic simulator, Ansoft v13. The optimal antenna design parameter was obtained through successions of parametric refinement. The prototype of the proposed antenna was manufactured using photolithography and etching technique. Several performance parameters which are impedance bandwidth, radiation pattern and the peak gain of the antenna were recorded during measurement process. Both the simulation and measurement results were compared and analyze for validation. Finally, a comparison was made with other similar existing metal mountable tag antenna to show the improvement of the proposed antenna over those in the literature especially in term of impedance bandwidth.

The accomplishments of this research work are summarized as follows:

i. The impedance bandwidth of 155 MHz (return loss ≤ -3 dB) and 117 MHz (return loss ≤ -6 dB) for both proposed antennas have achieved which is over the required 100 MHz for wideband UHF RFID application.

ii. The overall sizes of the antenna are $87 \times 55 \times 1.6$ mm^3 and $130 \times 63 \times 1.6$ mm^3 which are within the standard size for UHF RFID application (Rao et al., 2005).

iii. The peak gain of -7.2 dBi and -5.5 dBi have been achieved which were enough to provide a minimum read range of over 1 meter.

iv. The antenna have been successfully fabricated using a single copper cladding FR-4 board using photolithography and etching technique without the need of soldering and drilling process.

6.2 CONTRIBUTION

The main contribution of the research work is the development of planar wideband patch antenna for UHF RFID tag. The proposed antennas have half power impedance bandwidth of over 100 MHz to cover the entire operating frequency band of UHF RFID system (860 MHz to 960 MHz) where most of the tag antennas in the literature have low bandwidth thus limiting their usage only for a specific country or region. This wideband feature is very important for continuous tracking and monitoring of goods as they are being transported across the world. Moreover, the proposed antennas exhibit planar structure without any cross or multi-layer configuration such as shorting wall or via hole in order to simplify and to reduce the fabrication process

with the aim to reduce the cost of the antenna when being manufactured in bulk volume. Although some works have been done on this planar patch antenna, they are narrowband.

6.3   RECOMMENDATION

Although several accomplishments have been achieved in this research, there is still a lot of improvement that can be done for the proposed design. Several future directions were identified as follows:

    i.   The first proposed antenna exhibits half power impedance bandwidth performance (return loss ≤ -3 dB) of 155 MHz while the second antenna possesses an improved bandwidth of 117 MHz (return loss ≤ -6 dB). To further reduce loss due to impedance mismatch at the antenna input impedance, a patch antenna with impedance bandwidth of over 100 MHz based on 10 dB return loss performance should be designed. This would improve the power transmission coefficient of the antenna. As a result, a higher read range could be achieved.

    ii.   Size of tag plays a major role in determining the practicability of RFID systems. It is important to ensure a tag is small relative to the object it is attached to. The proposed patch antenna is aimed for tagging large metallic objects like metal container. However for tagging a small metal objects like drink can, it use would be unfeasible. Hence, a further reduction on the antenna size using exploiting interesting properties of meta-material should be explored.

iii.   One of the limitations of microstrip patch antenna is its low gain especially for thin and high permittivity substrate. The proposed antenna has gain varying from −5 dBi to −15 dBi which is low compared to commercial printed dipole tag antenna. This is due to the thin structure of the proposed antenna at 1.6 mm. For gain improvement, a usage of novel substrate that can increase the gain should be explored. With an improved gain, it is expected a higher maximum read range can be obtained.

iv.   Both of the proposed antennas are linearly polarized antenna. To ensure they are able to work properly, the antennas need to be oriented properly with respect to the reader antenna. As such, a wideband circularly polarized tag antenna is desirable to guarantee the tag is able to operate regardless its orientation with respect to the reader.

v.   To ensure RFID system is successfully implemented, the overall cost needs to be as minimum as possible. This is one of the reasons why a printed dipole antenna is widely used. However, it has been observed that printed dipole antenna does not work when used for tagging metallic objects, a metal mountable tag antenna such as microstrip patch antennas as proposed in this research are needed. Although the FR-4 substrate used in this research is one of the cheapest substrate available, other low cost substrate should also be explored.

vi.   Another sacrifice that was made in designing the proposed microstrip antenna is it rigid structure which would only be used for metal objects with flat surface. Some difficulties are anticipated if the surface on which the tag antenna is intended to be mounted on is curvy. This would not be the case for the printed dipole antenna which is flexible enough for tagging various object

shapes. Hence, a flexible wideband metal mountable tag antenna should be designed in the future.

REFERENCES

Abbaspour, M. and H. R. Hassani. (2008). Wideband star-shaped microstrip patch antenna. *Progress In Electromagnetics Research*, 1: 61-68.

Alienware. (2012). Alien Higgs 3 EPC Class 1 Gen 2 RFID Tag IC. Retrieved October 20, 2012. http://www.alientechnology.com/docs/products/Alien-Technology-Higgs-3-ALC-360.pdf.

Balanis, C. A. (1989). *Advanced Engineering Electromagnetics*. JohnWiley & Sons, New York.

Balanis, C. A. (2005). *Antenna Theory Analysis and Design*. (3rd Edn.). John Wiley & Sons, New Jersey.

Bird, T. S. (2009). Definition and Misuse of Return Loss. *IEEE Antennas and Propagation Magazine,* 51(2): 166-167.

Bjorninen, T., M. Nikkari, L. Ukkonen, F. Yang, A. Elsherbeni, L. Sydanheimo and M. Kivikoski (2008). Design and RFID signal analysis of a meander line UHF RFID tag antenna IEEE Antennas and Propagation Society International Symposium, pp**.** 1-4.

Chen, S.-L. (2009). A Miniature RFID Tag Antenna Design for Metallic Objects Application. *IEEE Antennas and Wireless Propagation Letters*, 8: 1043-1045.

Chen, H. D. and Y. H. Tsao (2010). Low-Profile Meandered Patch Antennas for RFID Tags Mountable on Metallic Objects. *IEEE Antennas and Wireless Propagation Letters*, 9: 118-121

Cho, C., H. Choo and I. Park (2008). Design of planar RFID tag antenna for metallic objects. *Electronics Letters*, 44(3): 175-177.

Cho, H.-G., N. R. Labadie and S. K. Sharma (2010). Design of an embedded-feed type microstrip patch antenna for UHF radio frequency identification tag on metallic objects. *IET Microwaves, Antennas & Propagation*, 4(9): 1232-1239.

Choi, W., H. W. Son, J.-H. Bae, G. Y. Choi, C. S. Pyo and J.-S. Chae (2006). An RFID Tag Using a Planar Inverted-F Antenna Capable of Being Stuck to Metallic Objects. *ETRI Journal*, 20(2): 216-218.

Choi, W., H. W. Son, C. Shin, J.-H. Bae and G. Choi (2006). RFID tag antenna with a meandered dipole and inductively coupled feed. IEEE Antennas and Propagation Society International Symposium, pp**.** 619-622.

Choi, Y., U. Kim, J. Kim and J. Choi (2009). Design of modified folded dipole antenna for UHF RFID tag. *Electronics Letters*, 45(8): 387-389.

Deavours, D. D. (2010). Improving the Near-Metal Performance of UHF RFID Tags. IEEE International Conference on RFID, Orlando, FL.

Delzo, K. M. E. (2010). *RFID Tags mountable on Metallic Surface,* Tampere University of Technology.

Derneryd, A. G. (1978). A Theoretical Investigation of the Rectangular Microstrip Antenna Element. IEEE Transaction, Antennas and Propagation 26(4): 532-535.

Dobkin, D. M. (2008). *The RF in RFID : Passive UHF RFID in Practice*. Elsevier Inc., Massachusetts.

Eunni, M., M. Sivakumar and D. D. Deavours (2007). A novel planar microstrip antenna design for UHF RFID. *Journal of Systemics, Cybernetics and Informatics*, 5(1): 6-10.

Finkenzeller, K. (2003). *RFID Handbook*. (2nd Edn.). John Wiley & Sons, West Sussex.

Garg, R., P. Bartia, I. Bahl and A. Ittipibon (2001). *Microstrip Antenna Design handbook*. Artech House, Noorwood, MA.

Ghannay, N., M. B. Ben Salah, F. Romdhani and A. Samet (2009). Effects of metal plate to RFID tag antenna parameters. Microwave Symposium Mediterrannean (MMS).

GS1 (2012). Regulatory status for using RFID in the UHF spectrum. Retrieved on September 28 2012. http://www.gs1.org/docs/epcglobal/UHF_Regulations.pdf.

Guha, D. and Y. M. M. Antar (2011). *Microstrip and Printed Antennas New Trends Techniques and Applications*. John Wiley & Sons

Hirvonen, M., P. Pursula, K. Jaakkola and K. Laukkanen (2004). Planar inverted-F antenna for radio frequency identification. *Electronics Letters*, 40(14): 848-850.

Huang, J. Z., P. H. Yang, W. C. Chew and T. T. Ye (2009). A compact broadband patch antenna for UHF RFID tags Asia Pacific Microwave Conference (APMC), pp. 1044-1047.

Huie, K. C. (2002). *Microstrip Antennas: Broadband Radiation Patterns Using Photonic Crystal Substrates*. Blackburg, VA, Virginia Polytechnic Institute and State University.

Kim, K.-H., J.-G. Song, D.-H. Kim, H.-S. Hu and J.-H. Park (2007). Fork-shaped RFID tag antenna mountable on metallic surfaces. *Electronics Letters*, 43(25): 1400-1402.

Kraus, J. D. and R. J. Marhefka (2003). *Antenna: For All Applications*. (3rd Edn.). McGraw-Hill, New York.

Kumar, G. and K. P. Ray (2003). *Broadband Microstrip Antenna*. Artech House, Noorwood, MA.

Kuo, S.-K., S.-L. Chen and C.-T. Lin (2008). An Accurate Method for Impedance Measurement of RFID Tag Antenna. *Progress In Electromagnetics Research*, 83: 93-106.

Kwon, H. and B. Lee (2005). Compact slotted planar inverted-F RFID tagmountable on metallic objects. *Electronics Letters*, 41(24): 1308-1310.

Loo, C.-H., K. Elmahgoub, F. Yang, A. Z. Elsherbeni, D. Kajfez, A. A. Kishk, T. Elsherbeni, L. Ukkonen, L. Sydanheimo, M. Kivikoski, S. Merilampi and P. Ruuskanen (2008). Chip impedance matching for UHF RFID tag antenna design. *Progress In Electromagnetics Research*, 81: 359-370.

Lu, J.-H. and K.-T. Hung (2010). Planar inverted-E antenna for UHF RFID tag onmetallic objects with bandwidth enhancement. *Electronics Letters*, 46(17): 1182-1183.

Lu, J.-H. and G.-T. Zheng (2011). Planar Broadband Tag Antenna Mounted on the Metallic Material for UHF RFID System. *IEEE Antennas and Propagation Magazine*, 10: 1405-1408.

Marrocco, G. (2003). Gain-optimized self-resonant meander line antennasfor RFID applications. *IEEE Antennas and Wireless Propagation Letters*, 2(1): 302-305.

Marrocco, G. (2008). The art of UHF RFID antenna design: impedance-matching and size-reduction techniques. *IEEE Antennas and Propagation Magazine*, 50(1): 66-79.

Ming, Y. L., Li R., M. M. Tentzeris (2010). Low-Profile Broadband RFID Tag antennas mountable on metallic objects. IEEE Antennas and Propagation Society International Symposium (APSURSI). Toronto, Canada.

Mo, L. and C. Qin (2010). Planar UHF RFID Tag Antenna With Open Stub Feed for Metallic Objects. *IEEE Transactions on Antennas and Propagation*, 58(9): 3037 - 3043

Mo, L. and C. Qin (2012). Tunable Compact UHFRFID Metal Tag Based on CPW Open Stub Feed PIFA Antenna. *International Journal of Antennas and Propagation*, 2012:

Mo, L., H. Zhang and H. Zhou (2008). Broadband UHF RFID tag antenna with a pair of U slots mountable on metallic objects. *Electronics Letters*, 44(20): 1173-1174.

Monti, G., L. Catarinucci and L. Tarricone (2010). Broad-band dipole for RFID applications. *Progress In Electromagnetics Research* C, 12: 163-172.

Obsiye, A. K. H. (2009). *Design of Microstrip Miniature Antenna for RFID Application*, International Islamic University Malaysia.

Obsiye, A. K. H. A.-R., H.E.; El-Islam, R. (2008). Modified printed crescent patch antenna for Ultrawideband RFID (UWB-RFID) tag IEEE International RF and Microwave Conference (RFM), pp. 274-276.

Palmer, K. D. and M. W. v. Rooyen (2006). Simple Broadband Measurements of Balanced Loads Using a Network Analyzer. *IEEE Transactions on Instrumentation and Measurement*, 55(1): 266-272.

Pan, B., Y. Yoon, J. Papapolymerou, M. M. Tentzeris and M. G. Allen (2005). A high performance surface-micromachined elevated patch antenna. IEEE Antennas and Propagation Society International Symposium, Washington D.C.

Paredes, F., G. Zamora, F. J. Herraiz-Martinez, F. Martin and J. Bonache (2011). Dual-Band UHF-RFID Tags Based on Meander-Line Antennas Loaded With Spiral Resonators. *IEEE Antennas and Propagation Magazine*, 10: 768-771.

Park, C. R. and K. H. Eom (2011). RFID Label Tag Design for Metallic Surface Environments. *Sensors*, 11: 938-948.

Pongpaibool, P. (2009). Wideband UHF RFID Tag. The 2009 International Symposium on Antennas and Propagation (ISAP 2009). Bangkok, Thailand, pp: 855-858.

Pozar, D. (1986). An update on microstrip antenna theory and design including some novel feeding techniques. *IEEE Antennas and Propagation Society Newsletter*, 28(5): 4-9.

Pozar, D. M. (1992). Microstrip Antennas. Proceedings of the IEEE, 80(1): 79-91.

Prothro, J. T. (2007). *Improved Performance of a Radio Frequency Identification Tag Antenna on a Metal Ground Plane*, Georgia Institute of Technology.

Prothro, J. T., G. D. Durgin and J. D. Griffin (2006). The Effects of a Metal Ground Plane on RFID Tag Antennas. IEEE Antennas and Propagation Society International Symposium J. T. Prothro, pp. 3241-3244.

Qing, X., C. K. Goh and Z. N. Chen (2009). Impedance Characterization of RFID Tag Antennas and Application in Tag Co-Design. *IEEE Transactions on Microwave Theory and Techniques*, 57(5): 1268-1274.

Rao, K., S. F. Lam and P. V. Nikitin (2008). Wideband metal mount UHF RFID tag. IEEE Antennas and Propagation Society International Symposium pp**.** 1-4.

Rao, K. V. S., P. V. Nikitin and S. F. Lam (2005). Antenna Design for UHF RFID Tags: A Review and a Practical Application. *IEEE Transactions on Antennas and Propagation*, 53(12): 3870-3876.

Rudge, A. W., K. Milne, A. D. Olver and P. Knight (1982). *The Handbook of Antenna Design*. Peter Peregrinus, London.

Sahin, C. and D. D. Deavours (2009). Wideband microstrip RFID tag: Theory and design. IEEE Antennas and Propagation Society International Symposium (APSURSI '09). Charleston, SC, pp**.** 1-4.

Son, H.-W., G.-Y. Choi and C.-S. Pyo (2006). Design of wideband RFID tag antenna for metallic surfaces. *Electronics Letters*, 42(5): 263-265.

Son, H.-W., H.-G. Jeon and J.-H. Cho (2012). Flexible wideband UHF RFID tag antenna for curved metal surfaces. *Electronics Letters*, 48(13): 749-750.

Son, H.-W. and S.-H. Jeong (2011). Wideband RFID Tag Antenna for Metallic Surfaces Using Proximity-Coupled Feed. *IEEE Antennas and Wireless Propagation Letters*, 10: 377-380.

Son, H.-W. and C.-S. Pyo (2005). Design of RFID tag antennas using an inductively coupled feed. *Electronics Letters*, 41(18): 994-996.

Sood, D., G. Singh, C. C. Tripathi, S. C. Sood and P. Joshi (2008). Design, fabrication and characterization of microstrip square patch antenna array for X-band applications. *Indian Journal of Pure & Applied Physics*, 46: 593-597.

Swason, D. G. J. and W. J. R. Hoefer (2003). *Microwave Circuit Modeling Using Electromagnetic Field Simulator*. Artech House, London.

Tashi, M. S. Hasan and H. Yu (2011). Design and simulation of UHF RFID tag antennas and performance evaluation in presence of a metallic surface. 5th International Conference on Software, Knowledge Information, Industrial Management and Applications (SKIMA). Benevento, pp**.** 1-5.

Tashi, T., M. S. Hasan and H. Yu (2011). A complete planner design of microstrip patch antenna for a passive UHF RFID tag. 17th International Conference on Automation and Computing (ICAC), pp**.** 12-17.

Ukkonen, L., L. Sydanheimo and M. Kivikoski (2004). A novel tag design using inverted-F antenna for radio frequency identification of metallic objects. IEEE Symposium on Advances in Wired and Wireless Communication, pp**.** 91-94.

Ukkonen, L., L. Sydanheimo and M. Kivikoski (2005). Effects of metallic plate size on the performance ofmicrostrip patch-type tag antennas for passive RFID. *IEEE Antennas and Wireless Propagation Letters*, 3: 410-413.

Ukkonen, L., L. Sydanheirno and M. Kivikoski (2004). A novel tag design using inverted-F antenna for radio frequency identification of metallic objects. IEEE Symposium on Advances in Wired and Wireless Communication.

Venkatakrishnan, R. K. (2011). *Compact Metamaterial UHF RFID Tag Antennas*, University of Cincinnati.

Weinstein, R. (2005). RFID: A Technical Overview and its Application to the Enterprise. *IT Professional*, 7(3): 27 - 33

Wong, K.-L. (2002). *Compact and Broadband Microstrip Antennas*. John Wiley & Sons, New York.

Xu, L., B. J. Hu and J. Wang (2008). UHF RFID Tag Antenna with Broadband Characteristic. *Electronics Letters*, 44(2): 79-80.

Yang, B. and Q. Feng (2008). A folded dipole antenna for RFID tag. International Conference on Microwave and Millimeter Wave Technology (ICMMT) 2008, Nanjing.

Yang, P. H., Y. Li, L. Jiang, W. C. Chew and T. T. Ye (2011). Compact Metallic RFID Tag Antennas With a Loop-Fed Method. *IEEE Transactions on Antennas and Propagation,* 59(12): 4454-4462.

Yao, W., C.-H. Chu and Z. Li, 2011. The use of RFID in healthcare: Benefits and barriers. IEEE International Conference on RFID-Technology and Applications (RFID-TA) Guangzhou, China, pp**.** 128-134

LIST OF PUBLICATIONS

Journals

1. Bashri, M. S. R., Ibrahimy, M. I. and Motakabber, S. M. A., (2013).Design and Development of a Compact Wideband C-Shaped Patch Antenna for UHF RFID Tag. *Research Journal of Applied Sciences, Engineering and Technology,* 6(10), 2118-2126. (ISI THOMPSON &SCOPUS)

2. Bashri, M. S. R., Ibrahimy, M. I. and Motakabber, S. M. A., (2013). A Compact Wideband Patch Antenna for Ultra High Frequency Radio Frequency Identification Tag. *Automatika* **(*Submitted*)**

Conference/Proceedings

1. Bashri, M. S. R., Ibrahimy, M. I. and Motakabber, S. M. A., (2013).A Planar Wideband Microstrip Patch Antenna for UHF RFID Tag. Paper presented at the IEEE International Conference on Space Science and Communication (ICONSPACE), 2013.

2. Bashri, M. S. R., Ibrahimy, M. I. and Motakabber, S. M. A., (2013).A Planar Wideband Inductively Coupled Feed Patch Antenna for UHF RFID Tag, IEEE International Conference on RFID Technology and Applications (RFID TA), 2013.

LIST OF AWARDS

Bashri, M. S. R., Ibrahimy, M. I. and Motakabber, S. M. A. "A Planar Wideband Microstrip Patch Antenna for UHF RFID Tag", Kulliyyah of Engineering Research and Innovation Exhibition (KERIE 2013), June 2013, Kuala Lumpur. (**Bronze Medal**)

APPENDIX A: INDUCTIVELY COUPLED FEED STRUCTURE
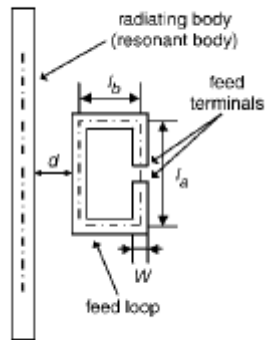
(a)
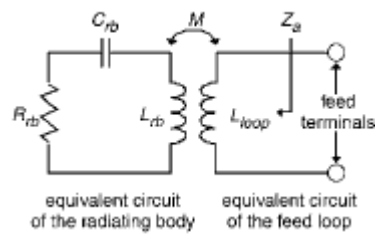
(b)

Inductively coupled feed structure and (b) its equivalent circuit network (Son and Pyo, 2005)

APPENDIX B: TRADE-OFF BETWEEN ANTENNA PARAMETERS
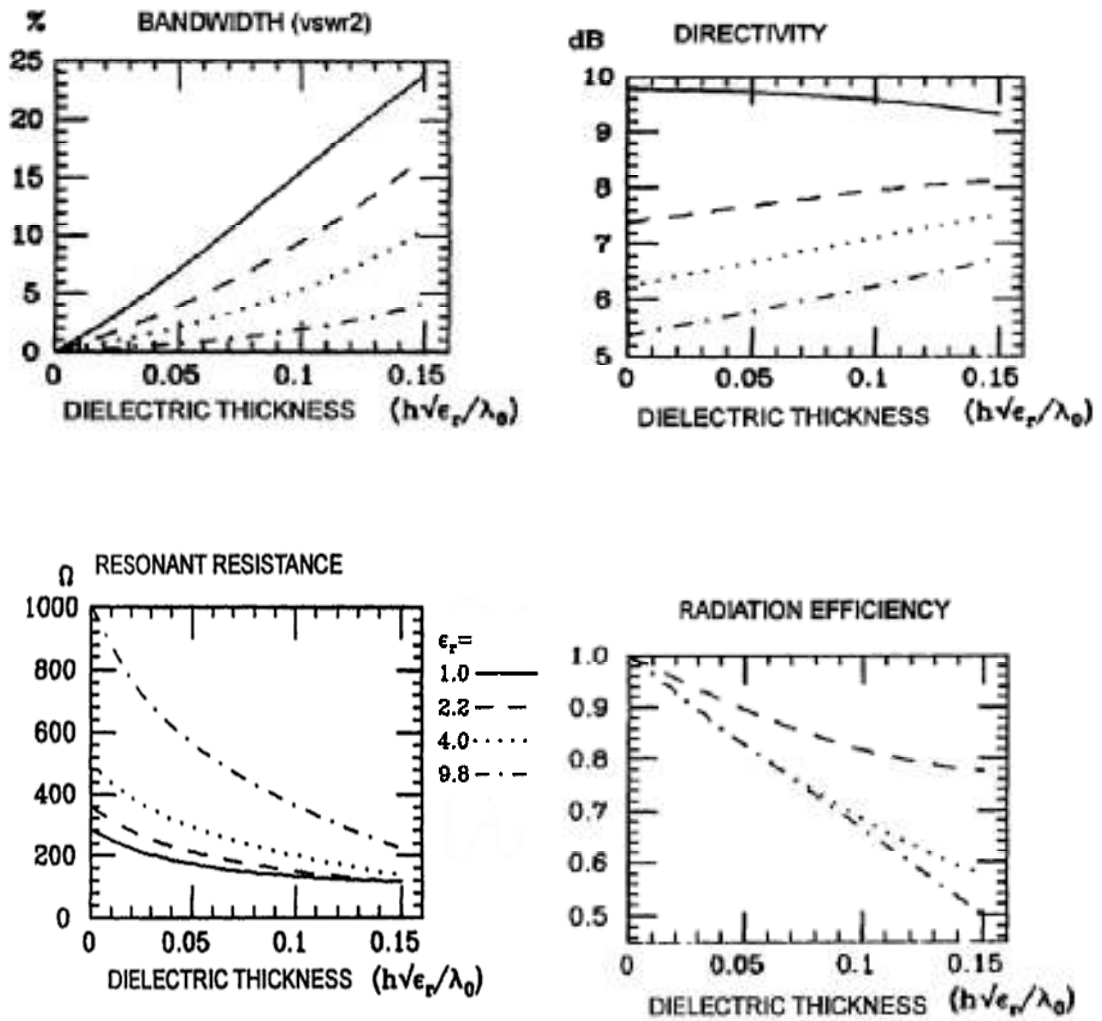
Trade-off between antenna parameters of square patch antenna (Garg et al., 2001)

APPENDIX C: DE-EMBEDDING THE EFFECT OF TEST FIXTURE

(a)

(b)

Screen snapshot of the measured impedance (a) before port extension (b) after port extension of the short circuited test fixture

APPENDIX D: RADIATION PATTERN MEASUREMENT DATA

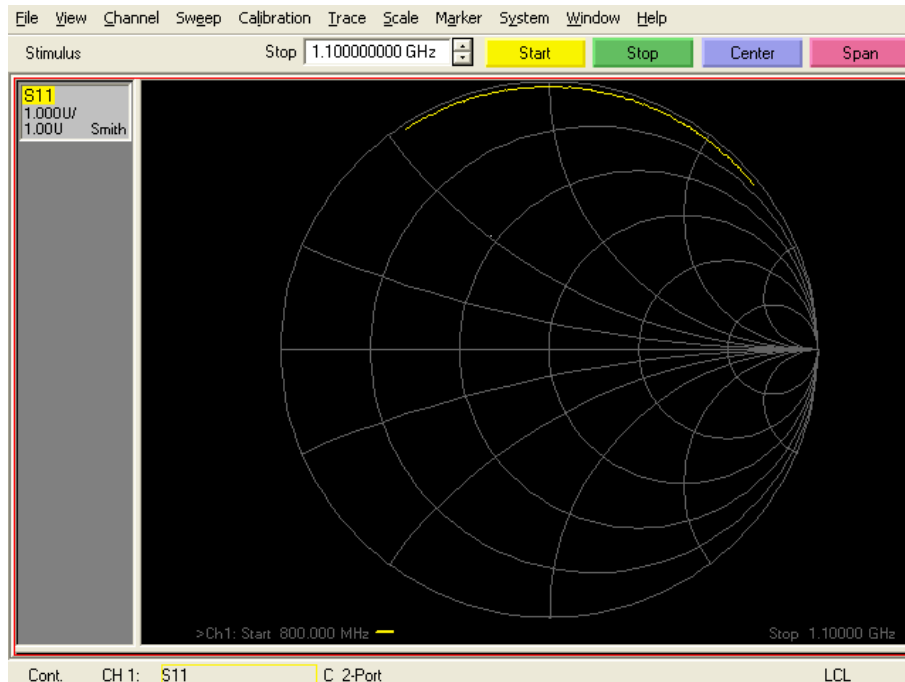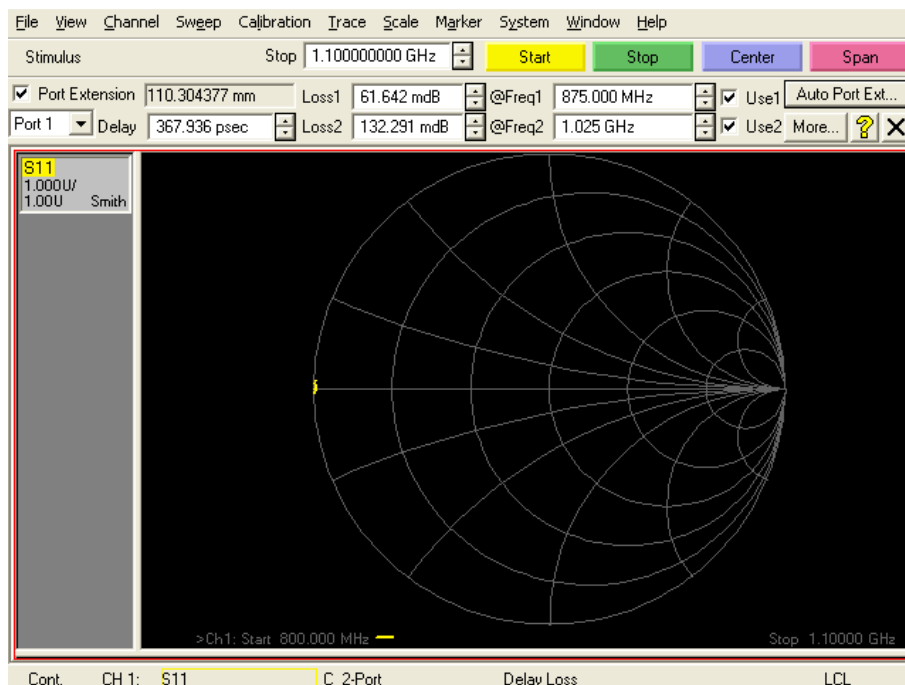| Theta [deg]	Double resonance antenna		Triple resonance antenna	
	E-plane (dB)	H-plane (dB)	E-plane (dB)	H-plane (dB)
0	-45.6747	-43.075	-47.7381	-44.5235
1	-45.9883	-43.3569	-47.4238	-45.1854
2	-46.1069	-42.5333	-47.3298	-44.6983
3	-45.2539	-42.8376	-46.7281	-44.6226
4	-45.3213	-43.0011	-46.9842	-44.5419
5	-45.6518	-42.5557	-46.966	-44.5387
6	-45.0564	-42.5429	-47.4673	-44.8699
7	-45.4332	-42.5999	-46.7474	-44.5932
8	-45.1846	-43.2317	-47.318	-44.6505
9	-44.6921	-43.176	-47.4995	-44.9164
10	-45.1496	-42.8393	-47.5895	-45.2738
11	-44.8371	-43.1172	-47.0079	-45.3792
12	-45.0678	-42.7806	-47.2766	-45.4522
13	-44.7597	-43.1832	-46.9685	-45.0012
14	-44.8822	-43.2838	-46.839	-45.2327
15	-45.0208	-42.8367	-46.9202	-45.3818
16	-44.8172	-43.4105	-47.6028	-45.4252
17	-44.8276	-43.6922	-47.0529	-45.0226
18	-44.9612	-43.2842	-46.9666	-45.0393
19	-44.52	-42.7477	-47.3678	-45.1451
20	-44.1342	-42.8805	-47.0876	-45.2332
21	-44.1881	-42.8469	-47.8516	-45.8213
22	-44.7621	-43.8023	-47.0942	-45.5327
23	-44.4826	-43.6007	-47.073	-45.9995
24	-44.3692	-43.3162	-47.2633	-46.1853
25	-44.2899	-43.74	-47.8555	-45.8816
26	-44.0102	-43.7011	-47.2715	-46.059
27	-44.0264	-43.5187	-47.8204	-45.5875
28	-44.3538	-43.5101	-47.9273	-45.9788
29	-44.0693	-43.2921	-47.9682	-45.7004
30	-44.2067	-43.3742	-47.4304	-45.656
31	-43.9995	-43.6095	-48.2276	-46.0591
32	-44.3525	-43.6745	-47.9367	-45.8999
33	-44.0375	-43.4547	-48.1642	-46.5775
34	-44.3263	-43.7801	-47.8486	-45.9002
35	-44.0623	-43.4071	-47.6236	-46.03
36	-44.4981	-43.7191	-48.6221	-46.3328
37	-44.7576	-43.7063	-48.0328	-46.6508
38	-44.0519	-44.3433	-47.811	-46.5259
39	-44.175	-43.7977	-48.2192	-46.6354

40	-44.5361	-44.3085	-48.5486	-46.709
41	-44.1545	-44.0745	-48.5147	-46.064
42	-44.7772	-43.8787	-48.9412	-47.0437
43	-45.0816	-43.7282	-49.1463	-46.5057
44	-44.6243	-43.9233	-49.1132	-46.2526
45	-44.9579	-44.2318	-48.6994	-46.8764
46	-45.05	-44.0497	-49.1575	-47.0722
47	-45.1515	-44.5235	-48.9797	-46.5509
48	-44.9335	-44.3502	-48.9278	-46.9899
49	-45.4443	-44.1367	-49.5415	-47.2021
50	-44.8432	-44.7871	-50.1399	-47.1896
51	-45.3686	-44.2838	-49.8915	-46.6813
52	-45.4068	-44.9524	-50.1235	-47.0745
53	-45.5829	-44.3975	-49.9998	-47.4178
54	-45.327	-44.8868	-50.4514	-47.2668
55	-45.7133	-45.0883	-50.5957	-46.8067
56	-46.0158	-44.8087	-50.3736	-47.4632
57	-46.2454	-45.1895	-50.7962	-46.9654
58	-45.8641	-45.1822	-51.3172	-47.012
59	-46.4547	-45.1491	-51.2094	-46.9302
60	-45.8151	-45.1548	-51.7554	-47.0007
61	-46.4295	-45.2723	-52.2287	-47.1716
62	-46.1324	-44.8832	-51.7355	-47.1527
63	-46.6993	-45.1013	-51.8171	-47.3866
64	-46.2929	-44.9034	-51.4335	-47.2891
65	-46.8194	-45.3859	-52.0487	-47.7674
66	-47.0023	-44.853	-52.723	-47.6942
67	-47.2911	-45.1548	-52.5568	-47.2493
68	-47.2064	-44.9393	-52.0836	-47.9985
69	-47.4172	-45.4851	-52.2403	-47.4146
70	-48.2954	-45.031	-53.0545	-47.953
71	-48.2795	-45.5343	-52.3225	-47.5082
72	-48.5106	-45.7406	-52.47	-48.218
73	-49.0286	-45.1444	-53.2069	-47.4765
74	-48.9662	-45.2538	-52.2943	-47.9721
75	-48.7279	-45.6218	-52.9675	-48.0127
76	-49.2072	-45.2855	-52.4798	-47.8479
77	-49.4237	-45.4278	-53.7452	-47.803
78	-49.8605	-45.8556	-52.975	-47.8836
79	-50.5929	-46.0519	-52.3313	-48.0057
80	-51.1973	-46.1358	-52.902	-48.5516
81	-51.1958	-45.5871	-52.0046	-48.3817
82	-51.7547	-45.7603	-52.6494	-48.5827
83	-51.3943	-46.0267	-51.9742	-48.3234
84	-51.8943	-46.1632	-51.2921	-48.554

85	-52.7749	-45.8147	-51.2743	-48.2641
86	-53.0114	-46.2709	-51.0894	-48.2267
87	-53.865	-45.9037	-51.6339	-48.3587
88	-54.5177	-45.6936	-51.1165	-48.1578
89	-55.0417	-45.9041	-51.2437	-48.3549
90	-55.8061	-46.1514	-50.1946	-48.5141
91	-56.914	-46.0809	-50.2305	-48.0841
92	-55.9726	-46.2655	-50.3662	-48.5449
93	-57.7326	-46.0127	-50.1591	-48.9259
94	-57.9767	-46.7891	-49.352	-48.777
95	-59.9213	-46.2008	-49.002	-48.7668
96	-58.9141	-46.5849	-49.0225	-48.9599
97	-60.0274	-46.6741	-49.3159	-48.9896
98	-61.7541	-46.7603	-49.2272	-48.5003
99	-62.5199	-46.7256	-48.8049	-49.0123
100	-63.7161	-46.4177	-48.5365	-48.562
101	-61.4992	-46.2798	-48.501	-48.9629
102	-60.7905	-46.7198	-47.5091	-48.5698
103	-60.0948	-46.8186	-47.1905	-48.6746
104	-59.3976	-46.6276	-47.7945	-49.1738
105	-58.4386	-46.9386	-47.0466	-49.1635
106	-56.7019	-46.3436	-46.5868	-48.9451
107	-55.9899	-46.5047	-47.152	-49.0692
108	-55.0145	-46.5391	-46.4655	-49.0944
109	-54.5687	-47.0144	-46.9348	-48.3773
110	-54.6402	-46.6268	-46.5536	-49.018
111	-53.0579	-46.7113	-46.7489	-48.4141
112	-53.5453	-46.7392	-45.7077	-48.3052
113	-53.5185	-46.2619	-45.5248	-48.4553
114	-52.6298	-46.8638	-45.6392	-48.729
115	-52.1788	-46.9402	-45.933	-48.2573
116	-50.971	-46.1959	-46.2199	-48.9022
117	-50.448	-46.7992	-45.4308	-48.1601
118	-50.0777	-46.6175	-46.0069	-48.3799
119	-50.078	-46.9844	-45.1597	-48.4728
120	-50.2366	-47.1267	-45.2623	-48.6591
121	-49.9961	-46.9863	-44.8636	-48.3681
122	-49.0923	-46.8582	-45.1004	-48.5761
123	-49.052	-47.1257	-44.9133	-48.5918
124	-49.2634	-46.9554	-44.8856	-48.5035
125	-47.8845	-46.9116	-45.1125	-48.5522
126	-48.4237	-47.2582	-44.6645	-48.6056
127	-47.4586	-46.9415	-44.83	-48.4335
128	-47.3227	-47.0609	-45.2473	-48.4985
129	-47.902	-46.9002	-44.2835	-48.9362

130	-47.3282	-46.9953	-44.471	-49.2304
131	-47.0221	-47.3106	-44.2212	-48.4731
132	-47.1341	-46.7239	-45.0021	-48.5787
133	-46.485	-46.9248	-44.6906	-48.3143
134	-46.8854	-46.7707	-44.5027	-48.9706
135	-46.9143	-47.4336	-44.2218	-49.1726
136	-46.1483	-46.969	-43.8274	-48.8547
137	-45.8818	-47.5641	-44.6982	-48.6543
138	-45.7434	-47.595	-43.8771	-48.7731
139	-45.4269	-47.234	-44.6777	-49.0488
140	-45.6545	-47.7183	-44.6049	-48.4529
141	-45.4537	-47.1123	-44.5857	-48.6928
142	-45.6832	-47.6349	-44.6668	-48.6978
143	-45.56	-47.3997	-44.0704	-48.6783
144	-44.822	-47.5774	-44.0326	-48.5999
145	-45.0383	-47.7832	-44.4795	-49.15
146	-45.2633	-47.8005	-44.6322	-48.9321
147	-45.111	-47.5928	-44.0402	-49.1145
148	-44.5075	-47.2818	-43.9526	-48.9304
149	-44.3032	-47.5966	-44.151	-49.2134
150	-44.8963	-47.3207	-44.6536	-48.5468
151	-44.2439	-47.7913	-44.8885	-48.5122
152	-44.6105	-47.1009	-44.1676	-48.645
153	-44.3748	-47.6088	-44.57	-48.4564
154	-44.6083	-47.206	-43.9868	-48.7888
155	-43.8457	-47.0479	-44.9363	-49.1741
156	-44.5261	-46.9971	-44.4589	-48.7833
157	-44.3772	-47.0197	-44.2399	-49.2204
158	-43.9403	-46.9606	-44.6246	-48.5569
159	-44.067	-47.2949	-44.1998	-49.5037
160	-43.6088	-47.0023	-44.9481	-48.7739
161	-44.7378	-47.2065	-44.4258	-49.5924
162	-43.8591	-47.4873	-45.1388	-49.5087
163	-44.205	-47.4239	-44.3591	-49.3444
164	-43.6961	-47.5495	-44.8676	-49.2946
165	-44.0073	-47.5871	-44.9764	-48.9064
166	-43.7754	-47.3656	-44.8389	-49.0389
167	-43.7238	-47.5402	-45.1127	-49.491
168	-43.321	-47.64	-44.9526	-49.4976
169	-44.1203	-47.5296	-44.3505	-49.3947
170	-43.7844	-47.5085	-44.5238	-48.5616
171	-43.9913	-47.2447	-44.9445	-48.7824
172	-43.7935	-47.8763	-45.194	-49.3163
173	-43.8249	-47.9068	-44.4369	-49.445
174	-43.9302	-47.4473	-45.2961	-49.6497

175	-43.4514	-48.0386	-44.5435	-48.5919
176	-43.2479	-47.6332	-45.2264	-49.0919
177	-43.985	-47.3172	-45.4647	-48.696
178	-43.8541	-47.755	-45.1414	-48.9239
179	-43.1367	-47.4832	-45.4951	-48.815
180	-43.8441	-47.7223	-45.1109	-49.6529
181	-43.715	-47.6516	-45.0349	-48.7789
182	-43.7195	-47.3318	-44.9006	-49.3896
183	-43.0278	-47.5528	-45.1662	-49.0795
184	-43.7351	-47.9624	-45.2951	-49.6397
185	-43.7291	-47.769	-45.0874	-49.063
186	-43.3964	-47.8327	-44.9714	-49.1786
187	-43.2014	-47.657	-45.8074	-49.6941
188	-43.9267	-47.6724	-45.9871	-49.795
189	-43.8609	-47.6141	-45.2276	-49.4506
190	-43.962	-47.4367	-45.6244	-49.4325
191	-43.9294	-47.7176	-46.1745	-48.8572
192	-43.9612	-47.4273	-45.5898	-49.4406
193	-43.9653	-47.4058	-46.3948	-49.7927
194	-43.5462	-47.1559	-45.8682	-49.4941
195	-44.2424	-47.4819	-45.9683	-49.3129
196	-43.3706	-47.9384	-46.3335	-49.5652
197	-43.865	-47.2825	-45.8554	-49.9576
198	-44.0181	-47.3196	-45.8933	-48.9472
199	-43.4724	-47.4382	-46.5075	-49.0008
200	-44.3322	-47.7108	-46.8508	-48.967
201	-44.3231	-47.7242	-46.3582	-49.6498
202	-43.7584	-47.126	-45.9895	-48.9998
203	-44.3428	-47.0904	-46.091	-49.5741
204	-44.3602	-47.4569	-46.7252	-48.72
205	-44.3969	-47.2999	-46.3013	-48.7745
206	-43.782	-47.4279	-46.8776	-48.7127
207	-44.2838	-47.5631	-46.3969	-48.8749
208	-43.6943	-47.669	-46.6918	-49.3889
209	-43.4621	-47.635	-47.376	-49.8218
210	-44.5976	-47.7089	-47.0314	-48.7289
211	-44.5322	-47.1069	-47.4233	-48.5935
212	-43.9284	-47.0922	-46.6773	-48.531
213	-43.8353	-46.9452	-47.4278	-48.4951
214	-43.7745	-47.3072	-47.3686	-48.7308
215	-43.8054	-46.9653	-46.8161	-49.5765
216	-44.4601	-47.1899	-47.1031	-48.854
217	-44.5742	-46.8586	-47.9002	-49.3461
218	-44.1517	-46.9719	-47.2427	-49.4235
219	-44.5893	-47.0305	-47.3472	-48.6209

220	-44.8165	-47.3407	-47.2805	-49.1445
221	-45.3238	-47.4233	-48.3838	-49.1952
222	-44.8553	-47.115	-48.0554	-48.7406
223	-45.2406	-47.2698	-48.4565	-48.6534
224	-45.1254	-47.3351	-48.8418	-48.9892
225	-45.3286	-47.2596	-48.9215	-49.3642
226	-44.7626	-47.1989	-49.2115	-48.5656
227	-44.3136	-46.7967	-49.4528	-48.6835
228	-45.3005	-47.3353	-48.4307	-48.4392
229	-45.5282	-47.178	-48.4382	-48.6464
230	-45.0736	-47.2002	-48.8518	-49.162
231	-44.8567	-47.3727	-48.0831	-49.3177
232	-44.7464	-46.5587	-47.8547	-49.6053
233	-44.6684	-46.9411	-47.4906	-48.6607
234	-44.9284	-46.3672	-47.8928	-49.2549
235	-44.5641	-46.8937	-47.6229	-49.514
236	-44.3615	-46.3875	-47.8964	-49.285
237	-45.0539	-46.6437	-47.0206	-48.9852
238	-44.997	-46.7689	-47.3109	-49.5937
239	-45.0044	-46.1607	-47.0907	-48.6377
240	-44.2481	-46.5046	-46.8724	-48.7799
241	-44.7702	-45.9335	-47.317	-48.5169
242	-44.2876	-46.6286	-47.6068	-49.2119
243	-44.2404	-46.3985	-47.2323	-48.9548
244	-44.1492	-45.7705	-46.8175	-49.1849
245	-44.4752	-46.3742	-46.4978	-49.3033
246	-44.3953	-46.3081	-47.1395	-49.1537
247	-44.1159	-45.6115	-47.2152	-49.5863
248	-43.9576	-45.8491	-46.3691	-49.484
249	-44.2493	-45.9271	-46.8043	-48.4161
250	-44.6509	-46.159	-46.2643	-48.5942
251	-44.547	-46.2051	-46.1595	-48.9462
252	-44.759	-45.4716	-46.7221	-49.1446
253	-44.7376	-45.7987	-46.4078	-49.489
254	-44.615	-45.7424	-46.0682	-48.544
255	-43.9244	-45.3487	-46.2171	-48.4056
256	-44.0368	-45.124	-46.7561	-48.4957
257	-45.1084	-45.0473	-45.8922	-49.4149
258	-44.0171	-45.1296	-46.4227	-48.4745
259	-44.7133	-45.1121	-45.973	-49.2839
260	-44.1721	-45.3176	-45.6511	-48.3555
261	-44.4735	-44.8056	-45.7532	-48.4746
262	-44.0858	-45.3247	-45.6725	-48.7159
263	-44.2901	-45.5058	-46.3733	-49.2929
264	-44.675	-44.9439	-45.4754	-48.2958

265	-44.1584	-45.4601	-46.2794	-48.536
266	-44.7945	-44.5689	-46.1651	-49.1214
267	-44.8355	-45.2212	-45.7395	-49.0385
268	-44.8337	-44.7678	-45.4038	-48.7778
269	-44.0741	-45.0677	-45.8016	-48.6594
270	-44.0025	-44.6218	-45.1214	-48.4712
271	-44.909	-45.0652	-46.1814	-49.4718
272	-44.0564	-44.7762	-45.0462	-48.6527
273	-44.801	-44.8167	-45.651	-48.66
274	-44.2631	-44.3051	-45.5881	-48.5111
275	-44.1387	-44.3513	-45.4944	-49.0178
276	-44.8072	-44.5358	-45.509	-49.3002
277	-44.0079	-45.0969	-44.8559	-48.9627
278	-43.9731	-44.661	-45.6576	-49.039
279	-44.4556	-44.9556	-45.1175	-49.3483
280	-43.9767	-44.7816	-45.6225	-49.711
281	-43.8972	-44.4988	-45.2138	-49.8171
282	-44.0695	-45.2399	-44.8457	-48.698
283	-44.027	-45.0506	-44.979	-48.9744
284	-43.9432	-45.213	-45.5255	-49.7379
285	-44.5674	-44.4751	-44.698	-48.8456
286	-44.2866	-44.259	-45.7304	-48.9612
287	-44.7192	-45.0958	-45.3541	-49.5664
288	-44.3465	-44.152	-45.7802	-48.7006
289	-45.0804	-44.6723	-45.5805	-49.6292
290	-44.0434	-44.7523	-44.9424	-48.8404
291	-44.6551	-44.2515	-45.1314	-48.8678
292	-44.6475	-45.1893	-45.749	-48.8139
293	-44.2884	-44.9652	-44.7826	-49.7694
294	-44.5953	-45.0988	-45.1302	-49.5171
295	-44.1416	-44.6224	-45.7255	-49.8118
296	-44.8204	-44.6031	-45.091	-48.6708
297	-44.9047	-45.1125	-45.5497	-49.0295
298	-44.6323	-44.1307	-45.5363	-48.8651
299	-44.4645	-45.1744	-45.644	-50.1179
300	-44.917	-44.8773	-45.6058	-49.2207
301	-44.0989	-44.6453	-45.0433	-48.7976
302	-44.0247	-45.1624	-45.0638	-49.8107
303	-44.7837	-44.7367	-45.1824	-49.6451
304	-44.7541	-44.5103	-45.1757	-49.9476
305	-44.6054	-44.4651	-45.7792	-49.3222
306	-43.9913	-44.7747	-45.0531	-49.205
307	-44.0895	-44.572	-44.8849	-49.1434
308	-44.8627	-45.2017	-44.9107	-49.8926
309	-44.1872	-44.486	-45.4536	-49.9898

310	-44.7703	-45.168	-44.9283	-49.4309
311	-44.1721	-45.2607	-44.8295	-50.3937
312	-44.0577	-45.0259	-45.2808	-50.3981
313	-44.1554	-45.0915	-45.0955	-50.1648
314	-44.6515	-44.2561	-45.8575	-49.487
315	-44.3413	-44.438	-45.6522	-50.2651
316	-44.2066	-44.1989	-45.571	-49.9943
317	-45.038	-44.5659	-45.6896	-50.0098
318	-44.1103	-44.8137	-45.4744	-50.0566
319	-44.8446	-44.215	-45.7318	-50.4451
320	-44.0686	-44.9216	-45.8679	-49.3762
321	-44.332	-44.3429	-46.3464	-50.1106
322	-44.7268	-44.2978	-46.3884	-49.7559
323	-44.963	-44.0722	-45.7068	-50.5134
324	-44.07	-45.0637	-46.0229	-50.347
325	-45.0538	-44.1521	-46.3452	-50.5497
326	-44.6696	-44.2921	-45.8118	-49.8137
327	-44.5476	-44.6481	-45.9259	-50.3147
328	-44.7894	-44.3536	-46.3232	-49.6831
329	-44.26	-44.0058	-46.7707	-49.6597
330	-44.8338	-44.7877	-46.0377	-50.2289
331	-44.9071	-43.9247	-46.6472	-49.6132
332	-44.7764	-44.0747	-47.2498	-50.4732
333	-45.0068	-43.8362	-47.4467	-49.766
334	-45.3624	-44.3806	-47.4072	-49.6505
335	-45.3833	-44.4419	-46.8185	-50.5381
336	-45.621	-44.4087	-46.9513	-49.5403
337	-45.3716	-44.1399	-46.9713	-49.934
338	-44.8929	-43.9075	-47.632	-49.9071
339	-44.8183	-43.4961	-47.6244	-49.7545
340	-45.5537	-43.6983	-47.9863	-50.3391
341	-45.6702	-43.6189	-48.0425	-50.481
342	-45.2864	-43.6056	-48.24	-49.8746
343	-45.0606	-44.1553	-48.2545	-49.9802
344	-45.7363	-44.334	-48.146	-50.3412
345	-45.5801	-44.2259	-49.0632	-49.6874
346	-45.2436	-44.127	-49.3498	-50.4976
347	-45.1755	-44.3369	-49.3436	-49.6737
348	-46.2429	-43.6302	-49.0504	-50.4544
349	-46.6452	-43.6681	-49.7103	-50.1014
350	-46.1986	-43.4648	-49.4194	-50.6317
351	-46.0785	-43.8259	-49.678	-50.369
352	-46.079	-43.7148	-50.2556	-50.6408
353	-47.0039	-44.0097	-50.2151	-50.17
354	-46.5959	-43.3301	-49.9633	-49.6838

355	-47.6412	-43.4501	-50.279	-50.0552
356	-47.4526	-43.5979	-50.4445	-49.9774
357	-47.3054	-43.4645	-51.0893	-50.1828
358	-47.7251	-43.9623	-51.9568	-50.1828
359	-47.9213	-43.9623	-52.1942	-49.9774